SEPT 2012
Vol. 1, Issue 1

સર્જન

SARJAN

SOCET Journal

Silver Oak College of Engineering & Technology
WE THINK ABOUT YOUR FUTURE

Silver Oak College of Engineering & Technology
Ahmedabad

MESSAGE FROM CHAIRMAN

It is a matter of great pleasure to me that our College starts 'SARJAN' SOCET Journal. My professors are always eager to share their knowledge and experience for the benefit of the students and engineering community. This Journal is the result of their efforts. My dream has come true with the opening of this Journal. I appreciate all those who have contributed and worked for this Journal. This Journal will surely be useful to my faculty and students. I appreciate the efforts of Vice chancellor of GTU who has inspired us to carry out such activities. I assure you all my support at any time. My blessings are always with you.

Shital Agrawal

Chiarman, SOCET

MESSAGE FROM THE EXECUTIVE DIRECTOR

I am happy to see 'SARJAN', SOCET Journal in my hand. I welcome the efforts of professors who have contributed and shared their experience through this Journal. My ambition of imparting the research knowledge to faculty members and students is fulfilled with this Journal. Our Vice Chancellor of GTU has always put efforts to bring GTU at international level. Our SOCET Journal is one step in this direction. I am sure that this Journal will be helpful to educational community to enhance their knowledge. My good wishes and support are always there with you.

Janak Khandwala

Executive Director, SOCET

MESSAGE

SOCET is bringing out “SARJAN”, a technical journal with papers submitted by the staff. Hearty congratulations to the staff for their innovative thought of a journal having technical ideas and papers of their own members. This gives a platform to hone the technical awareness towards research and development. Such initiatives in the technical institutions will create an environment of knowledge sharing between the peers and will in turn prove beneficial to the student community. This gives an opportunity for the staff to present the analysis in the area of their specialization which forms a base for further study.

Once again congratulations to all the faculty members who offered their papers for the journal. Trust that many more contributions will flow in the future volumes of the journal.

Let the “SARJAN” nurture eternally…… Best Wishes.

Prof. Ravikumar K.
Director (Academics)

MESSAGE FROM THE PRINCIPAL

I am indeed happy to note that our college is coming up with first issue of “SARJAN - SOCET Journal”. I strongly feel that it is need of hour, as today we are witnessing era of technological revolution. One has to update him/her self to keep up with this change. Publishing a paper at this juncture will provide good platform to our faculty members those who wish to excel in their academic career and explore further in the topic of interest.

I congratulate faculty members those who have contributed for “birth (SARJAN)” of first issue of journal and expect that this will motivate others as well, to come forward and contribute for upcoming issues of journal.

My heartiest congratulations to Dr. P. K. Shah (Dean), Prof. Jagat Shah, Prof. Harshid Patel and team who have given shape to this initiative.

I look forward for grand success of the journal in time to come.

Dr. Saurin Shah
Principal

EDITORIAL

'સર્જન', SOCET Journal is a Journal of Research & Educational activities. 'સર્જન',SARJAN means creation. It is something that is newly created for the benefit of human society. It is our great pleasure that our college starts this type of Journal which will enhance the technical progress of the society. It is a big step towards the advancement of research & development. The knowledge and intelligence of learned professors will be reflected in this Journal, which would benefit the faculty members, students & society. We specially thank the Vice Chancellor of GTU who always promotes such educational activities. Our Chairman, Executive Director, Principal and Director(Academics) have motivated and continuously inspired the team preparing this Journal. We are thankful to them for their inspiration and support. We also thank to the authors who have contributed their research papers for this Journal. We extend our thanks to the team members who have worked to bring this Journal out at the earliest. We thank Prof. Dulari Mehta and Mr. Dhruv Saidava for designing front page of the Journal. We are sure that in future also; we will receive the whole hearted support from all. We hope that this Journal will be much useful to educational and other communities also.

Dr. P. K. Shah Chief Editor
Prof. H. R. Patel Co-ordinator
Prof. J. K. Shah Co-ordinator
Prof. I. B. Thakar Co-ordinator

INDEX

Heat exchanger networking for the ammonia plant Using pinch technology

Umang Patadiwala

Email: umangpatdiwala@gmail.com

Mechanical Engineering Department, Silver Oak College of Engineering & Technology, Ahmedabad

Abstract:

Pinch technology is a set of conceptual tools and techniques for analyzing and optimizing total energy systems in any process unit. Components of energy systems in process plants include Heat Exchanger Network (HEN), utility system, combined heat and power cycle and heat pumping system which can be designed together by considering entire view involving the interactions among them. Pinch technology is not only used for energy savings but also enhanced operation flexibility and reduced environmental impact.

The initial phase of finding pinch point temperature in this technology is carried out in two different ways: Composite Curve Method which uses graphical analysis method and Problem Table Method which uses an algorithm for setting the targets algebraically.

From the analysis, an optimum Heat Exchanger Networking has been designed for the existing plant, as well as optimum number of heat exchangers and total heat load required for hot and cold streams has been carried out which results in reduction of capital cost and complexity of HEN.

Keywords: Heat exchanger technology, pinch technology

Nomenclature:

CP	heat capacity-flow rates (kW/K)
ΔH	change of flow enthalpy (kW)
Ts	supply temperature of process stream (K)
Tt	target temperature of process stream (K)
$_{H, HOT}$	relating to hot stream
$_{C, COLD}$	relating to cold stream

1. Introduction

Developing the best integrated process designs for both new plants and retrofits pinch technology has proved to be very effective. This has been demonstrated in numerous successful projects in traditional sectors such as oil refining, petrochemical, fertilizers, general chemical, and specialist sectors like food and drink, pulp and paper etc. Recent developments extend the Pinch technology from single processes to total sites, i.e. factories incorporating several processes, serviced by and linked through a central utility system.

In at least half of the new design projects, capital cost implications were saving rather than expenditure in other words, more elegant integration made it possible to identify process that would not only be cheaper to run but also cheaper to build. Benefits of this technology can be

- Energy saving identified ranged from 6% to 60% of the original design.
- Corresponding capital savings were as high as 30% of the original design.
- Payback time in plant modifications was improved by factors up to four.
- The improved designs do not tend to present unusually difficult control and operability problems and indeed some featured better control characteristics than the original designs.

This success is due to two main reasons as the techniques are based on completely new principles and concepts which is simple. The heat recovery “Pinch” is a new thermodynamic concept at the center of the techniques. Following on from the “Pinch” there are many new concepts and techniques. Between them, these concepts and techniques make it possible for the
user to deal quickly and confidently with problems so far thought too complex to be properly understood.

2. Practical thermodynamic performance target

In most people’s minds, thermodynamics is associated with energy costs and thermodynamic arguments are only practical if capital costs are low. Consider appropriate Fig. 1; at the top a heat exchanger network is shown that would seem appropriate to most when energy is cheap but with expensive capital. There is no process heat recover-

only utility usage. At the bottom a network is shown which would seem appropriate to most when energy is expensive. There is as much process heat recovery as is possible in preference to utility usage. The implicit assumption is that heat recovery (instead of utility use) saves energy but costs the capital.

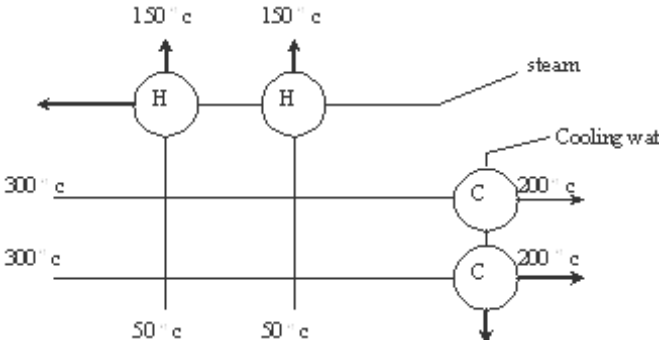

Fig.1 Networks for minimum cost

3. Application of the integration techniques

The initial phase of finding Pinch point temperature in this technology is carried out with two different ways, namely composite curve method and Problem table method. First method uses graphical analysis method (graph paper & scissors approach) and later uses an algorithm for setting the targets algebraically.

3.1 Composite Curve Method

A single composite of all hot and a single composite of all cold streams can be produced in the T/H diagram. Considering an example of two hot streams whose heat capacity-flow rate, CP (mass flow rate x specific heat at constant pressure) is A & B kW/ ^{o} C. Graphical construction is briefly shown in fig 2

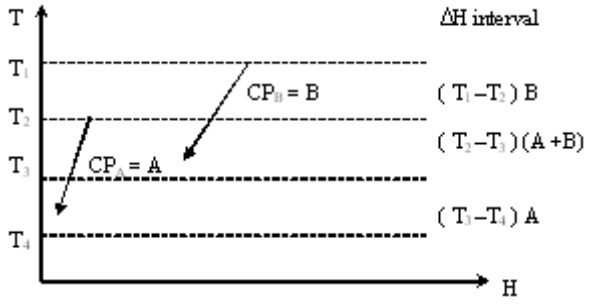

Fig.2a Construction for Hot Composite curves

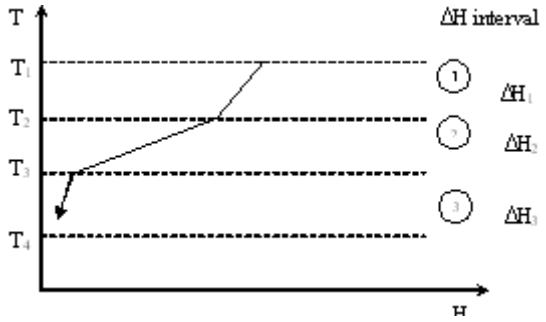

Fig.2b Hot Composite curves

In Figure 2 (a) their hot streams are plotted separately, with their supply and target temperature defining a series of "interval" temperature T_1 to T_2. Between T_1 and T_2 only stream B exists, and so the heat available in this interval is given by CP_B . $(T_1 – T_2)$. However between T_2 and T_3 both streams exists and so the heat available in this interval is $(CP_A + CP_B)(T_2 – T_3)$. A series of value of ΔH for each interval can be obtained in this way, and the result re-plotted against the interval temperature as shown is Figure 2. (b). The resulting T/H plot is a single curve representing all the hot streams. A similar procedure gives a composite of all cold streams in a problem.

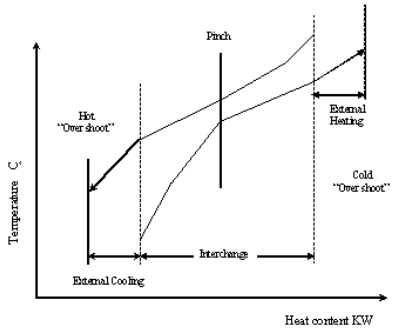

Fig.3

Figure 3 shows a typical pair of composite curves. Shifting of the curves leads to behavior similar to that shown by the two-stream problem. Now, though, the "kinked" nature of composites means that ΔT_{min} can occur anywhere in the interchange region and not just at one end. For a given value of ΔT_{min} the utility quantities predicted are the minima required to solve the heat recovery problem. Note that although there are many streams in the problem, in general ΔT_{min} occurs at only one point, termed the "pinch". This means that it is possible to design a network, which uses the minimum utility requirements, where only the heat exchangers at the pinch need to operate at ΔT values down to ΔT_{min}.

The overlap between the composite curves represents the maximum amount of heat recovery possible within the process. The "over-shoot" of the hot composite represents the minimum amount of external cooling required and the "over-shoot" of the cold composite represents the minimum amount of external heating. Because of the "kinked" nature of the curves, they approach most closely at one point. This is the "pinch". Remaining procedure is common with next method.

3.2 Problem Table Method

Taking an case study of Ammonia-II plant, GSFC fertilizer complex, data from technical dept. was provided. From Process flow diagrams of whole plant, a problem is identified as Table-1.

Table1 Problem of Ammonia-II plant at GSFC Fertilizer complex hot utility purge & associated gas at 1050°C cold utility water at 15 ° C.

Sr. No.	Stream	CP KW/° C	T_i ° C	T ° C	Load kW
1	Cold	10.327	15	382	3790
2	Cold	92.482	360	812	4180186
3	Hot	53.637	954	360	3186037
4	Hot	44.438	423	221	8976.47
5	Hot	126.245	235	172	7953.43
6	Cold	22.867	70	340	6174.09
7	Hot	24.171	370	40	7976.43
8	Cold	77.075	108	248	10790.5
9	Cold	22.71	15	207	4360.32
10	Cold	576.92	93	119	15000
11	Hot	429.28	172	135	1588336
12	Hot	338.94	125	78	15930.23
13	Hot	199.15	103	40	12546.45
14	Hot	326.8	127	70	18627.88
15	Hot	134.016	218	41	237208
16	Cold	73.047	108	147	2848.83
17	Cold	5.305	60	163	546.41
18	Hot	4.076	214	40	709.224

The hot and cold streams in a process can be represented on a temperature-heat content (enthalpy) graph once there input and output temperatures (or "supply" and "target" temperatures) and their flow rates and physical properties are known.

Streams are shown in a scheme representation with a vertical temperature scale. Temperature interval boundaries are superimposed. The interval boundary temperatures are set as ½ ΔT_{min} (5^0C in this example) below hot stream temperature and ½ ΔT_{min} above cold stream temperature. This data can be graphically presented as per fig. 4

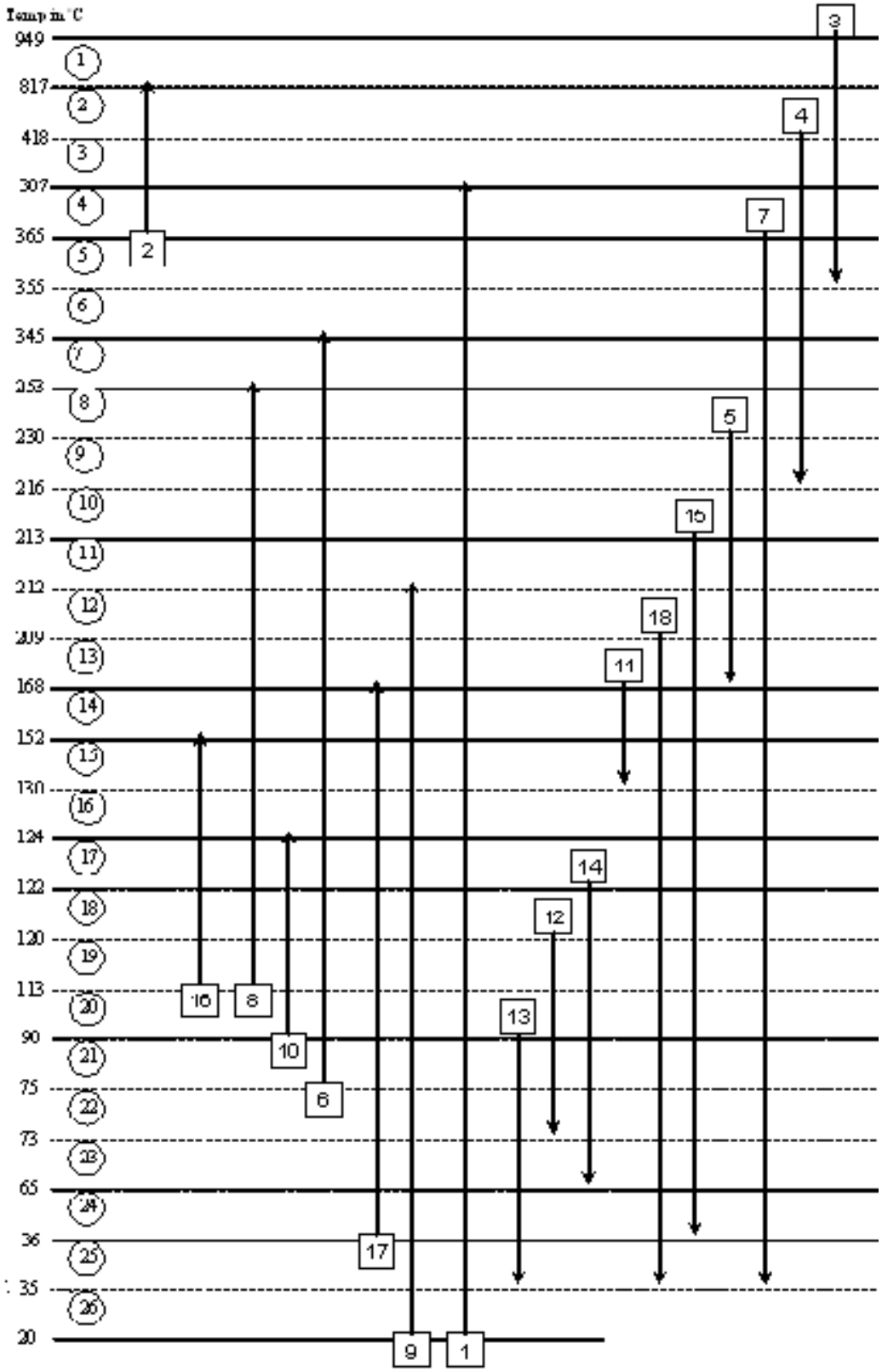

Fig.4 Stream Requirement

Setting up the intervals in this way guarantees that full heat interchange within any interval is possible. Hence, each interval will have either a net surplus or net deficit of heat as indicated by enthalpy balance, but never both. This is shown in fig 5(a). Knowing the stream population in each interval, enthalpy balances can easily be calculated for each according to:-

$\Delta H_i = (T_i - T_{i+1}) \times (\sum CP_C - \sum CP_H)_i$ for any interval i.

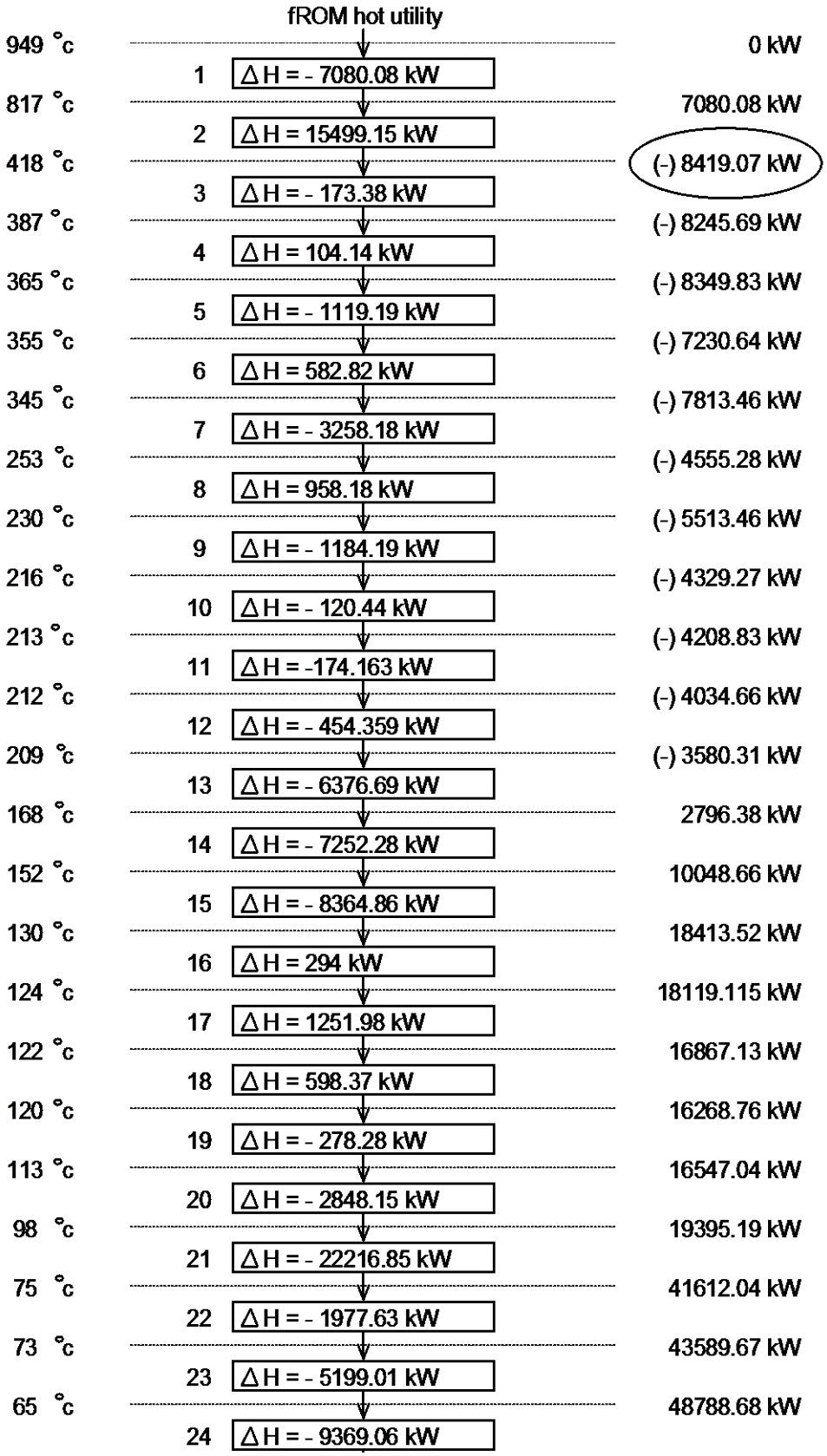

Fig. 5(a) Heat Cascade (Infeasible)

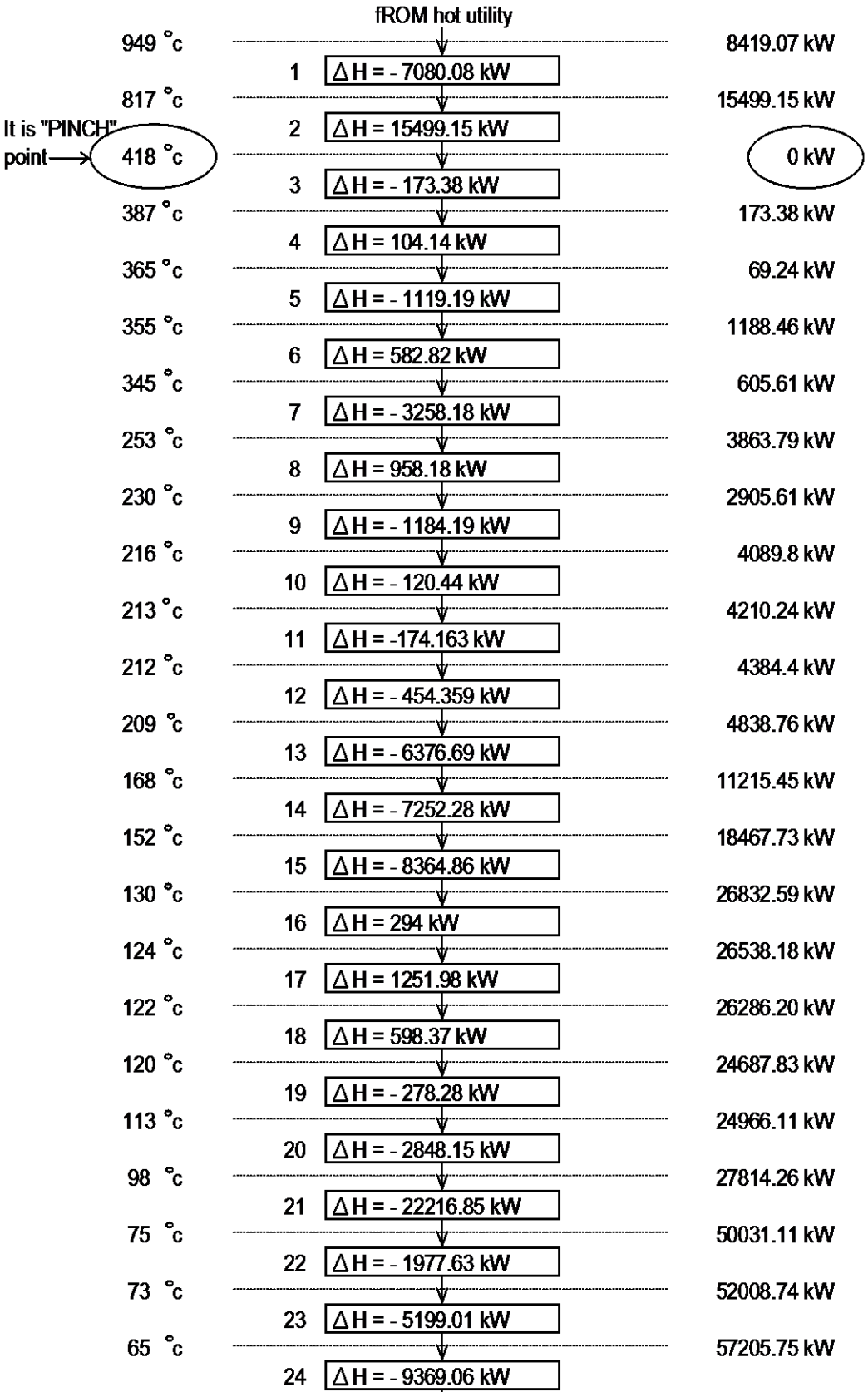

Fig. 5(b) Heat Cascade (Feasible)

Exploit a key feature of the temperature intervals. Namely, any heat available in interval 1 is hot enough to supply any duty in interval i + 1. Instead of sending the 7080.08 kW of surplus heat from interval 1 into cold utility. It can be sent down into interval 2. It is therefore possible to set up heat "cascade" as shown in Figure 5(a). Assuming that no heat is supplied to the hottest interval (1) from hot utility, In second interval with surplus of 7080.08 kW, deficit of 15499.15 kW is added, resulting deficit of 8419.07kW is passed to interval 3. Then in interval 4, has a 173.38 kW surplus, hence after accepting the –8419.07 kW it can be regarded as passing on a 8245.69 kW deficit to interval 4. After going through all intervals 57856.55 kW is the final cascaded energy to cold utility. This in face is the net enthalpy balance on the whole problem. Looking back at the heat flows between intervals in Heat Cascade fig 5(a), clearly the negative flow to 8419.07 kW between intervals 2 and 3 is thermodynamically infeasible. To make it just feasible (i.e. equal to zero), 8419.07 kW of heat must be added from hot utility as shown in fig 5(b), and cascaded right through the system. By enthalpy balance this means that all flows are increased by 8419.07 kW. The net result of 8419.07 kW hot and 66275.62 kW cold. Further, the position of the pinch has been located. This is at the 418^0 C interval boundary temperature (i.e. hot streams at 423^0 C and cold at 413^0 C) where the heat flow is zero.

So for the designer wishing to produce a minimum utility design, the firm message is:-

- Don't transfer heat across the Pinch.
- Don't use Cold utilities above.
- Don't use Hot utilities below.

4. Design for maximum energy recovery (MER)

The data in Table 1 were analyzed by the Problem Table method with the result that the minimum utility requirements are 8419.07 kW hot and 66275.62 kW cold. The pinch occurs where the hot streams are at 423^0 C and the cold at 413^0 C.

Briefly this design was produced by

- Dividing the problems at the pinch, and designing each part separately.
- Starting the design at the pinch and moving away.
- Immediately adjacent to the pinch, obeying constraints:
- $CP_{HOT} \leq CP_{COLD}$ (above pinch temp)
- $CP_{HOT} \geq CP_{COLD}$ (below pinch temp)
- Maximizing exchanger loads.
- Supplying external heating only above the pinch, and external cool below the pinch.

Finally the problem is resulting on a sheet for MER (Maximum Energy Recovery), considering steam splitting for necessary conditions, trading off energy & targeting for minimum number of units, energy relaxation and breaking loops is shown in fig. 6

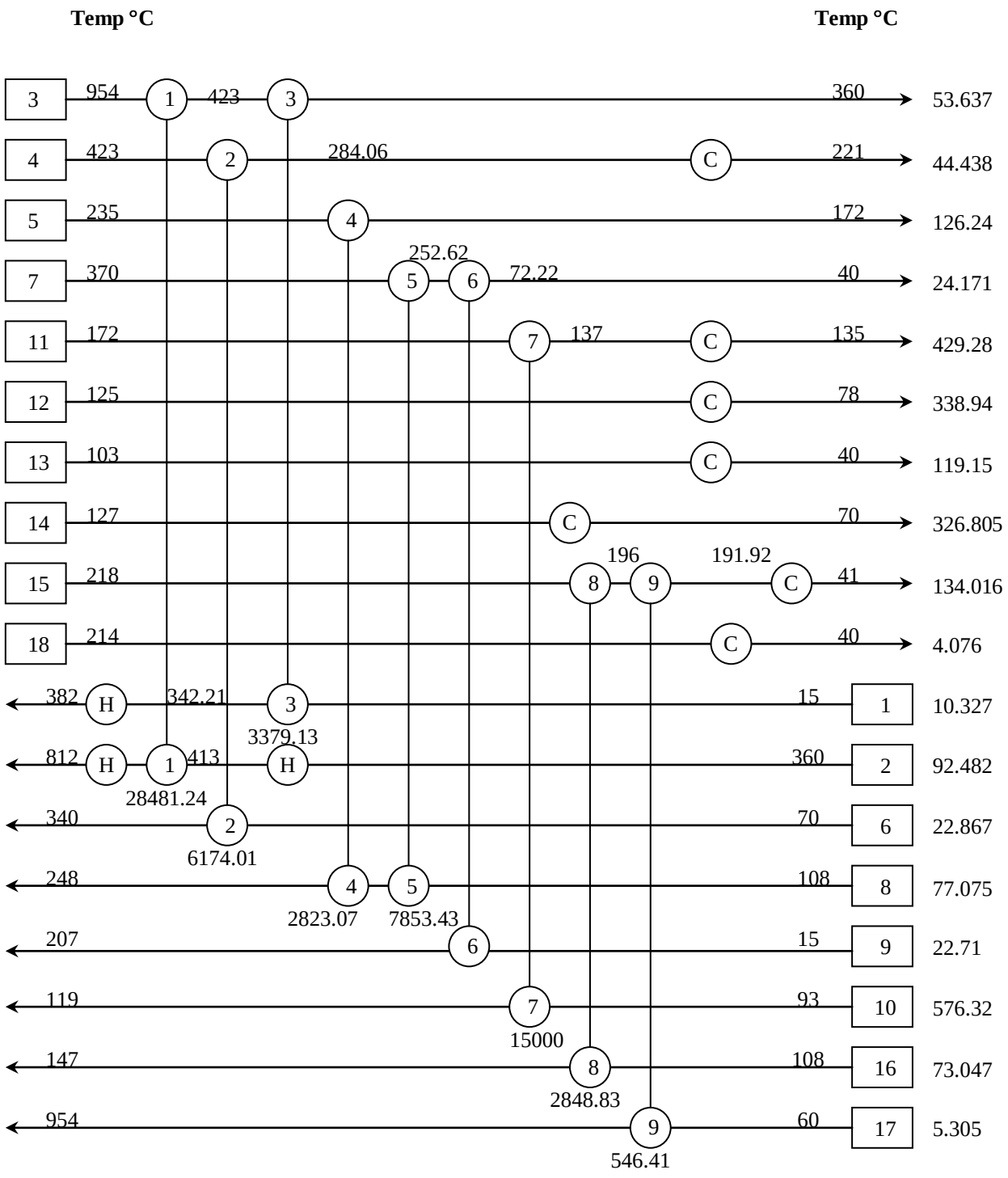

Fig.6 Optimum Network Diagram for HEN

5. Conclusion

Comparing both existing and new designed network, following conclusions can be made:

1. Hot utility load of 49953.48 kW (in existing network) is reduced to 13731.9 kW; this will decrease overall running cost of plant significantly.
2. Cold utility load of 54255.81 kW (in existing network) is increased to 67432.01 kW, but running cost will not effect much as cold water is freely available.
3. Number of heat exchangers used in network is reduced from 23 to 20 in new design, resulting in less capital cost and complexity.

6. Acknowledgements

The authors wish to express their sincere thanks to Gujarat State Fertilizer Corporation Limited (GSFC Ltd.) for granting permission and coordination for the present work.

7. REFERENCES

[1] B. Linnhoff, New concepts in thermodynamics for better chemical process design, Chem. Eng. Res. Des., 61, p207-223, 1983.
[2] B. Linnhoff and E. Hindmarsh, The pinch design method for heat exchanger networks, Chem. Eng. Sci., 38,5, p745-763, 1983.
[3] D. Boland and B. Linnhoff, The chemical engineer, 343, 222, 1979.
[4] D. W. Townsend and B. Linnhoff, Heat and power network in process design, AIChE J., 29,5,p742-771(2-parts),1983.
[5] R. A. Bowman et al Trans. ASME, 62, 283, 1940.
[6] F. J. Steinmetz and M. O. Chaney, Total plant energy integration, CEP, p27-32, july, 1985.
[7] B. Linnhoff and S. Ahmad, SUPERTARGETING: Optimum synthesis of energy management systems.
[8] Dr. A. K. Saboo, Pinch technology-theory into practice, sep. 1996.
[9] E. Chem. User guide on process integration for the efficient use of energy, 1982.
[10] B. Linnhoff and J. A. Turner, Heat recovery networks: New insights yield big saving, imperical chemical industries ltd.
[11] Y.K.Rastogi, Chemical industry digest: Special issue on energy conservation, October, 1994.
[12] A. M. Whistler, Heat exchangers as money makers, petroleum refiner, 27,1,p83-86, 1948.
[13] A. Saboo, Improved utility and cost targeting for heat exchanger networks.
[14] E. C. Hohmann, Optimum Networks for heat exchange, Ph.D. Thesis, University of Southern California, USA, 1971.
[15] J. L. Su, A loop-breaking evolutionary method for the synthesis heat exchanger networks, M.S. Thesis, Washington University, USA, 1979.
[16] S. P. Patel, Pinch technology used for heat exchanger network, M.E. Thesis, M.S. University, India, 1999.

Effect of tooth deformation on contact ratio and tooth stresses in plastic spur gears

Rudresh Makwana

Email: rudresh_makwana@yahoo.com

Mechanical Engineering Department, Silver Oak College of Engineering & Technology, Ahmedabad

Abstract:

This paper deals with the effect of deformation on contact ratio and stress behavior of plastic spur gear. It is shown that when one tooth of gear comes into contact with pinion tooth it gets some amount of deformation and due to this deformation the behavior of second tooth coming in contact changes and it also affects the contact ratio. The contact ratio in actual practice differs from the theoretical results. For getting deformation and stresses on gear tooth FEA is done. Results obtained indicate that in actual practice contact ratio is higher compared to the theoretical results in case of plastic gears.

Keywords: Plastic spur gear, contact ratio, tooth deformation

1. Introduction

Plastic gears are widely used now in many applications like electronic power steering, robots. It needs to understand the behavior of plastic gears as it is significantly different than metal gears. As modulus of elasticity of plastic gears are much less compared to metal gears their behavior changes as compared to metal gears. Because of the low elasticity the amount of deformation in plastic gears are much higher than metal gears. In metal gears the deformation are very less. We can say it is negligible in metal gears, while in case of plastic gears the deformations are high. As the gear tooth in contact deforms it will affect the behavior of the next tooth coming into contact.

In the proposed work, one initial position of gear is taken as the case 1, and then rotation of some degree is given in each case and the deformation on first tooth which is in contact and stresses on second tooth is obtained. These cases are taken as the cases in which effect of deformation on first tooth is not considered on second tooth. Contact ratio is calculated for the cases which is theoretical contact ratio. After finishing, new cases are taken in which deformation on first tooth is taken into consideration for finding contact points on second tooth and then again the stresses are obtained. The stresses obtained by both method, one without taking into consideration the effect of deformation and second by taking into consideration the effect of deformation are compared. The actual contact ratio is obtained in the second method.

1.1. Theoretical and actual contact ratio

The figure 1 given below shows the path of contact while gear rotation. The line passing through A an A' is line of action which is cutting the addendum of gear and addendum of pinion at A' and A respectively. This distance AA' is the distance through which the tooth remains in contact. In other words when the contact between the tooth of pinion and gear starts at the point when the addendum of gear crosses the line of action which is point A' and the contact ends at the point when the addendum of pinion crosses the line of action which is point A. So we can say that AA' is length of contact.

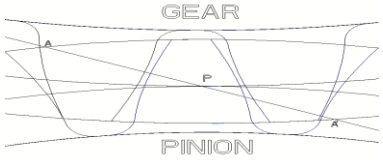

Fig. 1 line of action

The line passing through A an A' is line of action which is cutting the addendum of gear and addendum of pinion at A' and A respectively. This distance AA' is the distance through which the tooth remains in contact. In other words when the contact between the tooth of pinion and gear starts at the point when the addendum of gear crosses the line of action which is point A' and the contact ends at the point when the addendum of pinion crosses the line of action which is point A. So we can say that AA' is length of contact.

The path of contact consists of two parts one is path of approach and second is path of recess. These two paths are divided by pitch point P. As per the definition the contact ratio is ratio of length of contact to base pitch, so from figure it can be stated that contact ratio = AA'/ $P_{b.,}$ where $P_{b=}$ base pitch.

1.2. Deformation in gear tooth

When the gears are rotating they are transmitting power and forces like tangential, normal, radial, acts upon its tooth. Due to these forces gears deform at the point of contact. However in most of the cases this deformation is very minor and within elastic limit, but it affects the behavior of the gear tooth.

In the figure both, the original and deformed profile of a tooth is shown. The circle indicates the deformation in tooth 1 due to loading. This deformation causes the next tooth, tooth 2 to come into contact earlier. That means if the deformation is not considered the length of action would be AA', but if we consider the deformation the length of action is changed compared to AA' because the tooth 2 comes in contact with corresponding pinion tooth before the point A.

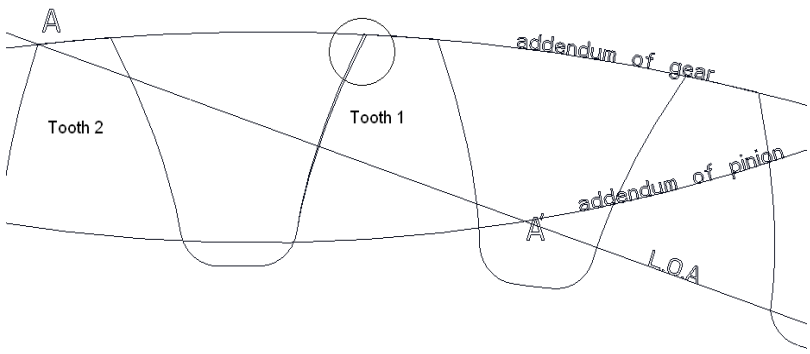

Fig. 2 Tooth deformation

2. FEA of plastic spur gear with and without effect of deformation

2.1 Material properties and dimensions of the gear

Material considered is Sustamid 66 which has following properties,

Table 1 Material Properties

Material Name	Sustamid 66
E (Modulus of Elasticity)	3200 Mpa
V (poission's ratio)	0.35
Yield point	85 Mpa

Table 2 Dimensions of gear

pressure angle	20°
Module m	6 mm
Addendum a	5 mm
Dedendum d	6.5 mm
Zg	44
N	500 rpm

2.2 Contact points

As per the dimensions of gear a 2d sketch is prepared according the geometry of gear. The involute were sketched by the usual method. The gear profile was put in position where the first tooth contact begins. It is as given in figure 3.

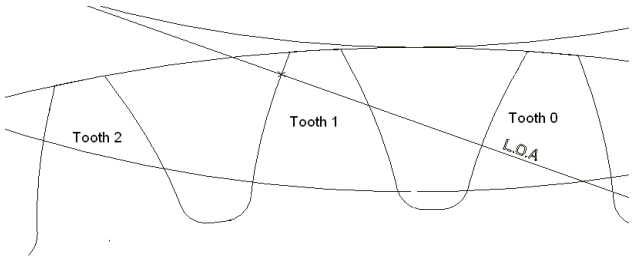

Fig. 3 contact points

The line of action crossing the tooth profile gives contact point at the particular position. In figure that is shown by a marked point on tooth 1. Here two teeth are in contact tooth 0 and tooth 1,it was assumed that gear starts rotating from this position. After getting the point the co ordinates of the point were found, this point was taken as first point of contact. For all 2d sketching, sketcher module of Pro-E was used.

2.3 Calculation of transmitted load

While gear when a single pair of teeth is engaged, this pair transmits the full load or the full load is then applied on the one meshing tooth only. When double pair of teeth are engaged, the transmitted load will be divided between two meshing teeth.

Torque transmitted $T = P/\omega$ (1)

The normal load applied on meshing teeth can be found as following

$F = T/r_b$, Where $r_b = r.\cos ø$ (2)

The stress analysis problem in this study is assumed as a plane elastic problem, since the applied transmitted load is assumed to be distributed uniformly across the width of the meshing tooth. Therefore the load had been depended per unit width of tooth as following

$F_n = F/b$ (3)

The component (F_x) and (F_y) will be

$F_x = F_n . \cos ø$, (4)

$F_y = F_n . \cos ø$ (5)

2.4 Finite Element Analysis

Analysis of each case was carried out in ANSYS by applying appropriate boundary conditions, loads and then solving it. The model was eliminated from whole gear to the three tooth gear to reduce calculation time.

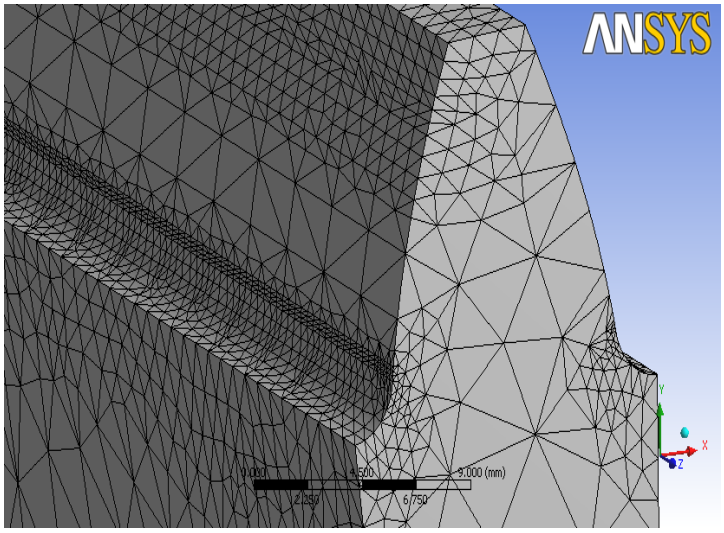

Fig. 4 Meshing

Mesh Refinement was given at the needed areas as shown in Fig. 4. The calculated load was applied on the contact line and results were obtained.

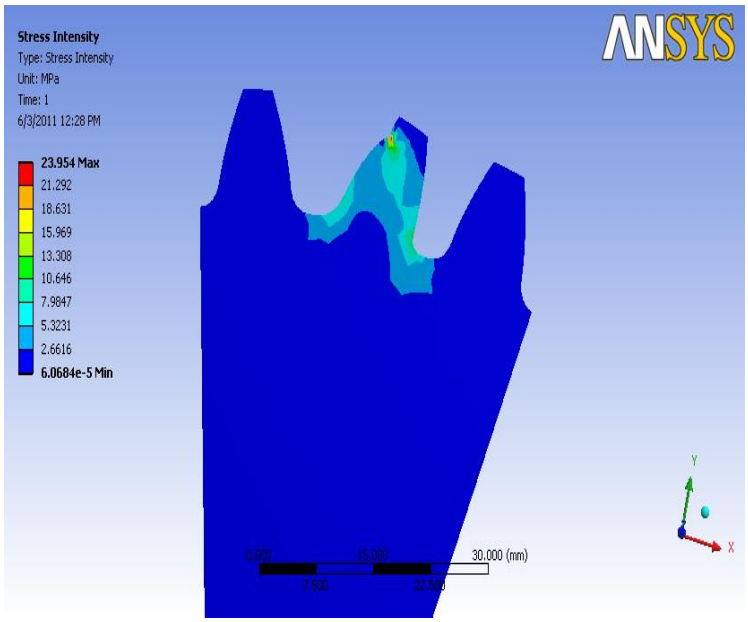

Fig. 5 Results in ANSYS

In the same manner the contact points and stresses on tooth 2, taking into account the deformation on tooth 1 are obtained.

3. Contact ratio calculations

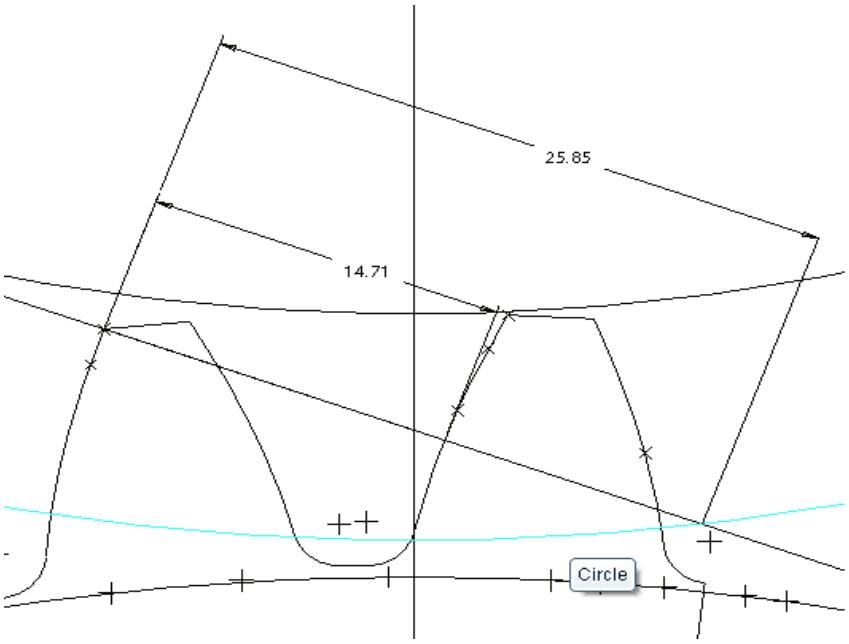

Fig. 6 Length of path of contact

The figure above shows the length of path of contact when deformation is not considered. And the figure below shows the length of path of contact in actual action.

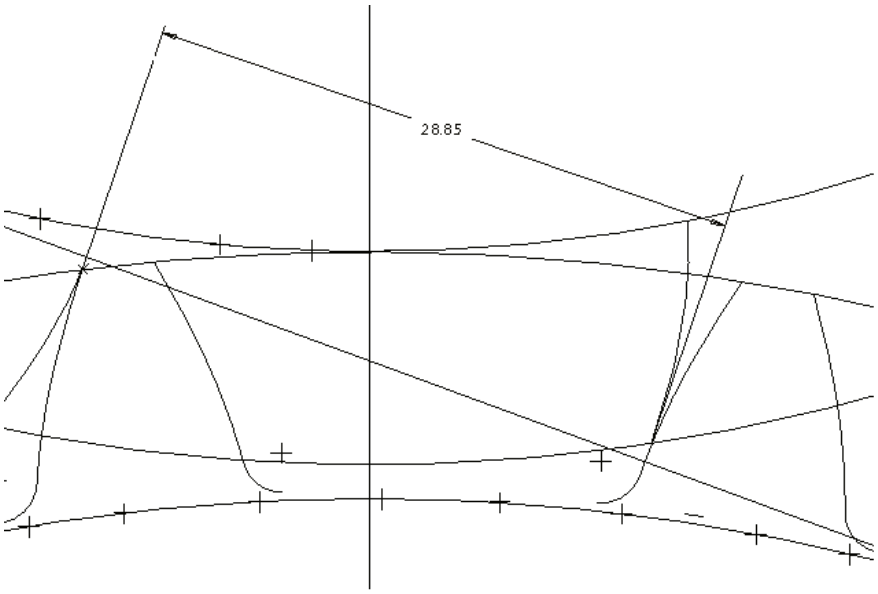

Fig. 7 Actual contact length

The stresses are obtained for both cases, one without the effect of deformation and second with the effect of deformation. For both the cases stresses induced in the tooth 2 were different. This difference was because of different contact points and different loading.

Series 1 shows stresses (MPa) on tooth 2 without effect of deformation on tooth 1

Series 2 shows stresses (MPa) on tooth 2 with the effect of deformation on tooth 1

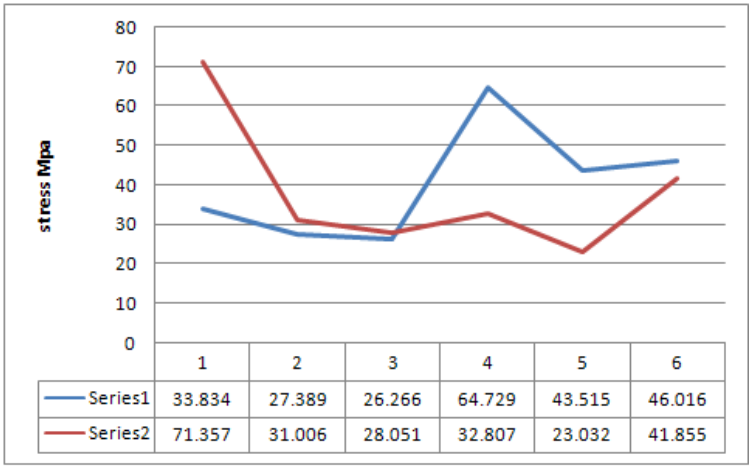

Fig. 8 stress plot

The contact ratio with effect of deformation is 1.9532 which is higher than the theoretical one which is 1.7508. This difference in contact ratio is because of the increased time of contact resulting from the deformation. These results show the actual contact ratio and stresses are different than the theoretical ones.

REFERENCES

[1] Ali Raad Hassan, 2009 - Contact stress analysis of spur gear teeth - world academy of science, engineering and technology.

[2] Alexander L. Kapelevich and Roderick E. Kleiss, 2002 – Direct gear design for spur and helical involute gears- Gear technology.

[3] Dr. Eng. Dimitrov L and De. Eng. Kovatchev I. -A computer model for determination of spur gear- teeth contact fatigue life.

[4] Sabah M.J.Ali, Load sharing on spur gear teeth and stress analysis when contact ratio changed.

[5] Evgueni Pdzharov, Almantas Mozuras – Design of high contact ratio spur gears cut with standard tools.

[6] Earle Buckingham – Analytical Mechanics of Gears

[7] Gitin M Maitra – Handbook of Gear Design

[8] H.E.Meritt – Gear Engineering

[9] Dudley – Handbook of Gear Design

Effect of Exhaust Back Pressure on Engine Performance by Altering Exhaust Manifold Position

Twinkle Collerwala

Email: twinkle_panch@yahoo.com

Mechanical Engineering Department, Silver Oak College of Engineering & Technology, Ahmedabad

Abstract:

The automobile plays an important role in the transport system of India. With increase in population and living standard, the vehicle population also increasing day by day. There is steep increase in the number of two wheelers during the last few years. All this are increasing exhaust pollution and particularly in metros as density of these vehicles is very high. As we know, more the emission, more the amount of fuel we have to burn in engine. Fuel consumption is directly depends on working conditions of an engine. Particularly for two wheelers, an extensive analysis of energy usage and pollution shows alternative power systems are still a long way behind the conventional ones. Therefore, all effort should be made to develop better engines in which specific fuel consumption should be less and also equipped with methods to reduce the pollution. The scavenging efficiency of engine is directly affected by speed of the engine, exhaust valve opening, and exhaust port dimensions, exhaust pipe location and position, dimensions of catalytic converter, muffler design. These all parameters are finally affect the back pressure of exhaust. So, this paper will help us to recognize the optimization of exhaust manifold to generate appropriate back pressure for particular two wheeler engine to reduce exhaust emission and improving fuel consumption.

Keywords: back pressure, manifold angle

1. Introduction

Research in three-dimensional manifold shapes by the unstructured, unsteady Euler code coupled with the empirical engine cycle simulation code had done. The result suggested that the pipe radius is important to improve the exhaust gas temperature and pressure. [1]

Conclusion was made by placing the catalytic converter downstream at the exhaust pipe, decreases the exhaust temperatures and pressure. No significant change was noticed in the volumetric efficiency. On the other hand, the brake specific fuel consumption increases, and the unburned hydrocarbon emissions decrease. [2]

Effect of Gas dynamics in the exhaust system of internal combustion engines had developed. They had developed the relation of volumetric efficiency and exhaust length. This relationship is illustrated in following figures.

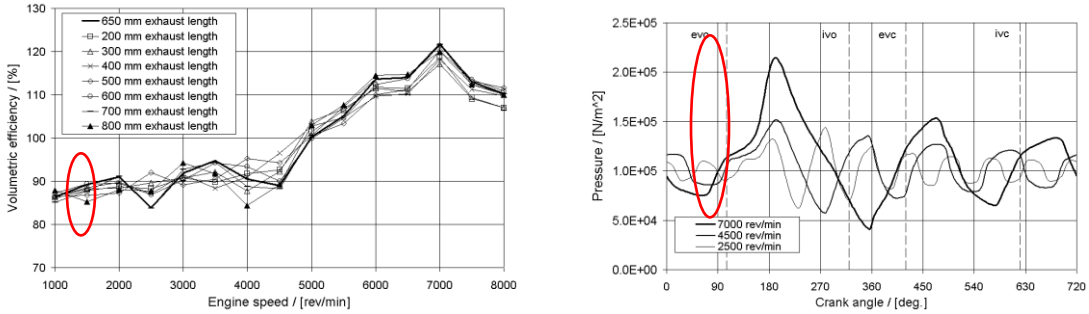

Fig.1 Variation of volumetric efficiency with engine speed for various exhaust pipe lengths

Above graphs show that the variation in pressure due to varying length of exhaust pipe affects the volumetric efficiency considerably. [3]

Investigation in the conversion efficiency of catalyst with the increase of catalyst length had done. The change in length is more important for short converters and it becomes gradually less important for long converters. Keeping other parameters constant, increasing the length of long converters may even have an adverse effect on the conversion efficiency and flow because of increased back pressure. [4]

Research work on designing of exhaust system design based on heat transfer computation had performed in 1999. According to their research the exhaust gas flow in the exhaust system is unsteady and compressible. The flow condition at each location is described by three independent parameters, namely velocity, density and back pressure. The following exhaust system design parameters they had optimized to get appropriate flow. [5]

- Exhaust manifold material, thickness and insulation
- Exhaust manifold and downpipe design (geometry)
- Position of catalytic converter in gasoline engines
- Position of particulate trap in Diesel engines

Research on optimal design of automobile exhaust system had done in 2007. The newly designed exhaust manifold shows lower back pressure which ultimately results better performance of the engine. They concluded that by reducing the angle of bend pipes, the back pressure reduced so that the exhaust gases removed easily from the engine cylinder and thus gave better breathing capability to the engine. [6]

The Effect of Exhaust Manifold Design on the Motorcycle Gasoline Engine Combustion Characteristics was examined. They had proved that the engine's volumetric efficiency can directly affect the engine's output and the emission levels. This research was done to modify the intake and exhaust manifold to understand the pipe boundary layer effects on the air's resistance entering the engine and the engine performance. These improved designed of intake and exhaust manifold resulted in good volumetric efficiency and lower back pressure. They concluded that the back pressure in the exhaust pipe can severely affect the intake flow characteristics. [7]

Work on increasing the combustion efficiency of the engine by reducing the backpressure in the exhaust manifold using Computational Fluid Dynamics was done in 2009. They have proved that the exhaust gas back pressure directly affects the combustion efficiency and volumetric efficiency of the engine.

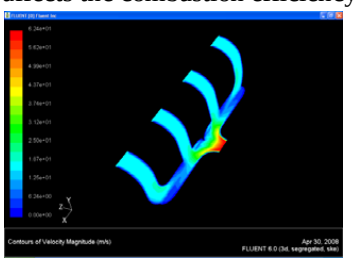

Fig.2(a) Existing Manifold

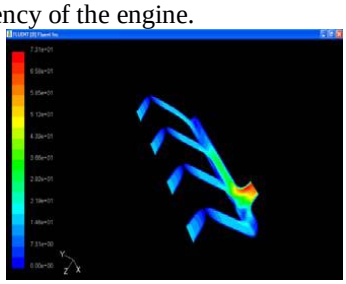

Fig.2(b)New Manifold Design

They observed that flow in a real exhaust port can easily be sonic with choked flow occurring and even supersonic flow in areas. The very high temperature causes the viscosity of the gas to increase, all at which alters the Reynolds number drastically. So by decreasing the back pressure in certain limit, they improved the volumetric efficiency as well as combustion efficiency. [8]

The research on optimization of exhaust system parameters for fuel economy improvement of small gasoline engine was done in 2008. The effects of exhaust pipe length and exhaust valve timing on the fuel economy performance of small gasoline engine were investigated based on thermodynamic cycle simulation. The calculation results demonstrated that the exhaust pipe length and exhaust valve timing exert great influences on the engine efficiency, mean pressure loss for gas exchange and indicated specific fuel consumption. [9]

2. Experiment Set Up

Definition of the core work could be given as a characterization and performance measurement of high speed, 4 stroke, Petrol engine for different exhaust manifold back pressure values. These values of back pressure have been generated by changing the angle of opening of exhaust manifold. The increment of opening angle had considered in clockwise direction as shown in fig 3.

Fig.3 Exhaust opening angle configuration

Fig 3 also shows the original position provided by the company and first performance and characterization was done with the same configuration to get standard performance data. The center for exhaust rotation has been chosen between muffler and catalytic converter same as shown in Fig 3. This would avoid difference in back pressure value arises because of catalytic converter.

The dynamometer was directly connected to engine crank shaft through universal coupling. The magnet mounting nut was used to couple the crank shaft to the dynamometer.

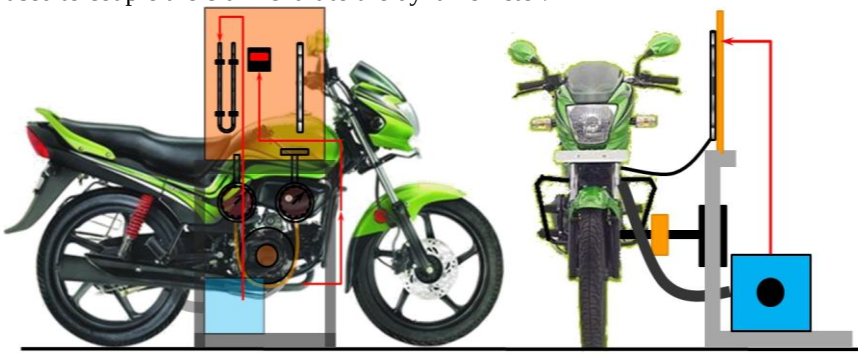

Fig.4 Schematic of entire experiment

Fig. 4 shows the experimental set up. The Rope brake dynamometer was used to load the engine. Universal joint was used to couple the dynamometer to engine. It also helped to eliminate the alignment difference between two shafts. The control panel contained manometer, digital temperature gauge and burette.

3. Results

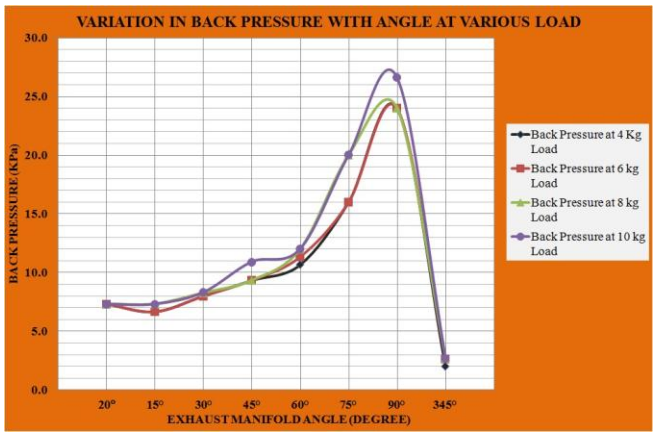

Fig.5 Variation in back pressure with Manifold Angle for 3000 RPM

Fig 5 shows the variation in back pressure with respect to different exhaust manifold angles at 3000 RPM. The standard value obtain for 20° is 7.3 KPa. As the angle decreases to 15°, back pressure reduces to 6.7 KPa. Afterward the back pressure increases as the angle increases by 30°, 45°, 60°, etc. Back pressure value suddenly increases at an angle of 75° and turn into maximum at 90°. Average value of back pressure at 90° is 24.7 KPa. This value is approximately 3.2 times more than the standard value. This rise in back pressure is result from chocking of exhaust gas flow. The velocity of gases decreases because; exhaust gas has to move through the gradient given to the manifold. As velocity decreases, pressure of flow increases. As an effect, back pressure on the engine also increases. Back pressure again decreases for 345° and settled at 2.7 KPa.

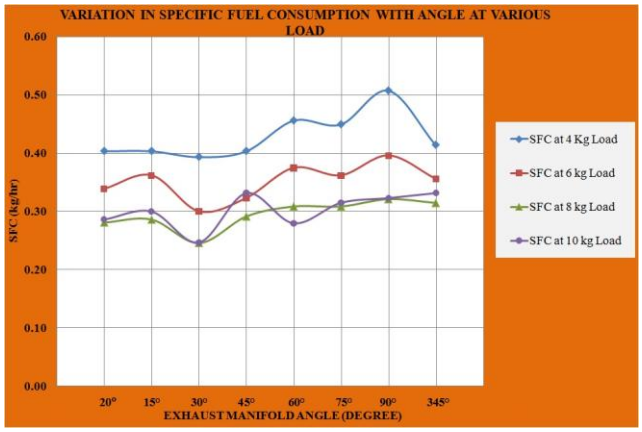

Fig.6 Variation in SFC with Manifold Angle for 3000 RPM

Fig 6 demonstrates the variation in SFC with respect to altering manifold angle at 3000 RPM. Lowest SFC indicates the best operating conditions for the engine. At 4 kg load, the value of SFC for 20° is 0.40 kg/ kW-hr. Minimum value of SFC is 0.39 kg/ kW-hr at 30° which indicate the best operating circumstance for the engine. Subsequently, the SFC increases with increased manifold angle and becomes maximum at 90° (0.51 kg/ kW-hr). That means the value of back pressure at 30° is providing the minimum SFC at 4 kg load. At 6 kg and 8 kg loads, curves behave just the same as for 4 kg load. Maximum SFC attained at 90° and minimum at 30°.

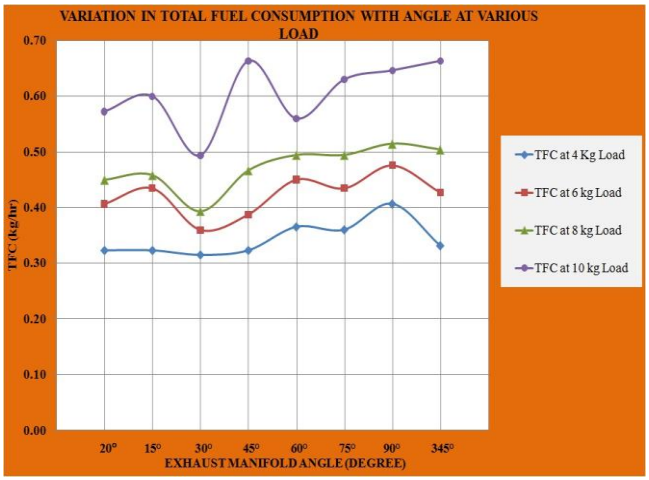

Fig.7 Variation in TFC with Manifold Angle for 3000 RPM

Fig 7 exhibits the variation in TFC with respect to altering manifold angle at 3000 RPM. Lowest TFC indicates the best operating conditions for the engine at constant load for 1 hour. The value of TFC for 20° is 0.32 kg/hr. Minimum value of TFC is 0.315 kg/ hr at 30° which indicate the best operating circumstance for the engine.

Subsequently, the TFC increases with increased manifold angle and becomes maximum at 90° (0.41 kg/hr). That means the value of back pressure at 30° is providing the minimum TFC.

4. Conclusions

- The standard value of back pressure obtain for 20° is 7.3 KPa for 3000 RPM. It nearly remains constant for each loading condition.
- The value of back pressure for 90° is approximately 3.2 times more than the standard value at 3000 RPM.
- Back pressure value increases 0.08 KPa with increase in manifold angle by 1°. This nature of back pressure is applicable up to 60°.
- After 60°, the increase in back pressure turns out to be 0.44 KPa with 1° rise in manifold angle.
- SFC increases 2.44 gm/kW-hr with increase in manifold angle by 1° at 3000 RPM.
- TFC increases 3.00 gm/hr with increase in manifold angle by 1° at 3000 RPM.
- η_B decreases 0.17 % with increase in manifold angle by 1° at 3000 RPM.

REFERENCES

[1] Masahiro Kanazaki, Masashi Morikawa, Shigeru Obayashi and Kazuhiro Nakahashi, 2002, "Multiobjective Design Optimization of Merging Configuration for an Exhaust Manifold of a Car Engine", 7-8

[2] K.A. Rezk a, M. M. Osman b and M.N. Saeed, 2004, "Effects of engine operating parameters and catalytic converter position on engine performance and hydrocarbon emissions", 5-9, Alexandria Engineering Journal, Vol. 43 (2004), No. 3, 313-321

[3] R Pearson, M Bassett, P Virr, S Lever and A Early, 2006, "EXHAUST SYSTEM GAS-DYNAMICS IN INTERNAL COMBUSTION ENGINES", 7-9, Proceedings of ICES 06, ASME Internal Combustion Engine Division 2006 Spring Technical Conference, May 7-10, 2006, Aachen, Germany

[4] Tariq Shamim and Huixian Shen, 2001, "Effect of Geometric Parameters on the Performance of Automotive Catalytic Converters", 7-8, Department of Mechanical Engineering, The University of Michigan-Dearborn, Dearborn

[5] I.P. Kandylas, A.M. Stamatelos, 1999, "Engine exhaust system design based on heat transfer computation", 11-16, Energy Conversion & Management 40 (1999) 1057-1072

[6] A.K.M. Mohiuddin, Ataur Rahamn and Mohd. Dzaidin, 2007, "Optimal Design of Automobile Exhaust System Using GT- Power", 5-7, International Journal of Mechanical and Materials Engineering (IJMME), Vol. 2 (2007)

[7] Meng-Chien Li and Dr. Kou-Liang Shin, "Effect of Exhaust Manifold Design on the Motorcycle Gasoline Engine Combustion Characteristics", 46-54, Institute for Mechanical Engineering, National Yunlin University of Science & Technology

[8] P. Gopal, T. Senthil Kumar and B. Kumaragurubaran, 2009, "Analysis of Flow Through The Exhaust Manifold of a Multi Cylinder Petrol Engine for Improved Volumetric Efficiency", 9-12, International Journal of Dynamics of Fluids, ISSN 0973-1784 Volume 5, Number 1 (2009)

[9] Peng He, Yunqing Li and Lifeng Zhao, 2008, "optimization of exhaust system parameters for fuel economy improvement of small gasoline engine", 3-7, Int.J. Thermodynamics.

Piezoelectric Gyroscopes: A review

[1]Jagat Shah, [2]Ishan Thakar

Email: jagat_sha@yahoo.com
Email: ibthakar@gmail.com

[1]Mechanical Engineering Department, Silver Oak College of Engineering & Technology, Ahmedabad
[2]Mechanical Engineering Department, Silver Oak College of Engineering & Technology, Ahmedabad

Abstract:

Piezoelectric plate gyroscope is a great improvement to the spinning mass gyroscopes because there is no wear, greater reliability and smaller size and weight. It is sensitive Device suitable for micro devices which can be easily incorporated with IC. Discussion is about the construction & working of the piezoelectric plate gyroscope with its merits over other types. It works on the piezoelectric principle in Which piezoelectric plate is used which is simple in design. Also the fabrications of such types of plate are discussed. At last the workings of PZT plate with different attributes with readings have been discussed.

Keywords: Gyroscope, Laser, MEMS, Piezoelectric, Vibrations

1. Introduction

In order to understand the mems gyroscope we first discuss the gyroscope in general & its engineering applications. Gyroscope is a spinning object which is free to rotate in any other direction. Whenever the object is spinning in a plane yz about an axis ox and that axis of spinning is made to process in another perpendicular plane xz couple is induced across the axis of spin in a third mutually perpendicular plane.

The more traditional spinning gyroscope was invented in the early 1800.s, and the French scientist Jean Bernard Leon Foucault coined the term gyroscope in 1852[1]. In the late 1800.s and early 1900.s gyroscopes were patented for use on ships. Around 1916, the gyroscope found use in aircraft where it is still commonly used today. Throughout the 20th century improvements were made on the spinning gyroscope. In the 1960.s, optical gyroscopes using lasers were first introduced and soon found commercial success in aeronautics and military applications.

2. Piezoelectric Gyroscope

2.1 Introduction

It is one of the MEMS Gyroscopes which use a PZT plate as its base. This method has been used to try to build macro-scale gyroscopes, is actually ideal for micro devices. At micro levels, an entire plate can be made of piezoelectric material. It has advantages over the common vibrating gyroscopes in that it requires a much smaller drive voltage to create readable outputs. [4]

2.2 Physical Description

The piezoelectric plate gyroscope is very simple in its design. . There is a piezoelectric plate, which has a length and width much larger than its depth. The plate has electrical leads connected to all 6 sides and sits on top of a thin membrane of a cavity in a silicon wafer. The cavity allows more freedom for the PZT to vibrate and deform. The leads provide the driving voltage and measure the output.

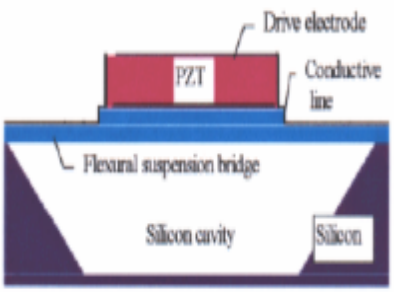

Fig.1 Cross Section of Gyroscope [3]

2.3 Fabrication

The following diagrams show a basic fabrication process that could be used to create the piezoelectric gyroscope.Fig.2 [3]

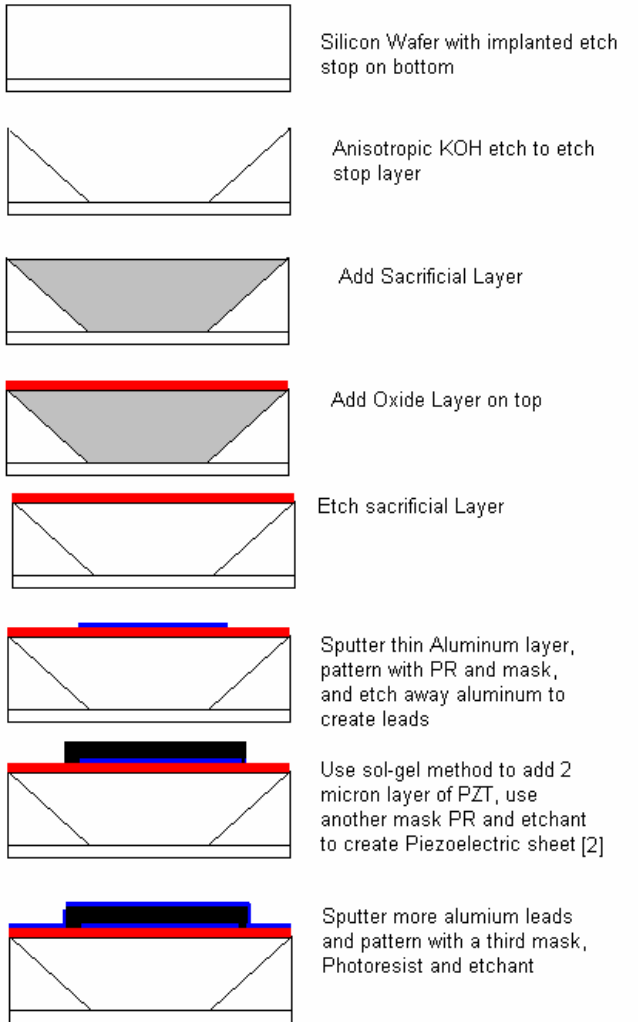

Fig.2

2.4 Functional Description

Like other MEMS gyroscope the piezoelectric plate gyroscope works on the principle of a vibrating body. In this case, the vibrating body is a piezoelectric sheet. The sheet does not vibrate like a plate or fork. Instead the Thickness vibrates which oscillates with time. This requires an AC driving voltage applied vertically across the plate, which uses the electro-mechanical properties of the PZT to create the vibration. Any piezoelectric material can be used, but PZT has high piezoelectric constants, and can be added at a precise thickness.

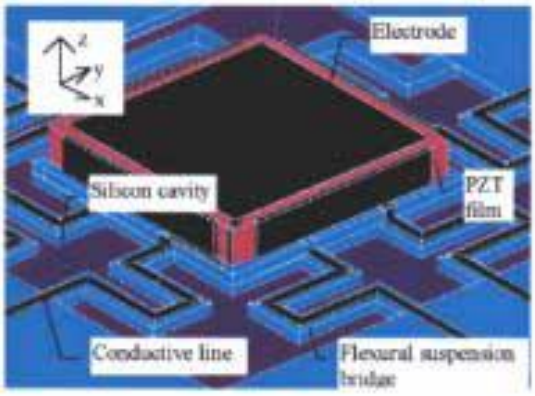

Fig.3 Piezoelectric Plate with orthogonal directions shown[3]

When the vibrating plate is rotated about an axis perpendicular to the drive voltage, a voltage is produced in the third perpendicular direction. This output voltage is proportional to the angular velocity. It can be proven that the relationship is

$$V_{Out} = -\frac{K}{\varepsilon_{11}^{T}}\frac{ac}{4}\left(d_{33} + |d_{31}|\frac{a^2}{c^2}\right)d_{15}$$
$$\cong \frac{V_A \rho\, \omega \cos\omega t}{\varepsilon_{11}^{T}}\frac{a^3}{4c}|d_{31}|d_{15}\Omega. \quad \textbf{[3]}$$

Here VA is the input voltage magnitude is the PZT density, ω is the input voltage frequency, t is time, a is the plate length perpendicular to the direction of rotation, c is the plate thickness, d31 and d15 are piezoelectric constants, ε11 is the permittivity constant and Ω is the angular velocity. Since the plate has x-y symmetry as shown above, it follows that a single plate can measure rotation in two directions. This is an added advantage when compared to traditional gyroscopes, which only measure one direction of rotation. Extensive testing has been conducted on piezoelectric plate gyroscopes and the following data has been determined. For a gyroscope with properties.[3]

Specifications	
Piezoelectric material	$Pb(Zr_{0.54}Ti_{0.46})O_3$
Density	7.5×10^3 kg m^{-3}
Piezoelectric constant d_{31}	700×10^{-12} m/V
Piezoelectric constant d_{15}	270×10^{-12} m/V
Permittivity $\varepsilon_{11}^T/\varepsilon_0$	3250
Plate length a	1000 μm
Plate width b	1000 μm
Plate thickness c	2 μm

The resulting attributes are as follows:

Measuring conditions and performance	
AC drive voltage V_A	1 V
Source frequency	100 kHz
Lock-in amplifier A_K	10 000
Thermal sensor noise	$< 1 \times 10^{-3}$ V
Maximum output voltage	5 V
Sensitivity ($A_K V_{out}/V_A/\Omega$)	0.0387 V/V/(deg/sec)
Accuracy	2.58×10^{-2} deg/sec
Range	129.2 deg/sec

Conclusion

The piezoelectric plate gyroscope is a feasible alternative to traditional MEMS gyroscopes. One of its advantages is a lower required drive voltage. However, the sensitivity is only about 38 microvolt, whereas the sensitivity of a ring gyroscope is around 200 microvolt [5]. Also, when there is no rotation, traditional gyroscopes come much closer to the ideal zero volts output than the piezoelectric plate gyroscope, which still outputs up to 100 mill volts. A major advantage and the one that could prove most practical is the versatility of the piezoelectric plate gyroscope. It can measure rotation in two directions. In addition, if the driving voltage direction is switched, the same device can measure rotation in the third direction, although with much less sensitivity. Since this device is easily incorporated into other IC chips, it could be controlled to do more things than a ring or tuning fork gyroscope, which require three gyroscopes to measure three rotation directions.

REFERENCES

[1] History of Gyroscopes, Glen Turner. 2004 (http://www.gyroscopes.org/history.asp)

[2] N. Yazdi, F. Ayazi, and K Najafi, .Micromachined Inertial Sensors,. *Proceedings of the IEEE*, Vol. 86, No. 8, (1998) 1640-1659.

[3] .Design and Analysis of a Micro-gyroscope with Sol.gel Piezoelectric Plate. Smart Material Structures. 1999 Vol. 8. 212-217. He, Nguyen, Hui, Lee, Luong.

[4] .Frequency locking and unlocking in a femtosecond ring laser with application to intracavity phase measurements. S. Diddams, B. Atherton, J.-C. Diels. Applied Physics B: Lasers and Optics Vol. 63 1996. p. 473-480

[5] .Micromachined Vibrating Gyroscopes: Design and Fabrication. Elliott, Gupta, Reed, Rodriguez. December 6th, 2002.

Emission analysis of single cylinder diesel engine fueled with sesame oil, diesel and its blend with ethanol

[1]Nilamkumar Patel, [2]Rupal Tank

Email: nilampatel_2008@yahoo.co.in
Email: rupaljtank@gmail.com

[1]Mechanical Engineering Department, Silver Oak College of Engineering & Technology, Ahmedabad
[2]Mechanical Engineering Department, Silver Oak College of Engineering & Technology, Ahmedabad

Abstract:

Recent decades continuous increased in the fuel price and fast depletion of the available fossil fuel reservoir, so it is necessary to find out the alternative fuel for the engine. Also global warming is becoming a problematic issued in the modern world .The use of vegetable oils as a fuel in diesel engines causes some problems due to their high viscosity compared with conventional diesel fuel. Various techniques and methods are used to solve the problems resulting from high viscosity. One of these techniques is fuel blending. In this study, a blend of sesame oil is in the various proportions like 20%, 30%, 40%, and up to 50% in the diesel fuel was used as an alternative fuel in a direct injection diesel engine. Find the optimum blend and add the ethanol in that blend in the 5%, 10%, and 15% find the emission characteristics .emission analysis were investigated and compared with the ordinary diesel fuel in a diesel engine. It is observed that the CO emission decreased with increase in sesame oil concentration in Diesel fuel but HC emission slightly increased .This can be minimized by adding the ethanol in the blend. It is concluded that it is possible to use Sesame oil in diesel engines as an alternate fuel in the future.

Keywords: Sesame oil; Ethanol; Emission characteristics.

1. Introduction

Now a day's Vegetable oils are the best alternative to diesel oil since they are renewable and have similar properties. Many researchers have studied the use of vegetable oils in diesel engines. Vegetable oils offer almost the same power output with slightly lower thermal efficiency when used in diesel engine [1-5]. It is known that the original diesel engine designed by Rudolph Diesel run with vegetable oil. Nowadays, vegetable oils are good alternative fuels to the fossil fuel and can be used instead of the ordinary diesel fuel as fuel in diesel engines [7, 8]. Vegetable oils have some merit as follows: they are renewable energy as the vegetables that produce oil are renewable, heat release rate is similar to diesel, its emissions (CO, HC and PM) rate is relatively low [6], they do not contain almost sulfur element, and they can be used with simple or without modifications in the diesel engine. The main problem of using neat vegetable oils as fuel in diesel engines is related to their high viscosity. The high viscosity generate the following problems in diesel engine; the choking of fuel lines and filters, poor atomization of the fuel, incomplete combustion, severe engine deposits, injector coking with trumpet formation and piston ring sticking, gum formation and thickening of the lubricating oil.

In order to solve these problems caused by the very high viscosity of neat vegetable oils, the following usual methods are adopted: blending in small blend ratios with normal diesel fuel, pre-heating, esterification. The blending method has the advantages of improving the use of vegetable oil fuel with minimal fuel processing and engine modification. Hence, mixing diesel fuel with vegetable oils with specific ratio reduces viscosity and consequently they can be used as alternative fuels in diesel engines. The main purposes of this study are to investigate the sesame oil - diesel fuel and ethanol blend as a fuel in a direct injection diesel engine and to determine engine performance and exhaust emissions characteristics. In the study, sesame oil is blended with diesel fuel at a various proportion like 20%, 30%, 40%, and 50% ratio on volume basis in order to reduce the high viscosity of sesame oil. Find the best suitable blend and add the ethanol in that blend. The experimental results are compared with those of ordinary diesel fuel.

2. Sesame oil

Soya bean oil is of primary interest as biodiesel source in USA, while many European countries use rapeseed oil, and countries with tropical climate prefer to use coconut oil or palm oil. Rapeseed oil has been grown in Canada since 1936. Hundreds of years ago, Asians and Europeans used rapeseed oil in lamps. Cottonseed oil is used almost entirely as food material. Sesame, olive, and peanut oil can be used to add flavor to foodstuff. Walnut oil is high-quality edible oil refined by purely physical means from quality walnuts. Poppy seeds are tiny seeds contained within the bulb of the poppy flower, also known as opium plant.

Dry oils such as Walnut, sunflower, safflower, dammar, linseed, poppy seed, and stillingia, tang, and vernonia oils are used for paint and wood-finishing applications. The solution to avoid twin problems of environmental pollution and energy shortage should be carefully planned gradual shift of our energy economy from fossil fuels to renewable sources of energy.

2.1 Property table

Table: 1 Comparison of sesame oil with diesel. [6]

Property	**Diesel**	**Sesame oil**
Heating value(KJ/Kg)	42900	39349
Viscosity(mm^2/s)	4.3(at 27 o C)	35.5 (at 38 o C)
Density (kg/l)	0.815	0.913
Cetane number	47	40.2
Flash point	58	260
Sulfar	< 0.01	0.01
Carbon residue(% by weight)	< 0.35	0.25

Property	**Diesel**	**Sesame oil**
Heating value(KJ/Kg)	42900	39349
Viscosity(mm^2/s)	4.3(at 27 o C)	35.5 (at 38 o C)
Density (kg/l)	0.815	0.913
Cetane number	47	40.2
Flash point	58	260
Sulfar	< 0.01	0.01
Carbon residue(% by weight)	< 0.35	0.25

3. Experimental setup

3.1 Engine set up

The schematic layout of the experimental set up is shown in Fig.1, and the specifications of the engine are shown in Table 2. The test engine used was a single cylinder, air cooled, direct injection stationary diesel engine. A Rope brake dynamometer was used to provide the engine load. A chromel alumel thermocouple, in conjunction with a digital temperature indicator, was used to measure the exhaust gas temperature. An air box and inlet manifold were fitted to the engine, and an air flow meter was used for airflow measurement. The fuel was passed from the fuel tank to the engine via the fuel injection pump and the fuel injector, and the fuel flow was measured on volumetric basis using a burette and a stopwatch. Initially, experiments were carried out using base diesel fuel. All the experiments were conducted at the rated engine speed of 1500 r.p.m.

Table: 2 Engine specifications

Parameter	Details
Engine	Single Cylinder High Speed Diesel Engine
Cooling	Water cooled
Bore × Stroke	80 mm × 110 mm
Compression ration	16 : 1
Maximum Power	5 hp or 3.7 kw
ated speed	1500 rpm
Capacity	553 CC

3.2 Test Procedure

In this experiments I use the diesel engine and it is connected with the rope break dynamometer with the help of dynamometer, varies the load on the engine or load remain constant .Gas analyzer is used to find the emission characteristic of exhaust gas. The reading takes by constant load or by varying the load on the engine using the dynamometer. Engine performance such as break power, indicated power, break specific fuel consumption etc find from the experiments .First only diesel fuel is used and engine performance is find .Then the blending of diesel and sesame oil at different proportion like 20%, 30%, 40% and 50% concentration in the diesel fuel takes and find the engine performance. By taking the analysis of the various blend of diesel and sesame oil it is shows that the best blend is to be S30 blend. After selecting the S30 blend as a best blend then ethanol is to be added in the 5%, 10% and 15% proportion in that blend and find the engine performance of diesel engine.

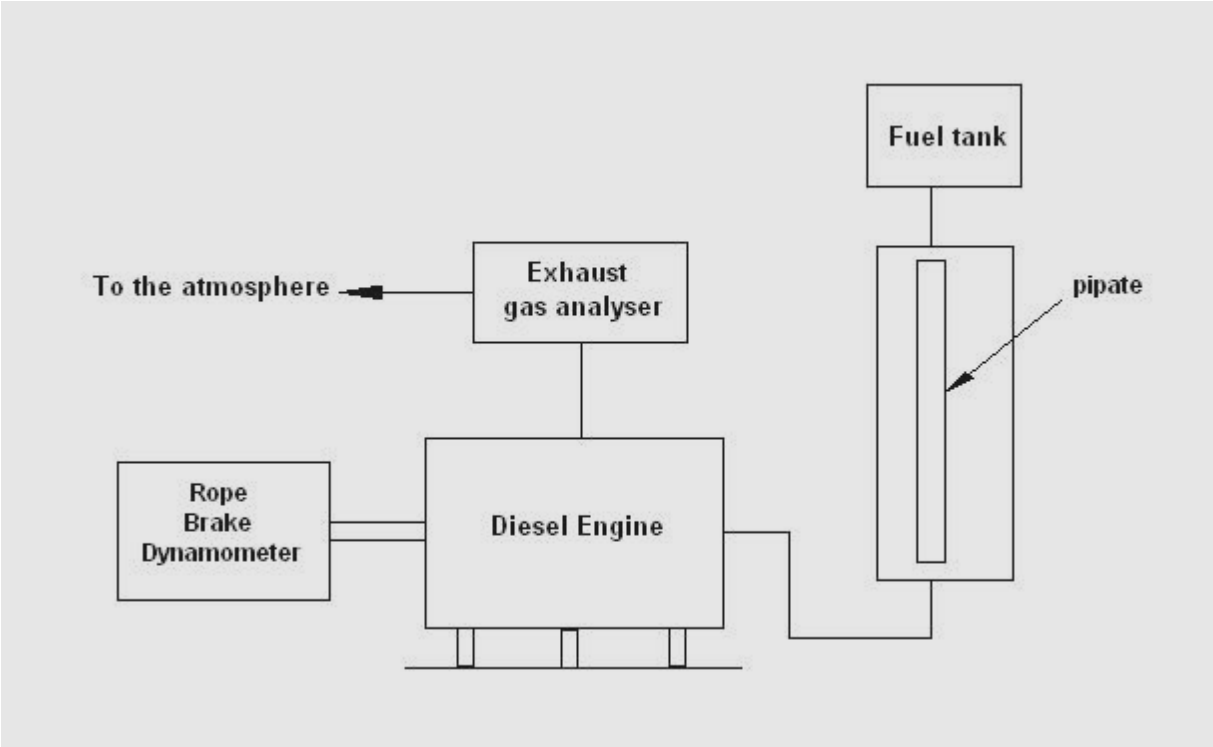

Fig. 1 Single cylinder diesel engine test rig with rope break dynamometer.

4. Results

4.1 Carbon Monoxide Emission:

The main reason of generation of CO emission is incomplete combustion and it is generally due to insufficient availability of oxygen. The graph shows that the CO emission reduced as the break power is increased.

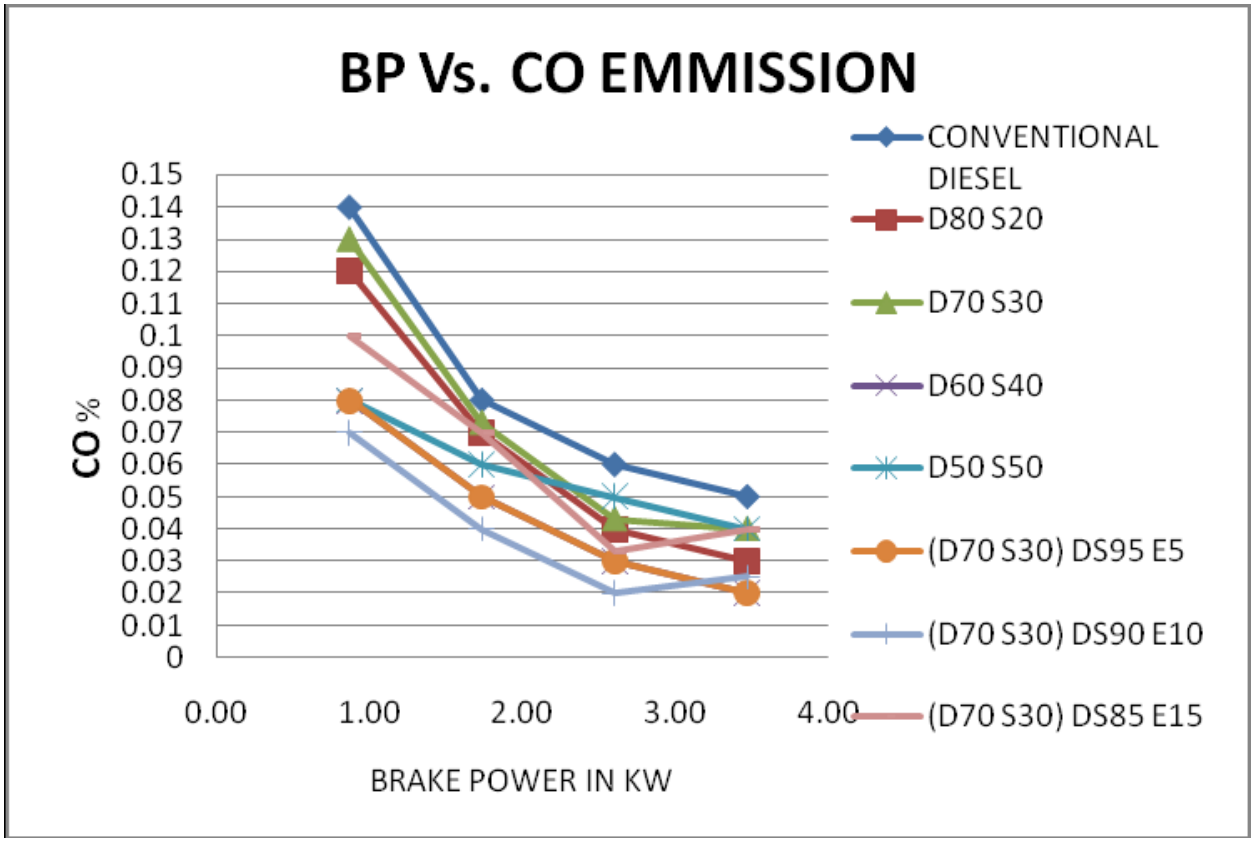

Fig.2 Effect of various blends on Carbon Monoxide Emission

At a full load condition the CO emission is minimum. As the percentage of sesame oil increased in the diesel fuel the CO emission decreased. By adding the ethanol in the proportion of 5%, 10% and 15% in the S30D70 blend the Co emission is less as compared to the diesel fuel.CO emission is minimum in the 10% ethanol blend with the S30D70 blend as compared to the diesel fuel.

4.2 Hydrocarbon Emission:

The hydrocarbon reacts with air to produce smog. This may reduce visibility. In conventional internal combustion engine the hydrocarbon fuel burns inside the engine in presence air. The amount of hydrocarbon fuel, which is not taking part in combustion process, is likely to come out as unburned hydrocarbon.HC

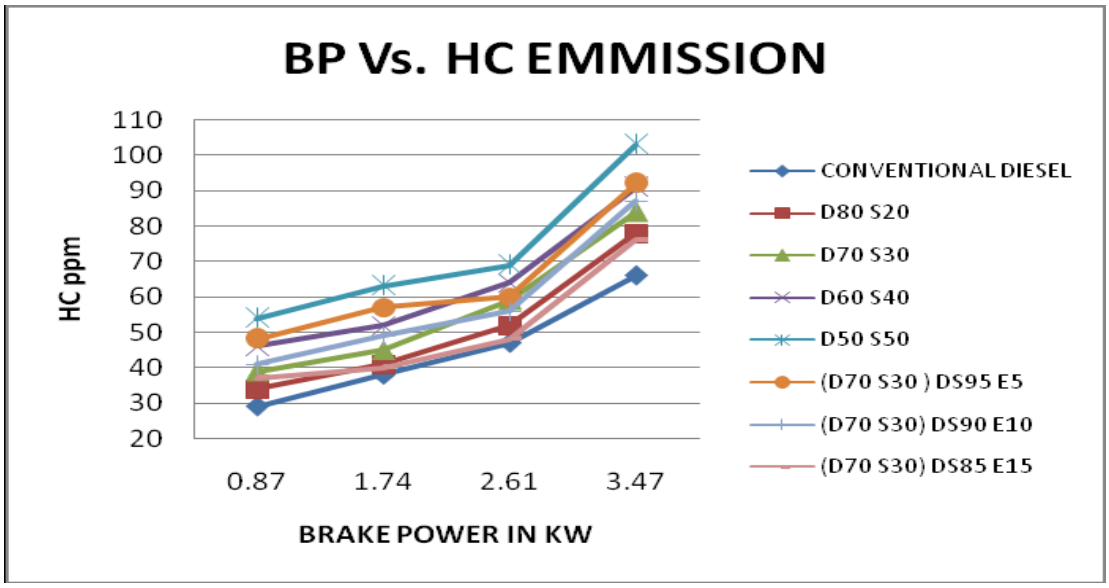

Fig.3 Effect of different blend on hydrocarbon (HC) emission.

HC emission increased with increased the sesame oil concentration this can be reduced by adding the ethanol in the blend. HC emission in the S30D70 blend have maximum but this can be minimize by adding the ethanol.

5. Conclusion

As sesame oil concentration increased in the diesel fuel the CO emission is reduced ,also by adding the ethanol in the S30D70 blend the CO emission further reduced compared to the diesel fuel.

The sesame oil reduced the CO but minor increased the HC which is reduced by adding the ethanol in the blend.

REFERENCES

[1] Srivastava A, Prasad R. Triglycerides-based diesel fuels. Renew Sustain Energy Rev 2000;4:111–33.

[2] Vellguth G. Performance of vegetable oils and their monoesters as fuels for diesel engines. SAE paper no. 831358, 1983.

[3] Demirbas A. Biodiesel production from vegetable oils via catalytic and non-catalytic supercritical methanoltransesterification methods.Int J Prog Energy Combust Sci 2005;31:466–87.

[4] Jajoo BN, Keoti RS. Evaluation of vegetable oils as supplementary fuels for diesel engines. In: Proceedings of the XV national conference on I.C. engines and combustion, Anna University, Chennai, 1997.

[5] N.R. Banapurmatha, P.G. Tewaria, R.S. Hosmath. Performance and emission characteristics of a DI compression ignition engine operated on Honge, Jatropha and sesame oil methyl esters. Renewable energy (2008) 1982–1988.

[6] S-ehmus Altun, Hu¨ samettin Bulut, Cengiz.The comparison of engine performance and exhaust emission characteristics of sesame oil–diesel fuel mixture with diesel fuel in a direct injection diesel engine. Renewable Energy 33 (2008) 1791–1795

[7] Choi CY, Bower GR, Reitz RD. Effects of biodiesel blended fuels and multiple injections on D.I. Diesel engine emissions. SAE paper, 1997, 970218.

[8] Graboski MS, McCormick RL. Combustion of fat and vegetable oil derived fuels in diesel engine. Prog Energy Combust Sci 1998;24:125–64.

[9] Rajashekhar s. Hosmath ,p. Mohanan. Evaluation of the performance and emission Characteristics of a 4-stroke single cylinder direct Injection diesel engine fuelled with sesame methyl Ester and diesel fuel blend san experimental investigation ICAER 2009.

Hardened properties of high Performance concrete

Anant Patel

Email: arp_925@yahoo.co.in

Civil Engineering Department, Silver Oak College of Engineering & Technology, Ahmedabad

Abstract:

Considering the economy and the durability of our present concrete structures, the quality and the density of the concrete cover, as well as the compaction of the concrete are main parameters. For this, Self-Compacting Concrete (SCC) offers new possibilities and prospects. As a result of the mix design, some properties of the hardened concrete can be different for SCC in comparison to normal vibrated concrete (NC). Therefore, it is important to verify the mechanical properties of SCC before using it for practical applications, especially if the present design rules are applicable or if they need some modifications.

Keywords: Super Plasticizers; Self-compacting concrete (SCC); Mix design; Compressive strength, Tensile strength; Rebound Hammer; Mix Design.

1. Introduction

Testing of Concrete in hardened states need to be carefully understood in order that adequate responses or proper corrective measures can be made to developing problems even before these develop. Oftentimes, the test results and what they tell the end user remain as merely test results because of a lack of understanding on what these test results are really indicating to us and how they could best be used or interpreted to result in adequate and timely corrective measures to address the problem. See fig-1 Self-Compacting Concrete (SCC) was first developed in Japan about 10 years ago in order to reach durable concrete structures. Since then, several investigations have been carried out to achieve a rational mix design for a standard concrete, which is comparable to normal concrete. Self-compacting concrete is defined so that no additional inner or outer vibration is necessary for the compaction. SCC is compacting itself alone due to its self-weight and is deaerated almost completely while flowing in the formwork. In structural members with high percentage of reinforcement it fills also completely all voids and gaps. SCC flows like "honey" and has nearly a horizontal concrete level after placing. SCC offers many advantages for the precast, SCC offers many advantages for the precast, prestressed concrete industry and for cast-in-situ construction SCC offers many advantages for the precast, SCC offers many advantages for the precast, prestressed concrete industry and for cast-in-situ construction.

- Low noise-level in the plants and construction sites.
- Eliminated problems associated with vibration.
- Less labor involved.
- Faster construction.
- Improved quality and durability.

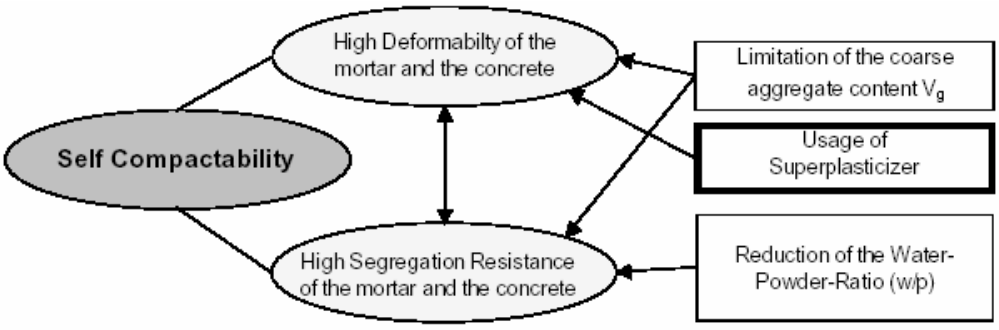

Fig.1 Typical Figure Showing SCC Nature

The objective of this paper is to study the Tensile Strength and Compressive Strength values of self compacting. Cylinder specimens were tested for Tensile and Compressive Strength after 28 days of standard curing, in order find out if self-compacting concrete would show an increase in these strengths and a better bonding between aggregate and cement paste, compared to normal concrete.

2. Self compacting concrete

Concrete that is able to flow under its own weight and completely fill the formwork, even in the presence dense reinforcement, without the need of any vibration, whilst maintaining homogeneity.(SCC = HPC)

Segregation Resistance (Stability)

The ability of SCC to remain homogeneous in composition during transport and placing.

Admixture

Material added during the mixing process of concrete in small quantities related to the mass of cement to modify the properties of fresh or hardened concrete.

Workability

A measure of the ease by which fresh concrete can be placed and compacted: it is a complex aspects of fluidity, cohesiveness, transportability, compatibility and stickiness.

Water/Cement Ratio

The water/cement ratio is the weight of the total amount of water relative to the weight of the total amount of cement used per cubic meter of concrete. In simple terms, the lower the water/cement ratio or the less water used for a ertain weight of Port in the mix, the better the concrete.

(SCC) of (stability) Combination of Portland cement

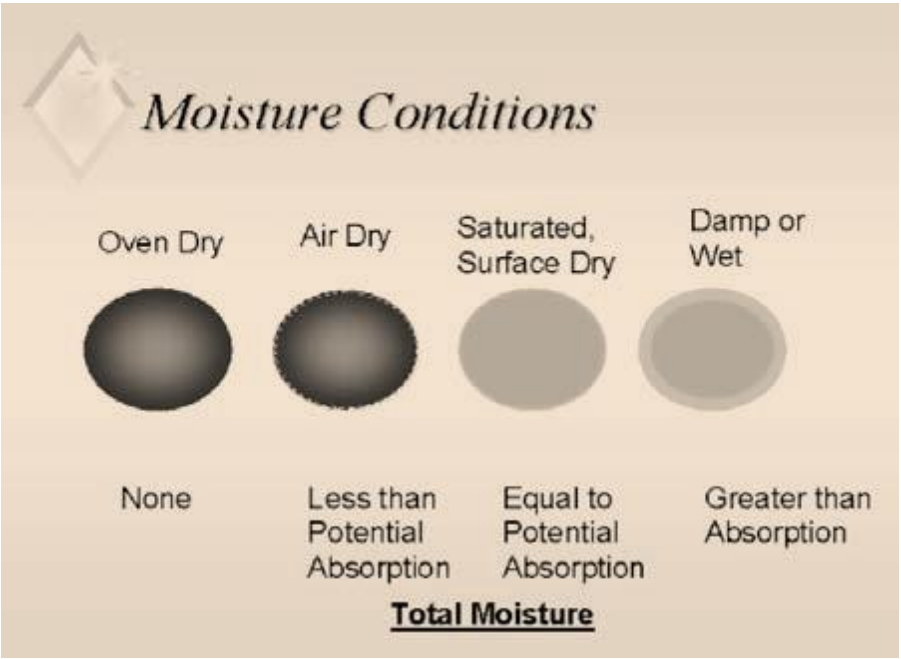

Fig.2 Moisture content

This is true to a point. Enough water is needed to be able to place and consolidate the concrete as well as achieve complete hydration reaction. The binding quality of the cement/water paste is due to the chemical reaction achieved when water is with cement. This reaction is called hydration. Very little water is needed for hydration. In fact, most concrete would look like a pile of rocks and be unworkable if the only water added was to hydrate the cement. Most of the water in concrete is "water of convenience" to help ease the task of placing concrete. The more water added to concrete the thinner the paste. The thinner the paste, the hardened concrete. The **Portland Cement Association** suggests using no more water than is absolutely necessary to make the concrete plastic and workable.

3. Super plasticizer

Super plasticizer (SP) is an essential component of SCC to provide the necessary workability. The super plasticizer to be selected should have:
(i) high dispersing effect for low water/powder ratio (less than 1 by volume),
(ii) maintenance of the dispersing effect for at least two hours after mixing,
(iii) less sensitivity to temperature changes.

The main purpose of using a super plasticizer produce flowing concrete with to be used in heavily reinforced structures and in places where adequate consolidation by vibration cannot be readily achieved. The other major production of high-strength concrete from 0.3 to 0.4.The ability of a super plasticizer to increase the slump of concrete depends on such factors as the type, dosage, and time of addition, w/c and the nature or amount of cement.

4. Double layer model

A "double layer" model explains the electrical repulsion mechanism and helps understand the definition of Zeta potential. A colloid (negative ion, co ion) will be surrounded by positive ions in the solution. The attraction from negative ion forces. See fig-2.

5. Plasticizer

Some of the positive ions to stick to its surface around colloid. This layer of counter ions is called "sternlayer".Additional positive ions are still attracted by the negative colloid, but with a small equilibrating force, and are now repelled by the stern layer counter ions and by other counter ions which are trying to approach the colloid.. Fig-3 presents the double-layer model.

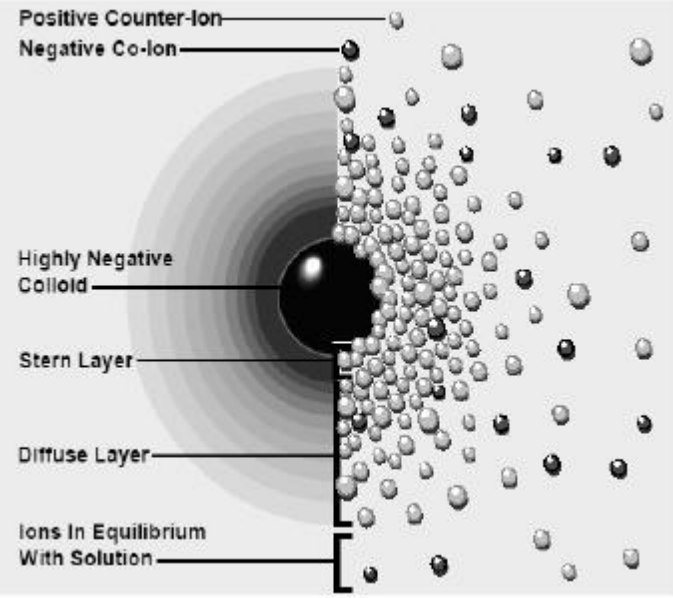

Fig.3 Double layer model

This dynamic equilibrium results in the formation of a "diffuse layer" of counter ions over-lapping the sternlayer. Diffuse layer is followed by a layer of ions which are in equilibrium with solution. In a similar but opposite fashion, there is a lack of negative ions in the neighborhood of the surface because they are repelled by the negative colloid. The concentration of co-ions gradually increases with the distance as repulsive forces of colloid are screened out by the positive ions until equilibrium is again reached. The diffuse layer can be visualized as a charged atmosphere surrounding the colloid. The stern layer and diffuse layers are called double-layer.

Some of the Benefits/Features of a Super Plasticizer are:

1. Specified strength can be achieved at high workability.
2. Faster placing with reduced labor and equipment costs.
3. Low permeable concrete leading to enhanced durability.

Some of Benefits of a High-Range Water Reducer are:

1. Higher strength can be achieved at "normal workability without the need for additional cement,
2. Reduction in water content typically reduces bleeding.
3. Produces cohesive and workable concrete at high slump, and
4. Reduction in striking times.

Some of the Applications of a Super Plasticizer are:

1. Incorporating the admixture during batching or on delivery at site increases workability to a flowing or self-leveling state,
2. Heavily reinforced sections,
3. Deep sections where normal consolidation is difficult,
4. High quality formwork finishes,
5. Pumped concrete (long pipelines), and
6. Compatible with all types of Portland cements, including sulfate-resisting cements and blends.

6. Properties of hardened scc structural properties

The basic ingredients used in SCC mixes are practically the same as those used in the conventional HPC vibrated concrete, except they are mixed in different proportions and the addition of special admixtures to meet the project specifications for SCC. The hardened properties are expected to be similar to those obtainable with HPC concrete. Laboratory and field tests have demonstrated that the SCC hardened properties are indeed similar to those of HPC. Table 3 shows some of the structural properties of SCC.

Compressive Strength

SCC compressive strengths are comparable to those of conventional vibrated concrete made with similar mix proportions and water/cement ratio. There is no difficulty in producing SCC with compressive strengths up to 60MPa. See fig-4 It appears that the strength characteristics of the SCC are related to the fineness and grading of the limestone filler used.

Fig.4 Compressive Strength Testing

SCC with a compressive strength around 60MPa can easily be achieved. SCC mixes with a high volume of cement – limestone filler paste can develop higher or lower 28-day compressive strength, compared to those of vibrated concrete with the same water material ratio and cement content, but without filler.

Tensile Strength

Tensile strengths are based on the indirect splitting test on cylinders. For SCC, the tensile strengths and the ratios of tensile and compressive strengths are in the same order of magnitude as the conventional vibrated concrete.

Bond Strength

Pull-out tests have been performed to determine the strength of the bond between concrete and reinforcement of different diameters. In general, the SCC bond strengths expressed in terms of the compressive strengths are higher than those of conventional concrete.

Modulus of Elasticity

SCC and conventional concrete bear a similar relationship between modulus of elasticity and compressive strength expressed in the form E/(fc)0.5, where E = modulus of elasticity, Fc=compressive strength. This is similar to the one recommended by ACI for conventional normal weight Concrete.

The Schmidt Rebound Hammer

The rebound hammer is an impact device that indicates relative and approximate concrete strength qualitatively through the rebound of the probe which has been calibrated against concrete strengths. It is useful in determining or locating weaker or stronger concrete qualitatively and in a relative sense or for locating areas with discontinuities and honeycombs. See fig-5.

It is not an accurate device even when calibrated against concrete cores extracted in the area and is not intended to replace the compression test. It should not be used as a basis for acceptance or non-acceptance of a particular pour.

The device when used properly could give useful indications such as to where weaker vs Stronger concrete is present but only in a relative sense.

Fig.5

A lot of consultants think that it is an accurate and absolute determinant of Concrete compressive strength which it is not. Dependence on this as the sole reference and basis for rejection is unwarranted, unsound and NOT VALID.

Concrete Compression Test ASTM C-39

A concrete test as technically defined should consist of tests on at least two standard cylinders taken from the same batch or pour.

ACI Requirements for Compressive Strength Test

For a strength test, at least two standard test specimens shall be made from a composite sample obtained as required in Section 16. A test shall be the average of the strengths of the specimens tested at the age Specified. If a specimen shows definite evidence other than low strength, of improper sampling, molding, handling, curing, or testing, it shall be discarded and the strength of the remaining cylinder shall then be considered the test result.To conform to the requirements of this specification, strength tests representing each class of concrete must meet the following two requirements mutually inclusive:The average of any three consecutive strength tests shall be equal to, or greater than, the specified strength,fc. No individual strength test shall be more than 500 psi [3.5 MPa] below the specified strength, f'c.

Failure Mechanism

Concrete failure in the compression test or in service is a result of the development of micro cracking through the specimen to the point where it can no longer resist any further load.The crack propagates through the weakest link whether it is through the aggregates or the cement matrix or both.For ultra high strength concrete aggregate strength becomes critical and it would be better to have smaller sized aggregates so that internal weaknesses in the aggregates would not be significant as a crack initiator.Also, the use of small sized aggregates increases the aggregate interlock and increases the chances for Crack Arrest.For normal strength concrete, failure normally propagates through the cement matrix unless internal planes of weakness in the aggregates give in more readily but the random distribution of these would arrest such crack propagation in the normally stronger aggregates.
In the compression test, because of scale effects, the plainness, perpendicularity and surface imperfections critically influence the results.

Factors Affecting Compressive Strength

Retempering of the mix with water in the concrete can cause a decrease in the mortar strength due to uneven dispersion of the retempering water which leads to pockets of mortar having a high water cement ratio.If concrete is allowed to dry rapidly, the available moisture for hydration reaction will be reduced and hydration ceases.

A smaller sized aggregate may have strength Advantage in that the internal weak planes may be less likely to exist.The bond between the mortar and coarse aggregate particles will be stronger for smaller sized aggregates which have a higher curvature.When concrete bleeds, the bleed water is often trapped beneath the coarse aggregate thus weakening the bond within the interfacial zone and allowing for weaker stress paths for cracks to initiate. Excessive bleeding will produce a high water cement ratio at the top portion leading to weakened wearing surfaces and dusting.

Factors Affecting the Compressive Strength Test Results:

Specimen geometry Size
End conditions of loading apparatus
Rigidity of Test Equipment
Rate of load application
Specimen moisture conditions

Requirements of Testing Machine Properties:

The Test Equipment used for the Compression test:

• Must be capable of smooth and continuous load application.
• Must have accurate load sensing and load indication.
• Must have two bearing blocks one fixed and the other spherically seated both satisfying plainness and rigidity requirements.
• Distortion of testing machine or of the bearing plates due to inadequate rigidity can cause strength reductions therefore; adequate rigidity needs to be assured.

Rate of Loading

ASTM C-39 requires that the loading rate for hydraulically operated test frames be controlled to within 20 to 50 PSI or about 500 Lbs per second. Other than making the test procedure follow consistent rates of loading and thus remove this as a variable effect on Concrete Strength, there are other reasons for prescribing a constant rate of loading. The apparent strength of the concrete increases with increasing loading rate and therefore the loading rate must conform to the required standard to produce consistent and accurate results. Higher strength concrete is more affected by the loading rate.

This dependence on loading rate has been found out to be due to the Mechanism of creep and Micro Thus, it has also been found out that when subject a sustained load of 75% its ultimate strength, concrete will eventually fail without any further load increases.

Concrete Flexural Strength:

Factors Affecting Flexural Strength Test Results

Specimen Size
Preparation
Moisture Condition
Curing
Where the beam has been molded or sawed to size
Aggregate Size

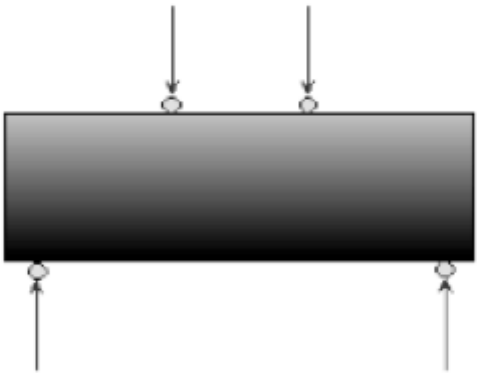

Fig.6 Flexure Test Break Patterns

Surface imperfections in the sample or the test platform can cause uneven break patterns strength results normally.

Break Patterns

Surface imperfections in the sample or the test platform can cause uneven break patterns strength results normally.

Fig.7 Uniaxial Test on Concrete Cylinder ASTM C-39

Micro-cracking.subjected to re which signal lower strength results normally.

Concrete shrinkage

Concrete shrinkage is primarily due to rapid and uneven loss of water. Therefore, improper curing of freshly poured concrete and control of environmental factors plays a key role in shrinkage control. Drying Shrinkage increases with increasing water content. Therefore control of mixing water to that required only for compl adequate flowability is important. In case such conditions cannot be met, it would be better to achieve these requirements by using water reducing plasticizers rather than by addition of more water. Although control of total wet primary objective to control shrinkage cracking, other factors contribute to the overall shrinkage cracking as the following Equation would suggest. Shrinkage cracking can be quantified or predicted based on **ACI 209R-92** following formula below. What is significant to note in this Formula is the contribution of other factors to the overall shrinkage magnitude which are controllable and thus points the way to the reduction of Shrinkage effects.

Prediction of Actual Shrinkage Values ACI 209R-92

Concrete shrinks due to moisture loss. However, the actual magnitude of ultimate shrinkage is dependent on a lot of factors as contained in ACI 209R. These factors are:

- Relative Humidity
- Minimum Thickness
- Cement Content
- Slump
- Air Content
- Fines Content

Mix Design Principles

To achieve the required combination of properties in fresh SCC mixes:

1. The fluidity and viscosity of the paste is adjusted and balanced by careful selection and proportioning of the cement and additions, by limiting the water/powder ratio and then by adding a super viscosity modifying admixture. Correctly controlling these components of SCC, their compatibility and interaction is thereshly complete hydration and desired not water in the mix is the procedures as given in the **Based on** 209R-92. plasticizer and (optionally) a key to achieving good filling ability, passing ability and resistance to segregation.
2. In order to control temperature rise and thermal shrinkage cracking as well as strength, the fine powder content may contain a significant proportion of type l or ll additions to keep the cement content at an acceptable level.
3. The paste is the vehicle for the transport of the aggregate; therefore the volume of the paste must be greater than the void volume in the aggregate so that all individual aggregate particles are fully coated and lubricated by a layer of paste. This increases fluidity and reduces aggregate friction.
4. The coarse to fine aggregate ratio in the mix is reduced so that individual coarse aggregate particles are fully surrounded by a layer of mortar. This reduces aggregate interlock and bridging when the concrete passes through narrow openings or gaps between reinforcement and increases the passing ability of the SCC.

Adjustment of the Mix

Laboratory trials should be used to verify properties of the initial mix composition. If necessary, Adjustments to the mix composition should then be made. Once all requirements are fulfilled, the mix should be tested at full scale at the concrete plant or at site. In the event that satisfactory performance cannot be obtained, then consideration should be given to fundamental re-design of the mix. Depending on the apparent problem, the following courses of action might be appropriate: · using additional or different types of filler, (if available); · Modifying the proportions of the sand or the coarse aggregate; using a viscosity modifying agent, if not already included in the mix; · adjusting the dosage of the super plasticizer and/or the viscosity modifying agent; · Using alternative types of super plasticizer (and/or VMA), more compatible with local materials; · adjusting the dosage of admixture to modify the water content, and hence the water/powder ratio.

7. Future scope

1. Despite its advantages as described in previous section, SCC has not gained much local acceptance though it has been promoted in the Middle East for the last five years.
2. The majority of applications thus far have been small niche pours into congested areas, domes, or thin wall sections.
3. In UAE, specifically in Dubai, there are a few high-rise structures under construction using SCC and many more are expected in future (Kapoor Awareness of SCC has spread across the world, prompted by concerns with poor consolidation and durability in case of conventionally vibrated normal concrete.
4. The scope of this work was limited to the development of a suitable mix design to satisfy the requirements of CC in the plastic stage using local aggregates and then to determine the strength and durability of such concrete exposed to thermal and moisture cycles.
5. The Implementations of new Techniques, new Plasticizers are under test.
6. Thus Improving the test results new plasticizers are been tested.

8. Conclusion

The primary aim of this research was to design a suitable SCC mix with local aggregates and thereafter determine its durability due to exposure to moisture and thermal variations. Possessed maximum compressive strength. The compressive strength of SCC specimens increased with the time of curing. A considerable increase in the compressive strength of concrete specimens exposed to thermal variations was noted compared to specimens exposed to wet-dry and normal exposures. Further, compared to the compressive strength of specimens under normal exposure, the compressive strengths of specimens under wet-dry were higher. The SCC specimens displayed better performances with regard to water absorption. Water penetration depth value found in case of wet-dry exposure corresponds to the "low permeability" whereas the same in cases of normal and heat-cool exposures Correspond to the "moderate permeability.

REFERENCES

[1] Self Compacting Concrete(SCC) – Energy Conservation Technique, Dr. Rakesh Kumar, Scientist C, Bridges and Structures, CRRI, New Delhi, May 2009.
[2] Self compacting Concrete, Hajime Okamura and Masahiro Ouchi, Journal of Advanced Technology, Vol. 1, No. 1, P 5-15, April, 2003.
[3] Guidelines for testing fresh self-compacting concrete, May 2005, Principal author: G. DE SCHUTTER.
[4] Measurement of properties of fresh selfcompacting concrete, Acronym: TESTING-SCC, European Research Project: 2001-2004
[5] Kashima, S., Kanazawa, K., Okada, R., and Yoshikawa, S. (1999). "Application of selfcompacting concrete made with low-heat cement for bridge substructures of Honshu-Shikoku Bridge Authority." Proceedings of the International Workshop on Self-Compacting Concrete, 255-261.
[6] Nagamoto, N., and Ozawa, K. (1997). "Mixture pr oportions of self-compacting high performance concrete," ACI International, SP-172, 623-636.
[7] Okamura, H., Maekawa, K., and Ozawa, K. (1993). "High Performance Concrete ."Gihodo Publishing
[8] Americansoccity of civil engineers www.asce.org/membership/benefits.cfm
[9] Thomas, M.D.A., and Evans, C.M., (1998). "Chloride penetration in highperformance concrete containing silica fume and fly ash", Presented at Two-Day CANMET/ACI Inter. Workshop on Supplementary Cementing Materials, Superplasticizers and other Admixtures in Concrete, 10pp.
[10] Ramsburg, P. and Neal, R.E., (2003). "The use of a natural pozzolan to enhance the properties of selfconsolidating concrete", (www.oldcastle-precast.com), pp. 1-7.
[11] Nagamoto, N., and Ozawa, K., (1997). "Mixture proportions of self-compacting high performance concrete", ACI International, SP-172, pp. 623-636.
[12] Mata, L. A., (2004). Implementation of Self- Consolidating Concrete (SCC) for Prestressed Concrete Girders, MS Thesis, North Carolina State University, November.
[13] Gerwick, B. C., Holland, T. C., Komendant, G. J., 1981, "Tremie Concrete for Bridge Piers and Other Massive Underwaer Placements", Report No. FHWA/RD-81/153
[14] Khayat, K. H., Sonebi, M., Yahia, A., and Skaggs, C.B. (1996). AStatistical models to predict flowability,

washout resistance and strength of underwater concrete,@ Production Methods and Workability of Concrete published by E&FN SPON, London, U.K., pp 463-481 15. Yao, S., Berner, D., and Gerwick, B. (1999).
[15] “Assessment of Underwater Concrete Technology for In the Wet Construction of Navigation Structure”, US Army Corps of Engineers Research and Development Center, Technical Report INPSL-1.
[16] Kordts S., Grube H., Controlling the Workability Properties of Self-Compacting Concrete Used as Ready-Mixed Concrete. Düsseldorf, Germany, 2006.
[17] The European Guidelines for Self-Compacting Concrete. EN 12350-1: 1999 E.

Assessment of Water Supply at Patan, Gujarat

Mrunalini Rana

Email: mrunalini_rana@yahoo.co.in

Civil Engineering Department, Silver Oak College of Engineering & Technology, Ahmedabad

Abstract:

About 85% of the global population had access to piped water supply through house connections or to an improved water source through other means than house, including standpipes, "water kiosks", protected springs and protected wells. However, about 14% did not have access to an improved water source and had to use unprotected wells or springs, canals, lakes or rivers for their water needs. A clean water supply, especially so with regard to sewage, is the single most important determinant of public health. Destruction of water supply and/or sewage disposal infrastructure after major catastrophes (earthquakes, floods, war, etc.) poses the immediate threat of severe epidemics of waterborne diseases, several of which can be life-threatening.
Water supply systems get water from a variety of locations, including groundwater, surface water, conservation and the sea through desalination. The water is then, in most cases, purified, disinfected through chlorination and sometimes fluoridated. Treated water then either flows by gravity or is pumped to reservoirs, which can be elevated such as water towers or on the ground.

Keywords: Water supply system; water distribution network, intermittent water supply, water treatment plant, ESR, sump.

1. Introduction

Clean drinking water and safe water supply is vital to our life. Water planners have two fundamental options available to ease water restrictions – to encourage water conservation or to increase water supply. Voluntary water conservation is often the most affordable, environmentally sensitive option available to urban water users. In general practice the water is supplied for restricted hours in morning or in evening for various reasons, known as intermittent water supply (IWS). The main objectives is to bench–mark and improve the level, quality and sustainability of Urban Areas of importance and rapidly developing cities, with a strong focus on up-gradation of Civic Infrastructure and enhance delivery of Civic Services.

2. Salient features of the town

Patan, a capital of Gujarat during medieval times, is a historic town with a history spanning over centuries. It is an important settlement and a district headquarters. It has also one of the oldest Municipalities. Patan situated at a distant of 120 km from Ahmedabad and 108 km away from the state capital Gandhinagar, is an ancient town of temples and other architecture monuments. Patan is known for its numerous architectural and cultural heritages like Ranki Vav, Sahastralingi Talav, Fort Wall and Gates, Panchasara Parshvanath Jain Derasar, Hemachandracharya Jain Ghyan Mandir and Kalika Temple. It is an important settlement and a district headquarters. It is a class-I town as per census of 2001 with total population of 1,13,749. The Patan city has immense potential for growth and development as revealed by the figures made available by the census 2001. Presently, Patan is home to the Hemachandracharya North Gujarat University previously known as North Gujarat University. Patan is a prominent medical centre in North Gujarat with around 140 clinics and laboratories with almost 393 practicing medical professionals. Patan serves as a central market place for local farmers. Close to Patan, Unjha has the biggest Asian market in Zira, Isabgol. Patan is still known for its patola saree which are highly expensive, involve high degree of skill and time and is one of the finest hand-woven saree produced today in the world. Patan is also a tourist destination with a rich religious and cultural history and landmarks. Patan has numerous Hindu and Jain temples as well as Muslim mosques.

2.1 Topography

Patan city is situated at latitude of 76 m. (249 feet) and is located at 23.83°N 72.12°E. The city has shape like that of an inverted saucer. Most of the rain water flows through natural drains leading to ponds like Pitambar Talav, Gungadi (Anand Sarovar) Talav, Siddhi Sarovar, Sahastraling sarovar and Vatrasar canal. With the natural topography it is observed that there is no major problem of water logging in the city areas. The city has Sahastraling Talav – a beautiful lake present which forms a tourist attraction to the city. There is old historical fort and ancient Saraswati River which dignifies the city. Patan has a very old archaeological monument of sun temple nearby which is visited by the tourist both from the state and outside the state in large numbers. This sun temple is second in the country, first being in Konark.

2.2 Climate & Rainfall

Patan has large variation of temperature ranging from maximum of 41.7° C in summer and 11.3°C minimum in winter. The average rainfall recorded during last 17 years has been found to be order of 588.33 mm. However, there are not many water bodies within or outside the city which help in modulating the climate. The rainfall of the town has been found to be lower than that of state average. Lowest rainfall of 160.75 mm was recorded in the year 1999-2000 in highest of 1476.17 mm in the year 1997-98.The annual rainfall for the Patan city is given in Table-1.

Table 1 Rainfall Data for Patan City

Sr. No.	Year	Total Rainfall, mm.	Average Rainfall in the State, mm
1	1988-1989	752.75	-
2	1989-1990	430.00	-
3	1990-1991	623.00	-
4	1991-1992	563.25	658
5	1992-1993	563.25	859
6	1993-1994	614.00	823
7	1994-1995	1087.50	1407
8	1995-1996	543.25	636
9	1996-1997	312.50	848
10	1997-1998	1476.17	1088
11	1998-1999	605.00	1072
12	1999-2000	160.75	642
13	2001-2002	254.75	530
14	2002-2003	525.75	796
15	2003-2004	279.25	629
16	2004-2005	670.00	1073
17	2005-2006	540.50	-
	Average	**588.33**	**850.85**

2.3 Demography & Growth Pattern

Total population of Patan is 1, 1,749 as per the census 2001 Table-2. gives trends in urbanization in Patan between 1901 and 2001.

Table 2 Population Growth Trend of Patan City

Sr. No.	Year	Population	% Growth Per Decade
1	1901	31402	-
2	1911	28339	-9.75
3	1921	27017	-4.66
4	1931	29830	+10.41
5	1941	36549	+22.52
6	1951	43044	+17.77
7	1961	51953	+20.70
8	1971	64519	+24.19
9	1981	79196	+22.75
10	1991	97025	+22.51
11	2001	113749	+17.24

Patan city has shown a moderate rate of growth. During the last decade (1991-2001), the city recorded a growth rate of 17.24%. During the last century, the town has recorded negative growth rate during 1901-11 and 1911-21. As against a population of 31402 at the beginning of the century, the population recorded in 2001 was 113749. The percentage growth rate of population for the city, is given in the Table-2. Despite of enormous potential, city has, due to neglect, haphazard and unplanned growth, the population of the town is lower than the state and national average.

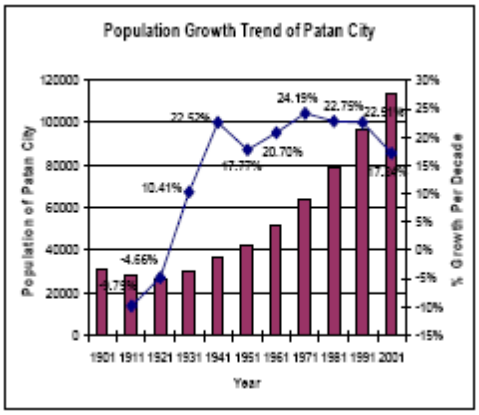

Fig.1 Population Growth Trend

There are 14 administrative wards within Patan city.Recently few areas of three outgrowths have been included in the total population of the city. The ward wise population for the Patan city is given in Table-3.

Table 3 Ward Wise Population Distribution

Sr. No.	Wards	Population	Residential Area*, sq.km.	Population Density, Persons/sq.km.
1	No. 1	7978	1.01	7903
2	No. 2	8622	0.68	12627
3	No. 3	8451	0.24	35459
4	No. 4	8503	1.81	4700
5	No. 5	7431	1.31	5667
6	No. 6	8630	0.82	10564
7	No. 7	8445	0.18	46913
8	No. 8	7918	0.20	38881
9	No. 9	7863	0.56	13952
10	No. 10	7767	0.18	42087
11	No. 11	8120	0.23	34563
12	No. 12	7447	1.79	4161
13	No. 13	7467	0.82	9143
14	No. 14	7477	0.71	10734
15	Matarwadi OG	330	0.43	767
16	Gungarpati OG	579	0.04	14367
17	Hansapur OG	621	0.37	1683
	Total	**113649**	**11.39**	**9990**

**** Excluding agricultural area and water bodies***

Ward no. 3, 7,8,10 and 11 covers old city area. These wards have high population density and limited growth. The total area of the Patan city is 12.09 sq. km. excluding the outgrowth areas.

2.4 Land Use Pattern

Table 4 Area Existing Land Use Map

Sr. No.	Type of Usage	Area in Hectares	Percentage of Total Area
1.	Residential Zone	888.65	67.64%
2.	Commercial Zone	48.67	3.80%
3.	Public Purpose	87.34	6.81%
4.	Industrial Zone	6.73	0.53%
5.	Open space/ Garden	10.05	0.78%
6.	Crematorium, Crematory	13.22	1.03%
7.	Water Body	21.34	2.13%
8.	Agriculture Zone	214.06	17.28%
	Total	**1290.07**	**100.00%**

Table-4 shows area under existing land use. There are very less industrial units in Patan city as GIDC which is a notified industrial having around 54 units. There is a spurt in residential demand beyond municipal limits and therefore the area has developed particularly for residential purpose. Patan city is growing extensively towards eastern side.

The commercial activities have developed along the main arterial roads of the city having a great impact over the land prices of the city. No commercial hubs have been established in the city, the gamtal area is one of the prominent commercial areas promoting traditional shopping to the citizens of the city.

2.5 Hydrology

The topography of the town is like a inverted saucer, so most of the rain water flows through natural drains leading to ponds like Pitambar Talav, Gungadi Talav, Siddhi Sarovar, Sahastraling sarovar and Vatrasar canal. With the natural topography it is observed that there is no major problem of water logging in the city areas. The storm water drainage system does not exist in Patan.

3. Existing water supply scenario

In Patan presently the source of drinking water is ground water. Water from 16 nos. of tube wells is being drawn. The town receives the water supply of 20.0 MLD water from ground water to supply to the town. The water from the tube wells is unpotable due to high TDS and fluoride content more than 2.5 mg. 2.15 m. dia. 20.5 km long NMC

Pipeline from Khorsam connecting Saraswati barrage is laid by irrigation department to pump water from NMC for Saraswati barrage and Siddhi Sarovar. Canal is constructed from Saraswati barrage towards Chanasma which is connected with Siddhi Sarovar. To supply surface water from Narmada Canal Water Treatment Plant (WTP) at Siddhi Sarovar is completed. WTP is to be connected with Sub-headwork's, for which ULB have invited the tender for laying pipelines to connect the Sub-headwork's with WTP. The water treatment plant near Siddhi sarovar pond is of capacity of 27.0 MLD. Water from Siddhi Sarovar pond will be pumped to WTP for Patan city. A sump of 20.0 Lacs litre and E.S.R. of 10.0 Lacs litre capacity are already constructed by GWSSB under Sujalam Sufalam Scheme. Intake well of 8m dia is constructed at Siddhi Sarovar. The water from intake well is supplied by 814 mm dia. M.S. rising main to Siddhi Sarovar filtration plant. The pipe is approximately 200 m in length. The water treatment plant of capacity 27.0 MLD near Siddhi Sarovar pond with a cost of Rs. 5.5 crores is already constructed.

Fig.2 Pump House at Siddhi Sarovar

Fig.3 Water Treatment Plant at Siddhi Sarovar

The treated water from Siddhi Sarovar filtration plant is being collected in clear water sump, which is again pumped into ESR constructed at main head works located within the filtration plant premises. It is proposed to supply treated water from ESR to sub stations in all different zones through gravity under Siddhi Sarovar Scheme. Presently the entire town is divided into 11 water supply zones. Water is distributed in the town through network of ESRs and underground sumps. The distribution network consists of pipelines varying from diameter of 50 mm to. 450 mm. The length of the total distribution network a is 120.0 km. However the actually marked distribution network on site comes out to be 110.01 km. Water is supplied for only 30 minutes in morning and evening. The existing pipelines are old and there are leakages at several places. The existing distribution network is laid in a haphazard manner.

4. Population projection

Population projection for the town can be done using four methods namely Arithmetic Increase Method, Increment Increase Method, Geometric Increase Method and Graphical Method. Considering the large variations of population arrived at by these methods, averages of the figures are proposed to be adopted for working out the population distribution.The population of Patan city for year 2001 is 1,13,749 as per census 2001 including three outgrowth areas viz.Matarwadi, Gungarpati & Hansapur shown in Table-5.

Table 5 Population Projection for Patan City

Year	Population of Patan City	Increment (X)	Incremental increase (Y)	Rate of Growth Per Decade
1961	50,264	--	--	
1971	64,519	14,255	--	0.28
1981	79,196	14,677	422	0.22
1991	97,025	17,829	3,152	0.22
2001	113,749	16,724	-1,105	0.17
Total		63,485	2,469	0.90
Average per decade		**15,871**	**823**	**0.22**

In calculating the water demand for the town the demand for the resident population, industrial demand and fire fighting demand has been taken into consideration.Considering Patan as city with piped water supply and where sewerage system will be provided in near future the residential demand of 135 LPCD has been taken into consideration. It is envisaged the design period shall be completed in one year and two to three years for construction activities. If design period has been considered as 2010 and proposes to complete the construction activities during 2011-2013.So for population projection the base year 2014 has been considered. Accordingly 2029 shall be the intermediate year and 2044 shall the ultimate design year for this project. Details of population projection is shown in Table-6.

Table 6 Summary of Population Projection

Year	Arithmetic Progression Method	Geometric Progression Method	Incremental Increase Method	Graphical Method	Average Population Considered
2001	---	---	---	---	113749
2010	128,035	136,445	128,740	142,000	133805
2014	134,385	147,935	135,615	152,500	142609
2029	158,190	200,330	162,570	198,500	179898
2044	181,995	271,275	191,375	269,500	228536

5. Water demand

In calculating the water demand for the town the demand for the resident population, industrial demand and fire fighting demand has been taken into consideration.

5.1 Residential Demand

The total demand for the city includes residential demand is shown in Table-7

Table 7 Residential Water Demand For Patan City

Year	2001	2010	2014	2029	2044
Population considered	113,749	133,805	142,609	179,898	228,536
Water demand @ 135 lpcd	15.36	18.06	19.25	24.29	30.85
Water Demand at ESRs & Sumps Including 15% UFW	18.07	21.25	22.65	28.57	36.30
Water Demand at Treated Water Sump Including2% Transmission Losses	18.50	21.76	23.20	29.26	37.17
Water Demand at WTP Including 2% Treatment Losses	18.96	22.30	23.77	29.98	38.09
Water Demand at Source Including 1% Treatment Losses	19.20	22.58	24.07	30.36	38.57
Total Demand, MLD	19.20	22.58	24.07	30.36	38.57

5.2 Industrial Demand

The Patan city has small industries within the municipal limits. Some industries use municipality water where as some of them has their own source of water. Per capita rates of supply recommended will ordinarily include the requirement of small industries (other than factories)distributed within a town.

5.3 Fire Fighting Demand

It is usual to provide fire fighting demand on the distribution system along with the normal supply to the consumers as assumed. A provision in KL/day based on the formula of $100\sqrt{P}$ where P=population in thousands and may be adopted for communities larger than 50,000. It is desirable that one third of fire-fighting requirements form part of the service storage. The balance requirement is distributed in several static tanks at strategic points. Fire demand is calculated in Table-8 by the formla given in CPHEEO manual.

Fired Demand = $100\sqrt{148391}/1000=1218$ Eq. (1)
KL/day=1218000 L/day=1.218 MLD

Table 8 Fire Demand For Patan City

Year	Population considered	Fire Demand, KL/day	Fire Demand, MLD
2001	113,749	1066.53	1.067
2010	133,805	1156.74	1.157
2014	142,609	1194.19	1.194
2029	179,898	1341.26	1.341
2044	228,536	1511.74	1.512

5.4 Total Water Demand

The total water demand including fire demand, industrial demand and losses for various stages of design, i.e. base year, intermediate year and ultimate year, for Patan city is given in Table-9.

Table 9 Total Water Demand For Patan City

Year	Population considered	Floating Popula -tion	Distri-bution Losses, 15%	Transmission Losses 2%	Treat-ment Losses 2%	Source Losses 1%	Total Demand , MLD (Table-7)	Fire Demand , MLD (Table-8)	Total Demand at Source, MLD	WTP Capacity, MLD (Excluding 1% source losses)
2001	113,749	0	18.07	18.50	18.96	19.20	19.20	1.067	20.2617	20.059
2010	133,805	0	21.25	21.76	22.30	22.58	22.58	1.157	23.7363	23.499
2014	142,609	0	22.65	23.20	23.77	24.07	24.07	1.194	25.2594	25.007
2029	179,898	0	28.57	29.26	29.98	30.36	30.36	1.341	31.6990	31.382
2044	228,536	0	36.30	37.17	38.09	38.57	38.57	1.512	40.0772	39.676

6.conclusions

The specific aims and objectives that are envisaged to be achieved by the implementation of the study are as follows:

-To optimize social and economic development in urban town like Patan, at Gujarat.

-To Improve and develop basic infrastructure in the Town water supply plays important role. It is observed from study that as population increases water demand also increases from 20.059 MLD in 2001 to 39.676 MLD in 2044.

7. Acknowledgements

I am also grateful to Patan ULB for providing me with the necessary details for my study.

REFERENCES

[1]CPHEEO-Central Public Health and Environmental Engineering Organization Manual on water supply and treatment, 3rd edn.

[2] Ministry of Urban Development and Poverty Alleviation, Govt. of India, New Delhi, 1999.

[3] Richard Francey and Anand Jalakam, Water and Sanitation Program Report, the Karnataka Urban Water Sector Improvement Project, 2010.

[4] Preliminary Design Report, Water Supply for Bhavnagar, Mott MacDonald Group Limited,2010

[5] Sathya Sai Baba, in Sathya Sai Speaks X, Chap. 19, 123; VII, Chap. 59, 350; VI, Chap. 58, 288

[6] Mysore water supply scheme - Mysore City Water Supply Augmentation Report, Mott MacDonald Group Limited

[7] City Assessment and Development Strategy Report

[8] DPR of water supply project for Rajkot City, Rajkot Municipal Cooperation.

Multi Objective Evolutionary Algorithms

[1]Kinjal Adhvaryu, [2]C. Bhensdadia, [3]Amit Ganatra

Email: kinjalvk@yahoo.com
Email: ckbhensdadia@ahoo.co.in
Email: amitganu@yahoo.com

[1]Computer Engineering Department, Silver Oak College of Engineering & Technology, Ahmedabad
[2]Computer Engineering Department, Dharmsinh Desai Institute of Technology, Nadiad
[3]Computer Engineering Department, Charotar Institute of Technology, Changa

Abstract:

Evolutionary Algorithms (EAs) are often well suited for optimization problems involving several coupled parameters. Since 1985, various evolutionary approaches to multi objective optimization have been developed, capable of searching for multiple solutions in a single iteration. These methods differ in the fitness assignment function obtained, however the decision to which method is best suited for a given problem depends mainly upon the nature of problem and its complexity. This paper utilizes three Evolutionary Algorithms, Vector Evaluated Genetic Algorithm, Non- dominated Sorting Genetic Algorithm and Nicked Pareto Genetic Algorithm and compared the performance of these algorithms in terms of closeness to the Pareto front and diversity of solutions for Multi Objective Traveling Salesman Problem (MOTSP) using two performance metrics, average set coverage and maximum spread. This paper concluded that NPGA algorithm is comparatively best suited for any Travelling Salesman Problem (TSP) type transportation applications.

Keywords: Diversity of solutions, Genetic algorithms, Optimization problems

1. Introduction

THE *Traveling Salesman Problem* is one which has commanded much attention of mathematicians and computer scientists specifically because it is so easy to describe and so difficult to solve. The problem can simply be stated as: if a traveling salesman wishes to visit exactly once each of a list of *m* cities and then return to the home city, which is the least costly tour the traveling salesman can take? And the *Multi-Objective Traveling Salesman* P*roblem* (MOTSP) is one in which a traveling salesman wishes to visit exactly once each of a list of *m* cities and then return to the home city but with more than one constraint like minimize the distance, cost, time or increase touring attractiveness etc. Here the problem is *symmetric multi-objective traveling salesman problem*. Much of the work on the MOTSP is not motivated by direct applications, but rather by the fact that the MOTSPprovides an ideal platform for the study of general methods that can be applied to a wide range of discrete optimization problems. This is not to say, however, that the MOTSP does not find applications in many fields. Indeed, the numerous direct applications of the MOTSP bring life to the research area and help to direct future work.

Different multi-objective genetic algorithm methods [2] have been proposed by the researchers and used for multi-objective optimization for number of years. Yet, in general, no method is superior to others in all the performance aspects. Different methods have their advantages and disadvantages. But still there is a scope for finding out which method is appropriate for particular Multi-Objective Traveling Salesman Problem. A comparative analysis of these methods is a new research area. The methods are mainly compared on the basis of diversity of solutions and closeness to the Pareto front. This paper takes three multi-objective genetic algorithms and compares their performance by applying them to a Multi-objective Traveling Salesman problem. Hence this project explores the performance of these MOEAs.

2. Genetic algorithm

Search and optimization techniques can be categorized into three classes: calculus based, enumerative, and random. Calculus based approaches usually require the existence of derivatives and the continuity. Therefore it is difficult to apply them to realistic problems where these assumptions often do not hold. Enumerative methods are straightforward search schemes. They can be applied to optimization problems when the numbers of feasible solutions are few. Most optimization problems in the real world, however, have countless possible solutions [13][16]. Therefore they cannot be applied to such complex problems. As for random searches, while they search in solution spaces without any kind of information, it may not be efficient. Therefore the search direction should be specified in order to improve their search ability. Genetic Algorithm (GA) is one of random searches because they use a random choice as a tool in their searching process. While a random choice performs an important role in GAs, the environment directs the search in GAs i.e. they utilize information from the environment in their searching process. The idea of Genetic Algorithms was introduced by John Holland.

Advantages of Genetic Algorithms over Traditional Methods

The Genetic Algorithms differ with traditional methods in the following ways:
1) Genetic algorithms work with a coded form of the function values (parameter set), rather than with the actual values themselves.
2) Genetic algorithms use a set, or population, of points to conduct a search, not just a single point on the problem space. This gives Genetic Algorithms the power to search noisy spaces littered with local optimum points. Instead of relying on a single point to search through the space, the GA looks at many different areas of the problem space at once, and uses all of this information to guide it.
3) Genetic Algorithms use only payoff information to guide themselves through the problem space. Many search techniques need a variety of information to guide them. The only information a Genetic Algorithm needs is some measure of fitness about a point in the space. Once the Genetic Algorithm knows the current measure of "goodness" about a point, it can use this to continue searching for the optimum.
4) Genetic Algorithms are probabilistic in nature, not deterministic. This is a direct result of the randomization techniques used by Genetic Algorithms.
5) Genetic Algorithms are inherently parallel. Here lies one of the most powerful features of genetic algorithms. Genetic Algorithms, by their nature, are very parallel, dealing with a large number of points (strings) simultaneously.

A. Multi-objective optimization problems

Besides having multiple objectives, there are a number of fundamental differences between single-objective and multi-objective optimization as follows:
1) Two goals instead of one;
2) Dealing with two search spaces;
3) No artificial fix-ups.

A striking difference between a classical search and optimization method [2][3][6][7][8] and a Genetic Algorithm is that in the latter a population of solutions is processed in each iteration (or generation). This feature alone gives Genetic Algorithms a tremendous advantage for its use in solving multi-objective optimization problems. Recall that one of the goals of an ideal multi-objective optimization procedure is to find as many Pareto-optimal solutions as possible. Since a Genetic Algorithm works with a population of solutions, in theory we should be able to make some changes to the basic Genetic Algorithm so that a population of Pareto-optimal solutions can be captured in one single simulation run of a Genetic Algorithm. This is the powerful feature of Genetic Algorithms that makes them particularly suitable to solve multi objective optimization problems. We don't need to perform a series of separate runs as in the case of the traditional mathematical programming techniques.
The first real implementation of a multi-objective genetic algorithm (vector valued GA or VEGA) was suggested

by David Schaffer in 1984. The name VEGA is appropriate for multi-objective optimization, because his GA evaluated an objective vector (instead of a scalar objective function), with each element of the vector representing each objective function. Although VEGA is simple to implement, it does not find diverse solutions in the population and converges to individual champion solutions only. Surprisingly, no significant study was performed for almost a decade after the pioneering work of Schaffer. Thereafter, several independent groups of researchers have developed different versions of multi-objective evolutionary algorithms [2][3][4]. Some of them are:-

1) Vector Evaluated Genetic Algorithm (VEGA) by David Schaffer (1984)
2) Non-dominated Sorting Genetic Algorithm (NSGA) by Srinivas and Deb (1994)
3) Nicked-Pareto Genetic Algorithm (NPGA) by Horn, Nafploitis and Goldberg (1994).

B. Vector evaluated genetic algorithm (VEGA)

VEGA is the simplest possible multi-objective Genetic Algorithm [2] and is a straightforward extension of a single-objective Genetic Algorithm for multi-objective optimization. Since a number of objectives (say M) have to be handled, Schaffer thought of dividing the population at every generation into M equal subpopulations randomly. Each subpopulation is assigned a fitness based on a different objective function. In this way, each of the M objective functions is used to evaluate some members in the population. The population at any generation is divided into M equal divisions. Each individual in the first subpopulation is assigned a fitness based on the first objective function only, while each individual in the second subpopulation is assigned a fitness based on the second objective function only, and so on. In order to reduce the positional bias in the population, it is better to shuffle the population before it is partitioned into equal subpopulations. After each solution is assigned fitness, the selection operator, restricted among solutions of each subpopulation, is applied until the complete sub-population is filled. This is particularly useful in handling problems where objective functions take values of different orders of magnitude. Since all members in a sub-population are assigned a fitness based on a particular objective function, restricting the selection operator only within a subpopulation emphasizes good solutions corresponding to that particular objective function. Moreover, since no two solutions are compared for different objective function, disparity in the ranges of different objective functions does not create any difficulty either. Schaffer used the proportionate selection operator.

VEGA procedure

1. Set an objective function counter i = 1 and define q = N/M.
2. For all solutions j = 1 + (i – 1) * q to j = i * q, assign fitness as $F(x^{(j)}) = fi(x^{(j)})$.
3. Perform proportionate selection on all q solutions to create a mating pool Pi.
4. If i = M, go to step 5. Otherwise, increment i by one and go to step 2.
5. Combine all mating pools together so that P = P1U P2U… U PM. Perform crossover and mutation on P to create a new population.

C. Non-dominated sorting genetic algorithm (NSGA)

The Non-dominated Sorting Genetic Algorithm (NSGA) was proposed by Srinivas and Deb [4], and is based on several layers of classifications of the individuals. Before the selection is performed, the population is ranked on the basis of non-domination. All non-dominated individuals are classified into one category. Then this group of classified individuals is ignored and another layer of non-dominated individuals is considered. The process continues until all individuals in the population are classified. This classifies the population P into a number of mutually exclusive equivalent classes called non-dominated sets P_j:

$$P = \bigcup_{j=1}^{\rho} Pj \qquad (3)$$

It is important to realize that any two members from the same class cannot be said to be better than one another with respect to all objectives. The total number of classes (or fronts), denoted as ρ in the above equation, depends on the population P and the underlying problem.

NSGA Fitness Assignment

1) Choose sharing parameter σ_{share} and a small positive number ε and initialize $F_{min} = N + \varepsilon$. Set front counter $j = 1$.
2) Classify population P according to non-domination to create non-dominated sets $P_1, P_2, \dots, P_\rho$.
3) For each $q \in P_j$
   a) Assign fitness $F_j^{(q)} = F_{min} - \varepsilon$.
   b) Calculate niche count nc_q among solutions of P_j only.
   c) Calculate shared fitness $F_j'^{(q)} = F_j^{(q)} / nc_q$. $F_{min} = \min (F_j'^{(q)} : q \in P_j)$ and set $j = j + 1$.
4) If $j \leq \rho$, go to step 3. Otherwise, the process is complete.

D. Niched pareto genetic algorithm (NPGA)

Horn and Nafploitis proposed a tournament selection scheme based on Pareto dominance [2][4]. Instead of limiting the comparison to two individuals, a number of other individuals in the population were used to help to determine dominance (typically around 10). When both competitors were either dominated or non-dominated (i.e., there was a tie), the result of the tournament was decided through fitness sharing. Population sizes considerably larger than usual with other approaches were used so that the emerging niches in the population could tolerate the noise of the selection method.

NPGA Tournament Selection Procedure

Arguments – i, j, Q.
Returns – winner

1) Pick a sub-population T_{ij} of size t_{dom} from the parent population P.
2) Find α_i as the number of solutions in T_{ij} that dominated i. Calculate α_j as the number of solutions in T_{ij} that dominates j.
3) If $\alpha_i = 0$ and $\alpha_j > 0$, then i is the winner. The process is complete.
4) Otherwise, if $\alpha_i > 0$ and $\alpha_j = 0$, then j is the winner. The process is complete.
5) Otherwise, if $|Q| < 2$, i or j is chosen as a winner with probability 0.5. The process is complete. Alternatively, the niche counts nc_i and nc_j are calculated by placing i and j in the current offspring population Q, independently. With the niching parameter σ_{share}, nc_i is calculated as the number of offspring ($k \in Q$) within a σ_{share} distance d_{ik} from i. The distance d_{ik} is the Euclidean distance between solutions i and k in the objective space.
6) If $nc_i \leq nc_j$, solution i is the winner. Otherwise, solution j is the winner.

NPGA Procedure

1) Shuffle P, set $i = 1$, and set $Q = \phi$.
2) Perform the above tournament selection and find the first parent, p1 = NPGA-tournament (i, i + 1, Q).
3) Set $i = i + 2$ and find the second parent, p2 = NPGA-tournament (i, i + 1, Q).
4) Perform crossover with p1 and p2 and create offspring c1 and c2. Perform mutation on c1 and c2.
5) Update offspring population $Q = Q \cup \{c1, c2\}$.
6) Set $i = i + 1$. If $i < N$, go to step 2. Otherwise, if $|Q| = N / 2$, shuffle P, set $i = 1$, and go to step 2. Otherwise, the process is complete.

E. Performance comparison

In the following discussion of the case study it has been carried out using the above three multi objective GAs for solving an extended Multiobjective Traveling Salesman Problem. There are two distinct goals in multi-objective optimization: (1) to discover solutions as close to the Pareto-optimal solutions as possible, and (2) to find solutions

as diverse as possible in the obtained non-dominated front [10]. A Multi-objective GA will be termed a good Multi-objective GA, if both goals are satisfied adequately. For that Set Coverage Metric and Maximum Spread Metric are used.

A. Implementation Details

This work describes implementation of different instances of two different numbers of objectives for Traveling Salesman Problem. All the programs were coded in C language. It uses Turbo C in DOS environment. This paper takes four instances of each algorithm for bi-objective traveling salesman problem. Also four instances of each algorithm for three-objective symmetric traveling salesman problem. In bi-objective TSP, the objectives are to minimize distance and cost. In three-objective TSP, the objectives are to minimize distance and cost and maximize touring attractiveness which are conflictive.

B. Simulation for Multi-Objective TSP

This paper uses the MOTSP with the problem-instances for 10-cities, 25-cities, 50-cities and 60-cities with 100 population size, maximum number of generation 100, crossover rate 0.8, mutation rate 0.1, niching parameter 0.185 and domination tournament set size 10.This analysis work contains total 24 graphs for bi-objective TSP and three-objective TSP[14]. This paper contains results of all instances of all three algorithms for three-objective TSP. The results are compared on the basis of performance metrics, average set coverage and maximum spread. There are two distinct goals in multi-objective optimization: 1) Discover solutions as close as to the pareto -optimal solutions as much as possible and 2) Find solutions as diverse as possible in the obtained non-dominated front. An Multi-objective GA will be termed as a good Multi-objective GA, if both goals are satisfied adequately. Here some results are given using these three algorithms for three-objective traveling salesman problem. For that two performance metrics are used, average set coverage metric and maximum spread metrics. Figure 1 to figure 12 shows the solution set for 10-cities, 25-cities, 50-cities and 60-cities instances for three-objective Traveling Salesman Problem for VEGA, MOGA, NSGA and NPGA.

For bi-objective TSP, the results for average set coverage metric are : VEGA gives 63%, NSGA gives 97% and NPGA gives100% for 10-cities instance. For 25-cities, VEGA gives61%, NSGA gives 100% and NPGA gives 69%. For 50-cities VEGA gives41% , NSGA gives 98% and NPGA gives 100%. For 60-cities instances, VEGA gives56% ,NSGA gives 100% and NPGA gives 100%. For maximum spread metric also, NPGA gives good results compared to remaining three algorithms.

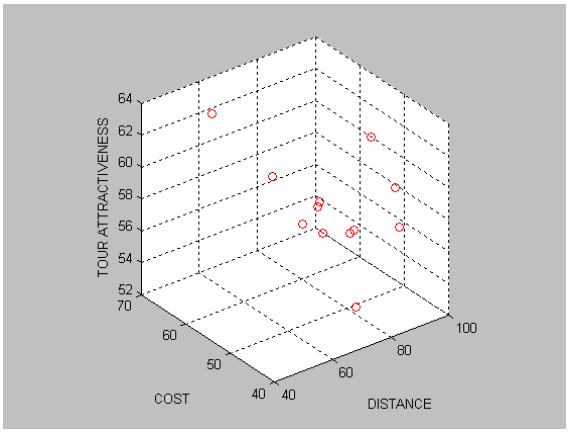

Fig.1 solution set for 10-cities(VEGA)

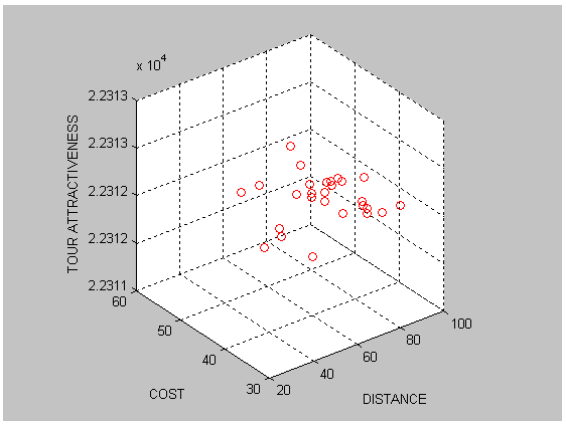

Fig.2 solution set for 10-cities (NSGA)

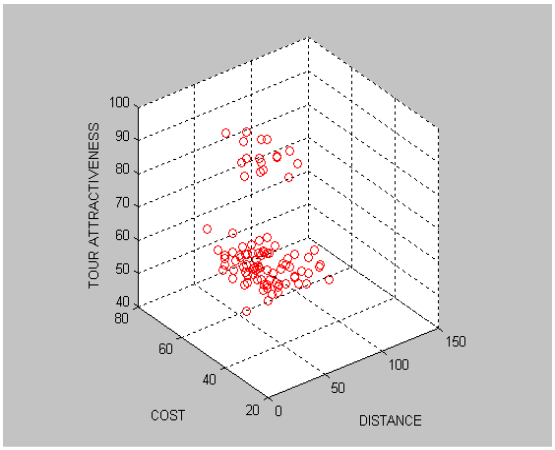

Fig.3 solution set for 10-cities (NPGA)

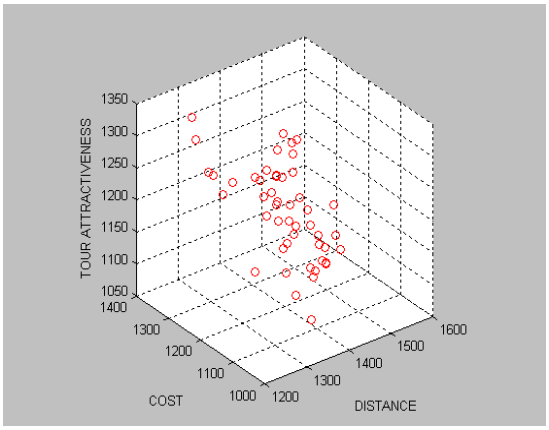

Fig.4 solution set for 25-cities (VEGA)

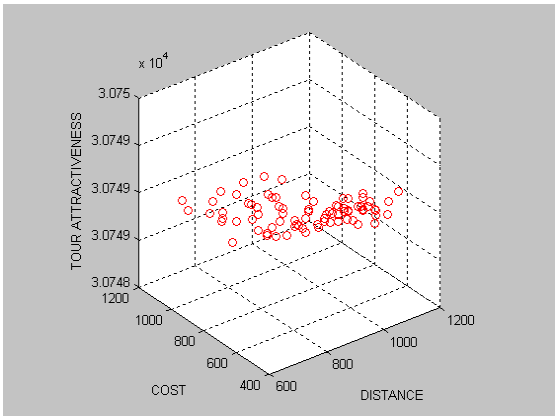

Fig.5 solution set for 25-cities (NSGA)

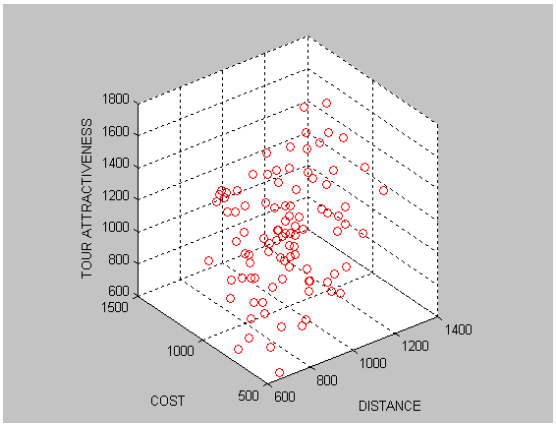

Fig.6 solution set for 25-cities (NPGA)

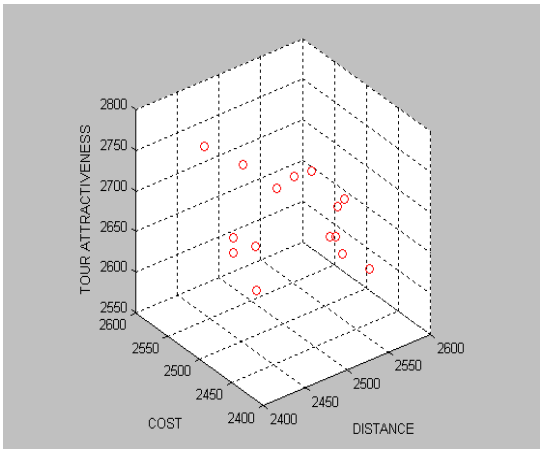

Fig.7 solution set for 50-cities (VEGA)

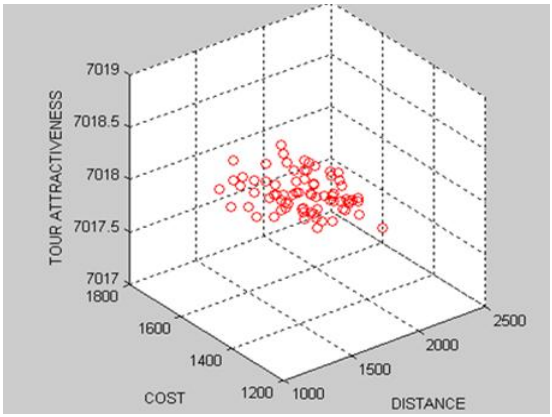

Fig.8 solution set for 50-cities (NSGA)

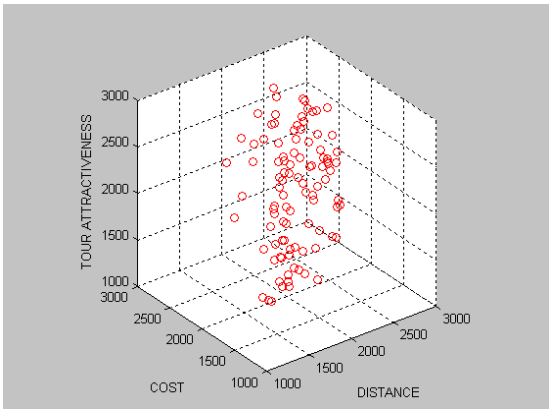

Fig.9 solution set for 50-cities (NPGA)

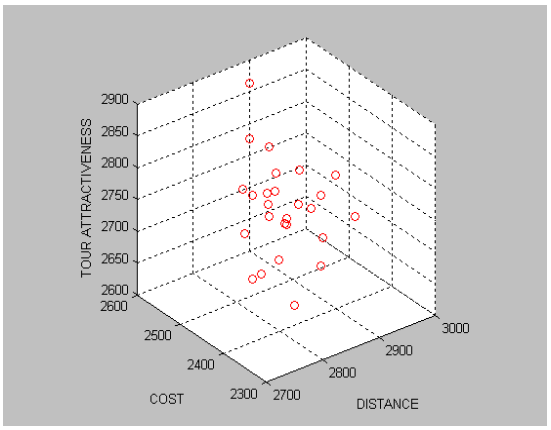

Fig.10 solution set for 60-cities(VEGA)

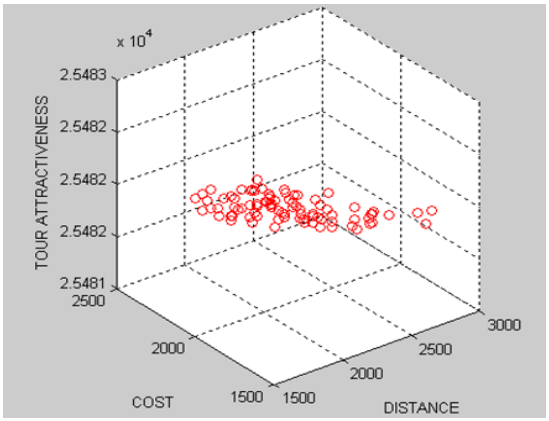

Fig.11 solution set for 60-cities (NSGA)

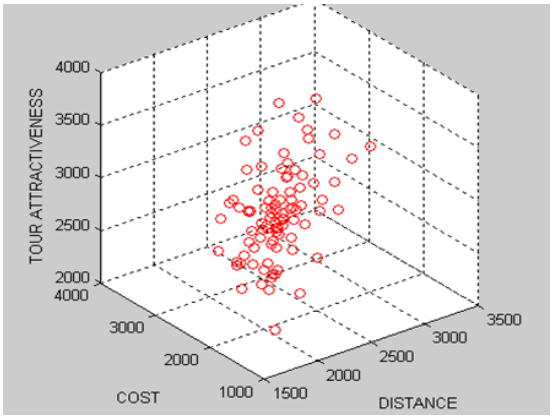

Fig.12 solution set for 60-cities (NPGA)

For three-objective TSP, NPGA gives good results compared to all remaining three algorithms. For maximum spread metric, results are: for 10-cities instance VEGA gives 50, NSGA gives 65 and NPGA gives 98. For 25-cities instance VEGA gives 453, NSGA gives 787and NPGA gives 1540.For 50-cities instance VEGA gives 245, NSGA gives 897 and NPGA gives 2487. For 60-cities instance VEGA gives 368, NSGA gives1279 and NPGA gives 2657.

3. Conclusions

Analyzing the drawn results of average set coverage metric, NPGA gives the good results compared to VEGA and NSGA since it selects individuals by directly checking them for the non-domination. Also, from the solution sets, we can see that NPGA gives more solution sets. From the results of maximum spread metric also, we can conclude that NPGA gives good results for MOTSP compared to remaining all two algorithms. From these performance metrics, it is clear that there is no effect of number of objectives on performance of NPGA. From all the above reasons we can analyze that NPGA is the best for Multi-objective traveling salesman problem and also for similar type of applications.

REFERENCES

[1] Goldberg, D.E. (1989). Genetic Algorithms in Search, Optimization, and Machine Learning. Singapore: Pearson Education.

[2] Deb, K. (2002). Multi-objective Optimization using Evolutionary Algorithms. West Sussex: John Wiley and Sons, Ltd.

[3] Coello, Carlos A. and Christiansen, Alan D. An Approach to Multi-objective Optimization using Genetic Algorithms. Department of Computer Science, Tulane University, New Orleans, LA, USA.

[4] D. S. Johnson and L. A. McGeoch, The Traveling Salesman Problem: A Case Study in Local Optimization, Local Search in Combinatorial Optimization, E. H. L. Aarts and J.K. Lenstra (ed), John Wiley and Sons Ltd, 1997, pp 215-310.

[5] Chang Wook Ahn. Advances in Evolutionary Algorithms. Theory, Design and Practice, Springer, ISBN 3-540-31758-9, 2006

[6] Zitzler, E. and Thiele, L. *An Evolutionary Algorithm for Multi-objective Optimization: The Strength Pareto Approach.* Computer Engineering and Networks Laboratory, Swiss Federal Institute of Technology, Zurich, Switzerland.

[7] Ajith Abraham, Lakhmi Jain and Robert Goldberg(editors).Evolutionary Multiobjective Optimization. Theoretical Advances and Applications, Springer, USA, 2005, ISBN 1-85233-787-7

[8] Coello, Carlos A. and Christiansen, Alan D. Two New GA based Methods for Multi-objective Optimization. Department of Computer Science, Tulane University, New Orleans, LA, USA

[9] G. B. Dantzig, R. Fulkerson, and S. M. Johnson, Solution of a large-scale traveling salesman problem, Operations Research 2 (1954), 393-410.

[10] S. Arora. Polynomial Time Approximation Schemes for Euclidean Traveling Salesman and other Geometric Problems. Journal of ACM, 45(1998), 753-782.

[11] N. Christofides, Worst-case analysis of a new heuristic for the traveling salesman problem, Report 388, Graduate School of Industrial Administration, CMU, 1976.

[12] C. H. Papadimitriou, S. Vempala: On the approximability of the traveling salesman problem (extended abstract). Proceedings of STOC'2000, 126-133.

[13] G. Gutin, Traveling Salesman and Related Problems, Royal Holloway, University of London, 2003

[14] G. Gutin, A. Punnen, The Traveling Salesman Problem and its variations, Kluwer Academic Publishers.

[15] M. Dorigo, L.M. Gambardella, Ant Colony System: A Cooperative Learning Approach to the Traveling Salesman Problem, IEEE Transactions on Evolutionary Computation 1(1) 53-66, 1997.

[16] C.M.Fonseca, and P.J.Fleming: "Genetic algorithms for multiobjective optimization: Formulation, discussion and generalization," *Proc. 5th ICGA* (University of Illinois at Urbana-Champain, USA, July 17-21, 1993), pp.416-423

Extended Performance Comparison of Pixel Window Size for Colorization of Grayscale Images using YIQ Color Space

Ankita Taparia

Email: enggankita.taparia@gmail.com

Computer Engineering Department, Silver Oak College of Engineering & Technology, Ahmedabad

Abstract:

There is no exact solution for colorization of grayscale images. In the initial work done [1], color traits transfer techniques to color grayscale images are proposed. The main focus of the techniques [1] is to minimize the human efforts needed in manually coloring the grayscale images. The human interaction is needed only to find a reference color image, and then the job of transferring color traits from reference color image to grayscale image is done by proposed techniques. This paper is an extension to [18].Here the technique of color traits transfer to grayscale images have been performed with respect to RGB color space only but with different pixel window sizes. The pixel window sizes used are total fifteen ranging from window with size1x2 to 4x4. So in all 15 different versions of color traits transfer to grayscale algorithms are tested over thirty-one different images for deciding the color space and pixel window size giving best quality of coloring. The experimental results give that the pixel window of size 4x4 suits the best in RGB color space.

Keywords: Colorization, Color Palette, Color Spaces, Color Transfer, Pixel Window.

1. Introduction

The task of 'color traits transfer to a grayscale image' is very difficult because it involves assigning three dimensional (RGB) pixel values to an image which varies along only one dimension (luminance or intensity) [3].Since different colors may have the same luminance value but vary in hue or saturation, the problem of colorizing grayscale images has no inherently 'unique' solution [2].Due to these ambiguities, human interaction usually playsa large role in the colorization process. Even in the case ofpseudocoloring, [4, 5] where the mapping of luminance values to color values is automatic, the choice of the color map is commonly determined by human decision. Pratt [5] describes this method as an image enhancement technique because it can be used to "enhance the detectability of detail within the image [2]".

Grayscale image colorization can find its applications in black and white photo editing [2, 6], classic movies colorization [7, 8, 9] and scientific illustrations [2, 3]. To enhance visual appeal of grayscale images and for perceptual enhancement of scientific illustrations, colorization plays a vital role. In medicine [2,5] , image modalities which only acquire grayscale images such as Magnetic Resonance Imaging (MRI), X-ray and Computerized Tomography (CT) images can be enhanced with color for presentations and demonstrations. Pseudo coloring is a common technique for adding color to grayscale images such as X-ray, MRI, scanning electron microscopy (SEM) and other imaging modalities so as to study the infected areas in a fine manner.

The re-coloring of grayscale images using semi-automated techniques, where users provide cues in order to facilitate the image re-coloring, has been investigated by several research groups.

In the color traits transfer techniques [1], the color palette is prepared using pixel windows of some degrees taken from reference color image. Then the grayscale image is divided into pixel windows with same degrees. For every window of grayscale image the palette is searched and equivalent color values are found, which could be used to color grayscale window.

Welsh et al. [2s] proposed a grayscale image colorization method that works very impressively for natural images and scientific illustration images. In general, Welsh et al.'s method works well on scenes where the image is divided into distinct luminance clusters or where each region has distinct textures. However, their technique does not work very well with human faces. Using a technique reminiscent of image analogies, Levin et al [10] produced grayscale re-colorizations of *video* by having users pick colors from a source image and draw freehand curves or

scribble the target frame to cue where and how color transfer should occur for selected destination *frames*. Also of interest is an image re-coloring scheme for *gamut* replacement described in [11, 12] that uses grayscale recolorization methods.

One of the most common tasks in image processing and editing is to alter an image's color. Recently, Rudermanetal. [13] Developed a color space, called L□ □ color space, which minimizes correlation between channels for many natural scenes. Reinhard et al. [3] used this color space to transfer color from one color image to another rand achieved impressive visual effect. The basic idea of that paper is to combine the color transferring technique in[3] with texture synthesis techniques. This technique works very well on scenes where the image is divided into distinct luminance clusters or where each of the regions has distinct textures.

However, the technique does not work very well with faces. It fails to classify the difference between skin and lip. More generally, this problem exists in colorizing grayscale images with regions with similar or confusing luminance distribution. Directly employing this technique will fail to colorize these different regions with user specified colors, even though with the help of swatches.

The techniques given in [3] and [13] are referred as no interactive (i.e. fully-automated) color transfer techniques, Reinhard et al [3] used statistical methods in order to *color correct* natural landscape images by transferring color "characteristics" from a source image to destination image. Their transfer methods relied heavily on the properties obeyed by natural images when they are analyzed in Ruderman's L□ □ color space [13].

In [14], [15], [16] grayscale image matting algorithms are used to combine with color transferring techniques to achieve object-based colorization, where objects in the same image are colorized independently. In [17], the authors have demonstrated the possibility to color many grayscale images in a way that is completely automatic. Here the source image is found from database of color images based on feature matching of target grayscale image with source color images. All the techniques except [1] are very complex and fail at one or other category of images, also computationally they are very heavy.

2. Color trait transfer algorithm

In order to transfer color traits to grayscale image, initially user needs to find an appropriate reference source color image. Then one can follow the steps given below to color the target grayscale image. The color traits transfer algorithm mainly has three steps

a. Generate color palette by traversing the source color image using a particular window size .
b. Search the respective matches for grayscale pixels in the color palette using the same window size .
c. Transfer the colors from best found palette match to grayscale pixels.

2.1 Color palette generation using source

We have purely worked in RGB color space and so there is no requirement of converting the source color image to any other color space. The source image is then divided into the pixel windows of size M x N. First M+N columns in the color palette, store the grayscale value of the corresponding pixels. Next M+N columns store the value of red component of those pixels and in the same way, values of green and blue components is stored. This array is referred as the color palette which is used to squirt colors in target grayscale image.

2.2 Search

The target grayscale image is also divided into the pixel windows of same size MxN. Every window is represented as array of grayscale intensity values of inclusive pixels. For every row of grayscale intensity values the best match is searched from the color palette using Mean Squared Error (MSE). Here the MSE value is computed of grayscale target pixel window in color palette from first record to last record. Wherever the MSE value is lowest that is considered to be best match. Thus for every pixel window of grayscale target image all the records in color palette are considered in exhaustive search.

2.3 Color Transfer to Grayscale image

As the appropriate row with lowest MSE value is found in the color palette, all the corresponding values of red, green and blue components in that row are transferred to the corresponding pixels in grayscale image. As a result, final image is obtained with all three R, G and B planes.

3. Quality of colored image

The objective criteria to measure the quality of colored target image cannot be considered because the process of coloring is very subjective to the target grayscale image and source color image. At the most one could convert some color images into their equivalent grayscale images and then recolor them using source as same original color image. Then the Mean Squared Error (MSE) difference of re-colored image with original one could be considered to compare the proposed algorithms with each other.

4. Results and discussion

To check the quality of color traits transfer algorithm for RGB color spaces along various window sizes, here we have considered various color images as shown in figure 1 for re-coloring their gray equivalents. Here we have considered only RGB color spaces for color traits transfer to grayscale images using fifteen varied pixel window sizes of 1x2, 1x3, 1x4, 2x1, 2x2, 2x3, 2x4, 3x1, 3x2, 3x3, 3x4, 4x1 and 4x2, 4x3 and 4x4. The combinations of RGB color space and window sizes resulted into 15 different versions of the original color traits transfer algorithms given in [1].

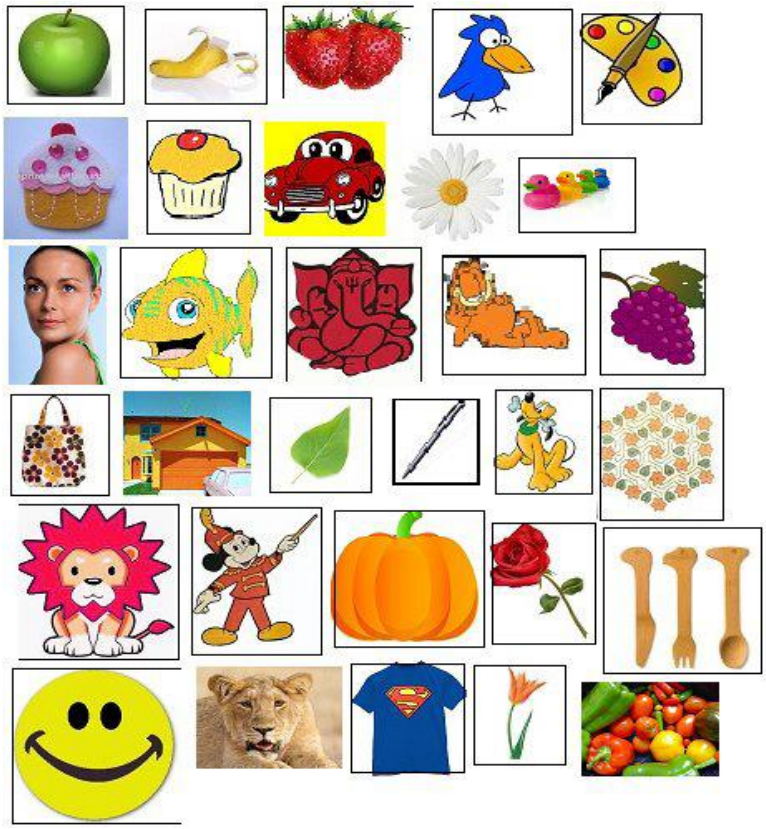

Fig.1 Sample Images considered for checking quality of color traits transfer technique using RGB color spaces for different window sizes

Fig 2, indicates the Mean Squared Error Difference between Original color Images and respective re-colored images using RGB color space plotted against various window sizes. The MSE values are averaged on all thirty one test mages shown in fig 1 for respective color space and respective window size

As , different pixel window sizes have been used here so to find out the best pixel window size, we have applied 6 different pixel window sizes on a grayscale image and colored it using a source color image, fig.3.

In fig.4, a grayscale image has been colored using colors of a source image with 6 different pixel window sizes. On seeing the results, it can be easily sketched out that pixel window size of 2x2 gives best results. Hence, considering pixel window size of 2x2, results of some more grayscale and source color images have been shown in fig 4.

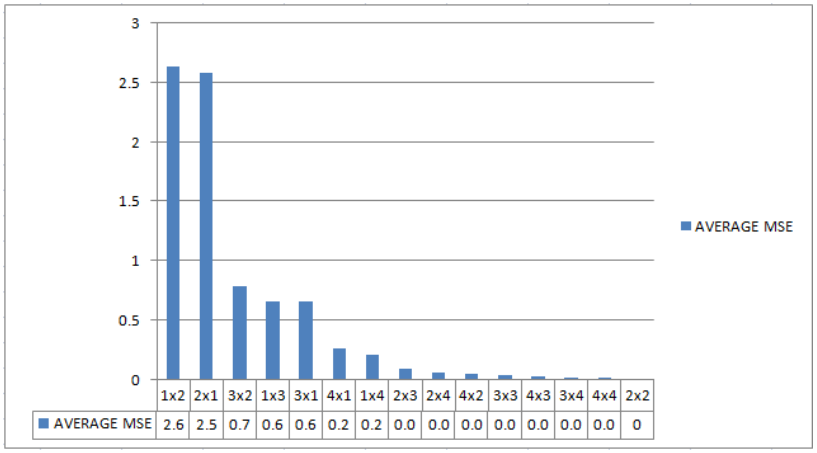

Fig.2 Average of Mean Squared Error Difference between Original Color Image and Image Re-colored using RGB Color Space Versus various Window Sizes

Fig.3 (a) Grayscale image (b) Source color image

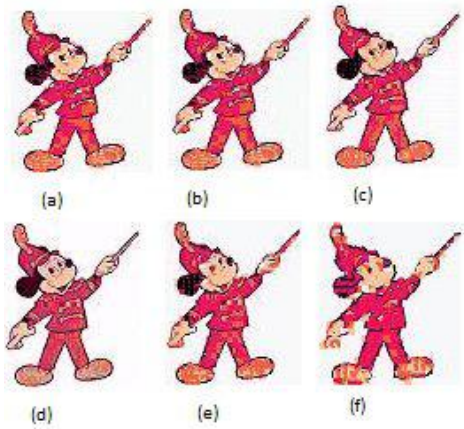

Fig.4 Colored image of grayscale Mickey in fig.3 (a) 2x2 (b) 2x4 (c) 3x2 (d) 3x1 (e) 3x3 (f) 4x4

After finding that the RGB is most suited along with the 2x2 pixel window size, for best quality color traits. Transfer, the same window size has been used in color traits transfer on various images, as shown in fig 5.

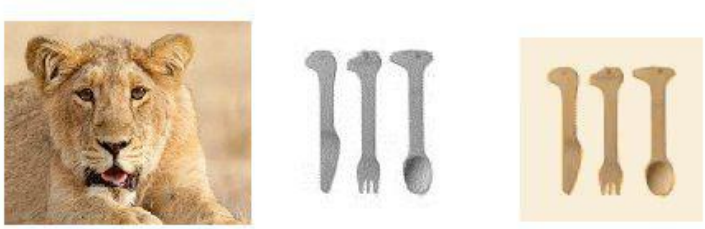

Fig.5(a)Color Traits transfer to grayscale spoons image

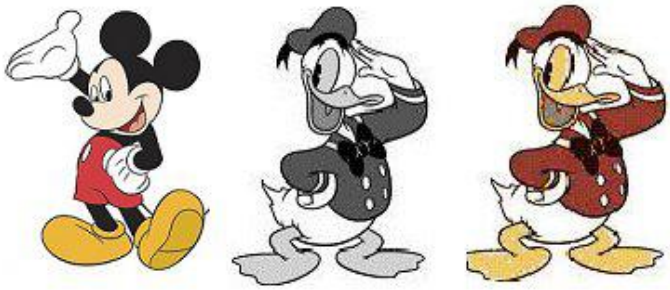

Fig.5(b) Color Traits transfer to grayscale donald image

Fig.5(c) Color Traits transfer to grayscale teddy bear image

Fig.5(d) Color Traits transfer to grayscale orange image

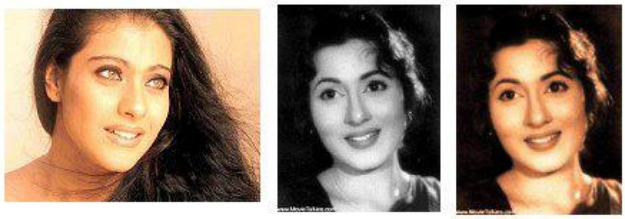

Fig.5(e) Color Traits transfer to grayscale face image

Fig.5(f) Color Traits transfer to grayscale umbrella image

Fig.5. Color Traits transfer to various grayscale images using RGB color space and pixel window size 2x2 [Here for all a-f from left first is source color image second is target grayscale image and third is colored target image using colors from source color image]

5. Conclusion

In this paper we have revisited color traits transfer to grayscale images with help of RGB color space and 15 different pixel window sizes. In all 15 versions of the color traits transfer technique are tested to decide the most suitable pixel window size to be used for RGB color space. As the color traits transfer technique is highly subjective, the quality of colored image cannot be expressed by any objective criteria. Just to compare the proposed techniques the same color source image can be re-colored and compared with the original color image. Here for comparing quality of coloring among 84 versions of color traits transfer technique, five different color images are considered to be re-colored.

6. REFERENCES

[1] H.B.Kekre, Sudeep D. Thepade, "Color Traits Transfer to Grayscale Images", In Proc. of Int. Conference on Emerging Tends in Engg. And Tech.,ICETET-2008, pp-

[2] T. Welsh, M. Ashikhmin, and K. Mueller,Transferring color to grayscale images," ACM TOG, vol. 20, no. 3, pp. 277–280, 2002.

[3] E. Reinhard, M. Ashikhmin, B. Gooch, and P.Shirley, "Color transfer between images," IEEE Computer grahics and applications, vol. 21, no. 5, pp.34–41, September/October 2001.

[4] Rafael C. Gonzalez & Paul Wintz, "Digital Image Processing", Addison-Wesley Publications, May,1987.

[5] Pratt, W. K. "Digital Image Processing", John Wiley& Sons, 1991.

[6] Tongbo Chen, Yan Wang Volker Schillings,Christoph Meinel, "Grayscale Image Matting And Colorization", In Proceedings of ACCV-2004, Jan27-30, 2004, Jeju Island, Korea, pp. 1164-1169.

[7] Rafael C. Gonzalez & Paul Wintz, "Digital Image Processing", Addison-Wesley Publications, May,1987.

[8] Y. Y. Chuang, A. Agarwala, B. Curless, D. Salesin, and R. Szeliski, "Video matting of complex scenes," ACM Transaction on Graphics, vol. 11, no. 4, pp. 348–372, 2002.

[9] A. R. Smith and J. F. Blinn, "Blue screen matting,"in Proceedings of ACM SIGGRAPH, 1996, pp. 259–268.

[10] Tongbo Chen, Yan Wang Volker Schillings,Christoph Meinel, "Grayscale Image Matting And Colorization", In Proceedings of ACCV-2004, Jan 27-30, 2004, Jeju Island, Korea, pp. 1164-1169.

[11] Karl Rasche, Robert Geist, James Westall, "Recoloring Images for Gamuts of Lower Dimension",EUROGRAPHICS , Volume 24 , Number ,2005.

[12] Stone M. C., Cowan W. B., Beatty J. C., "Color gamut mapping and the printing of digital color images", ACM Transactions on Graphics, Volume 7,No.4 October 1988, pp 249.292.

[13] D. L. Ruderman, T. W. Cronin, and C. C. Chiao, "Statistics of coneresponses to natural images: implications for visual coding," J. Optical Soc. Of America, vol. 15, no. 8, pp. 2036–2045, 1998.

[14] Tongbo Chen, Yan Wang Volker Schillings, Christoph Meinel, "Grayscale Image Matting And Colorization", In Proceedings of ACCV-2004, Jan27-30, 2004, Jeju Island, Korea, pp. 1164-1169.

[15] Y. Y. Chuang, A. Agarwala, B. Curless, D. Salesin,and R. Szeliski, "Video matting of complex scenes," ACM Transaction on Graphics, vol. 11, no. 4, pp.348–372, 2002.

[16] A. R. Smith and J. F. Blinn, "Blue screen matting," in Proceedings of ACM SIGGRAPH, 1996, pp. 259–268.

[17] Luiz Filipe M. Vieira, Rafael D. Vilela, Erickson R.do Nascimento, "Automatically choosing source color images for coloring grayscale images", In Proceedings of the XVI Brazilian Symposium on Computer Graphics and Image Processing (SIBGRAPI'03), 2003.

[18] Dr. H.B.Kekre , Dr. Sudeep Thepade, Archana Athawale and Adib Parker , "Using Assorted Color Spaces and Pixel Window Sizes for Colorization of Grayscale Images", ACM , January-February 2004

Digital Audio Broadcasting

Nisha Solanki

Email: nisha.ecr@socet.edu.in

Electronics & Communication Engineering Department, Silver Oak College of Engineering & Technology, Ahmedabad

Abstract:

Digital Audio Broadcasting, DAB, is the most fundamental advancement in radio technology. It gives listeners interference- free reception of high-quality sound, easy-to-use radios, and the potential for wider listening choice through many additional stations and services. DAB is a reliable multi- service digital broadcasting system for reception by mobile, portable and fixed receivers with a simple, non-directional antenna. It can be operated at any frequency from 30 MHz to 3 GHz for mobile reception (higher for fixed reception) and may be used on terrestrial, satellite, hybrid (satellite with complementary terrestrial) and cable broadcast networks. In addition to supporting audio programmes with a wide range of sound coding rates and hence qualities, it also has a flexible, general purpose digital multiplex which can carry a number of services, including audio-programmed associated data and independent data services. It is the only system available in the world to meet all the demanding requirements drawn up by the International Telecommunications Union (ITU), thus opening horizons for all-digital broadcasting of the future. This review paper would give the brief idea about the technologies involved in the Digital Audio Broadcasting.

Keywords: MPEG, OFDM, SFN

1. Introduction

Digital audio broadcasting (DAB), also known as digital radio and high-definition radio, is audio broadcasting in which analog audio is converted into a digital signal and transmitted on an assigned channel

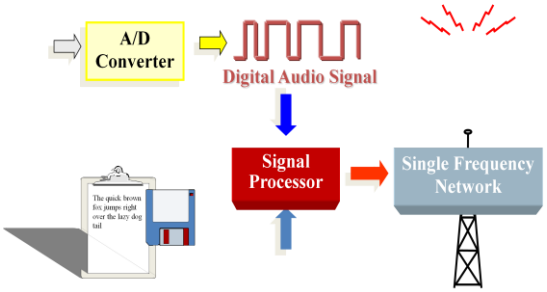

Fig.1 DAB block diagram

The EUREKA DAB System is a rugged, yet highly spectrum and power-efficient sound and data broadcasting system. It uses advanced digital audio compression techniques (MPEG 1 Audio Layer II and MPEG 2 Audio Layer II) to achieve a spectrum efficiency equivalent to or higher than that of conventional FM radio. A closely controlled coding redundancy is applied to the signal in order to provide strong error protection and high power efficiency. The transmitted information is spread in both frequency and time so that the effects of channel distortions and fades are eliminated in the receiver, even under conditions of severe multipath propagation whether at home or in the car.

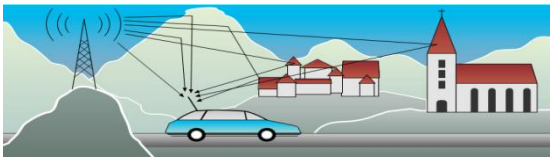

Fig.2 Multipath propagation

The efficiency of spectrum use is increased by a special feature called the Single Frequency Network (SFN). A broadcast network can be extended virtually without limit by operating all transmitters on the same radio frequency.

2. Main features of DAB systems

The DAB transmission signal carries a multiplex of several digital services simultaneously. Its overall bandwidth is 1.536 MHz, providing a useful bit-rate capacity of approximately 1.5 Mbit/s in a complete "ensemble". Each service is independently error protected with a coding overhead ranging from about 25% to 300% (25% to 200% for sound), the amount of which depends on the requirements of the broadcasters (transmitter coverage, reception quality). The ensemble contains audio programmes, data related to the audio programme and optionally other data services. Usually, the receiver will decode several of these services in parallel. A specific part of the multiplex contains information on how the multiplex is actually configured, so that the receiver can decode the signal correctly. It may also carry information about the services themselves and the links between different services. Following are the most important features of the DAB system.

Flexible audio bit-rate, from 8 kbit/s to 384 kbit/s, which allows the multiplex to be configured in such a way that it provides typically 5 to 6 high-quality stereo audio programmes or up to 20 restricted quality mono programmes.

Data services, each service can be a separately defined stream or can be divided further by means of a packet structure.

Programme Associated Data (PAD), embedded in the audio bit-stream, for data transmitted together with the audio programme (e.g. lyrics, phone-in telephone numbers). The amount of PAD is adjustable (min. 667 bit/s), at the expense of capacity for the coded audio signal within the chosen audio bit-rate.

Conditional Access (CA), applicable to each individual service or packet in the case of packet-mode data. Specific subscriber management does not form part of the DAB System Specification, however, the DAB ensemble transports the CA information and provides the actual signal scrambling mechanisms.

Service Information (SI), used for operation and control of receivers and to provide information for programme selection to the user. SI also establishes links between different services in the multiplex as well as links to services in other DAB ensembles and even to FM/AM broadcasts.

3. Generation of DAB signals

Figure 3 shows the block diagram of conceptual DAB signal generator.

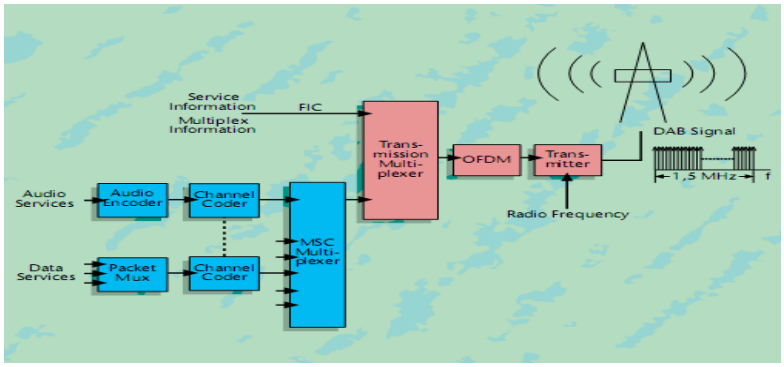

Fig.3 Generation of DAB signal

Each service signal is coded individually at source level, error protected and time interleaved in the channel coder. Then the services are multiplexed in the Main Service Channel (MSC), according to a pre determined, but adjustable, multiplex configuration.

The multiplexer output is combined with Multiplex Control and Service Information, which travel in the Fast Information Channel (FIC), to form the transmission frames in the Transmission Multiplexer. Finally, Orthogonal Frequency Division Multiplexing (OFDM) is applied to shape the DAB signal which consists of a large number of carriers. The signal is then transposed to the appropriate radio frequency band, amplified and transmitted.

4. Reception of DAB signal

Figure 4 shows the block diagram of conceptual DAB signal receiver.

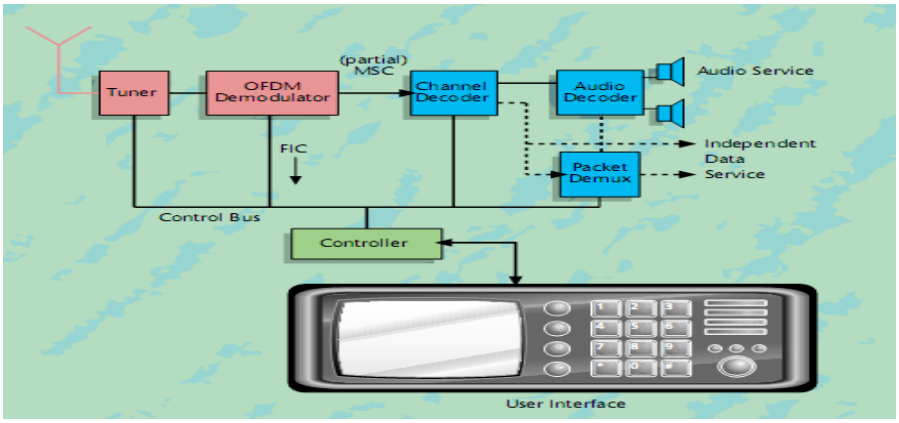

Fig.4 Reception of DAB signal[3]

The DAB ensemble is selected in the analogue tuner, the digitized output of which is fed to the OFDM demodulator and channel decoder to eliminate transmission errors. The information contained in the FIC is passed to the user interface for service selection and is used to set up the receiver appropriately. The MSC data is further processed in an audio decoder to produce the left and right audio signals or in a data decoder (Packet Demux) as appropriate.

5. Various services

5.1 Audio Services

Compared to conventional PCM sound coding, in DAB the bit-rate is reduced six fold to twelve fold by means of a digital audio compression technique.

The DAB Specification permits full use of the flexibility of MPEG Layer II except for the fact that only the standard studio sampling frequency of 48 kHz and the half sampling frequency of 24 kHz are used. Layer II is capable of processing mono, stereo and dual-channel such as bilingual programmes. Different encoded bit-rate options are available (8, 16, 24, 32, 40, 48, 56, 64, 80, 96, 112, 128, 144, 160 or 192 kbit/s per monophonic channel). In stereophonic or dual-channel mode, the encoder produces twice the bit-rate of a mono channel.

The range of possible options can be utilized flexibly by broadcasters depending on the quality required and the number of sound programmes to be broadcast. A stereophonic signal may be conveyed in the stereo mode, or particularly at lower bit-rates in the joint stereo mode. This mode uses the redundancy and interleaving of the two channels of a stereophonic programme to maximize the overall perceived audio quality.

5.2 Data Services

Programme Associated Data

Each audio programme contains Programme Associated Data (PAD) with a variable capacity (minimum 667 bit/s, up to 65 kbit/s) which is used to convey information together with the sound programme. Typical examples of PAD applications are dynamic range control information, a dynamic label to display programme titles or lyrics, speech/music indication and text with graphic features.

5.3 Independent Data Services

In addition to PAD, general data may be transmitted as a separate service. This may be either in the form of a continuous stream segmented into 24 ms logical frames with a data rate of n x 8 kbit/s or in packet mode, where individual packet data services may have much lower capacities and are bundled in a packet sub-multiplex. A third way to carry Independent Data Services is as a part of the FIC (Fast Information Channel). Typical examples of Independent Data Services are a Traffic Message Channel, correction data for Differential GPS, paging and an electronic newspaper.

5.4 Conditional Access

Every service can be fitted with Conditional Access if desired. The Conditional Access (CA) system includes three main functions:

1. **scrambling/descrambling**, - It makes the service incomprehensible to unauthorized users.
2. **entitlement checking** - It consists of broadcasting the conditions required to access a service, together with encrypted secret codes to enable descrambling for authorized receivers.
3. **entitlement management**. – It distributes entitlements to receivers.

5.5 Service Information

The following elements of Service Information (SI) can be made available to the listener for programme selection and for operation and control of receivers:

- basic programme-service label (i.e. the name of a programme service)
- Programme-type label (e.g. news, sports, classical music)
- Dynamic text label (e.g. the programme title, lyrics, names of artistes)
- programme language
- time and date, for display or recorder control
- switching to traffic reports, news flashes or announcements on other services

- Cross-reference to the same service being transmitted in another DAB ensemble or via AM or FM and to other services.
- transmitter identification information (e.g. for geographical selection of information)

Essential items of SI that are used for programme selection are carried in the FIC. Information that is not required immediately when switching on a receiver, such as a list of all the day's programmes, may be carried separately as a general data service (Auxiliary Information Channel).

5.6 Channel Coding and Time Interleaving

The data representing each of the programme services is subjected to energy dispersal scrambling, convolutional coding and time interleaving. For energy dispersal scrambling a pseudo-random bit sequence is added to the data in order to randomize the shape of the DAB signal and thus efficiently use power amplifiers. The convolutional encoding process involves adding redundancy to the data in order to help the receiver detect and better eliminate transmission errors. In the case of an audio signal, some parts of the audio frame are less sensitive to transmission errors than others and accordingly, the amount of redundancy added is reduced for these. This method is known as Unequal Error Protection (UEP)(Figure 4).

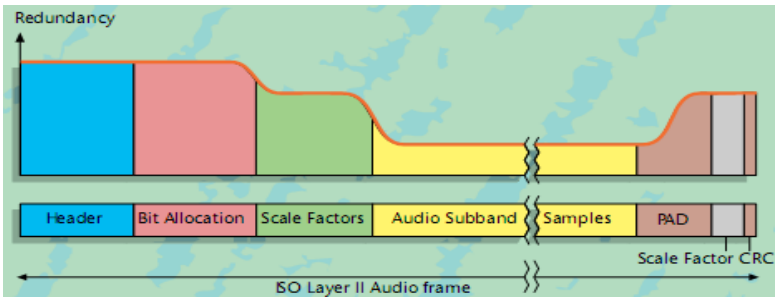

Fig.5 Unequal Error Protection

5.7 Main Service Multiplex

The encoded and interleaved data is fed to the Main Service Multiplexer (MUX) where every 24 ms the data is gathered in sequences. The combined bit-stream output from the multiplexer is known as the Main Service Channel (MSC) and has a gross capacity of 2.3 Mbit/s. Depending on the convolutional code rate, which can differ from one application to another, the net bit-rate ranges from approximately 0.6 to 1.8 Mbit/s, accommodated in a DAB signal with a 1.536 MHz bandwidth.

Transmission Frame

In order to facilitate receiver synchronisation, the transmitted signal is designed according to a frame structure with a fixed sequence of symbols. Each transmission frame(see Figure 6) begins with a null symbol for coarse synchronization (when no RF signal is transmitted), followed by a phase reference symbol for differential demodulation. The next symbols are reserved for the FIC and the remaining symbols provide the MSC. The total frame duration is 96 ms, 48 ms or 24 ms, depending on the transmission mode (see Table 1). Each service within the MSC is allocated a fixed time slot in the frame.

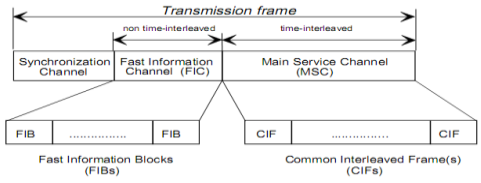

Fig.6 Transmission Frame

Table 1 – Transport Characteristics of Transmission Frame

Transmission mode	Duration of transmission frame	Number of FIBs per transmission frame	Number of CIFs per transmission frame
I	96 ms	12	4
II	24 ms	3	1
III	24 ms	4	1
IV	48 ms	6	2

Modulation with OFDM and Transmission Modes

The DAB system uses a multicarrier scheme known as Orthogonal Frequency Division Multiplexing (OFDM). This scheme meets the exacting requirements of high bit-rate digital broadcasting to mobile, portable and fixed receivers, especially in multipath environments. Before the transmission the information is divided into a large number of bit-streams with low bit-rates each. These are then used to modulate individual orthogonal carriers (differential QPSK) in such a way that the corresponding symbol duration becomes larger than the delay spread of the transmission channels. By inserting a temporal guard interval between successive symbols, channel selectivity and multipath propagation will not cause inter-symbol interference (Figure 7).

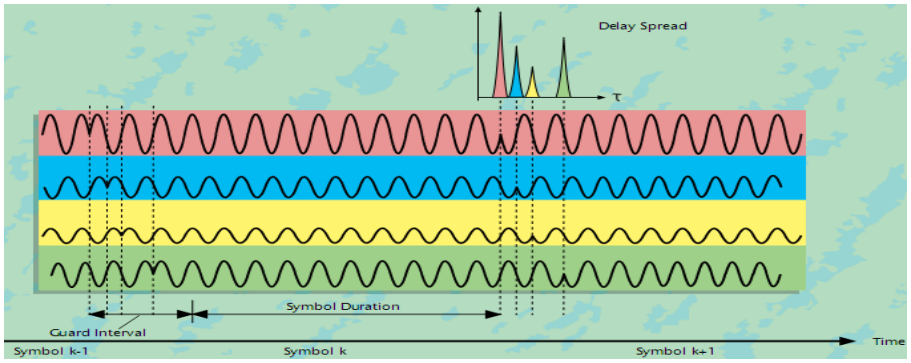

Fig.7 OFDM technique

The system provides four transmission- mode options which allow for a wide range of transmission frequencies between 30 MHz and 3 GHz and network configurations. For the nominal frequency ranges, the transmission modes have been designed to suffer neither from Doppler spread nor from delay spread, both inherent in mobile reception with multipath echoes.

Table 2 – Transmission Parameters[2]

System Parameter	*Transmission Mode* I	II	III	IV
Frame duration	96 ms	24 ms	24 ms	48 ms
Null symbol duration	1297 µs	324 µs	168 µs	648 µs
Guard interval duration	246 µs	62 µs	31 µs	123 µs
Nominal maximum transmitter separation for SFN	96 km	24 km	12 km	48 km
Nominal frequency range (for mobile reception)	≤ 375 MHz	≤ 1.5 GHz	≤ 3 GHz	≤ 1.5 GHz
Speed/coverage trade-off	No	No	No	Yes
Useful symbol duration	1 ms	250 µs	125 µs	500 µs
Total symbol duration	1246 µs	312 µs	156 µs	623 µs
No. of radiated carriers	1536	384	192	768

Table 2 gives the temporal guard interval duration, the nominal maximum transmitter separation and frequency range for mobile reception for the different modes. The noise degradation at the highest frequency is equal to approximately 1dB at 100 km/h under the most critical multipath conditions, which do not occur frequently in practice. The table shows that the higher the frequencies, the shorter the guard interval available and hence the smaller the maximum non-destructive echo delay. Mode I is most suitable for a terrestrial Single-Frequency Network in the VHF range, because it allows the greatest transmitter separations. Mode II will preferably be used for medium-scale SFN in L-band and for local radio applications that require one terrestrial transmitter. Larger transmitter spacing can be accommodated by inserting artificial delays at the transmitters and by using directional transmission antennas. Mode III is most appropriate for cable, satellite and complementary terrestrial transmission, since it can be operated at all frequencies up to 3 GHz for mobile reception and has the greatest phase-noise tolerance. Mode IV is also used in L-band and allows greater transmitter spacing in SFNs. However, it is less resistant to degradation at higher vehicle speeds. The large number of orthogonal carriers (see Table 2), which can be easily generated by a Fast Fourier Transformation (FFT) process, is known collectively as a "DAB block". The spectrum of the signal is approximately rectangular, Gaussian noise-like, and occupies a bandwidth of 1.536 MHz. Figure 3-5 shows an example of the transmitter output spectrum after it has been amplified and filtered. In practice, the peak-to-mean ratio can be limited to about 8 dB by digital processing, al- though this may be further reduced by additional signal conditioning when amplifying it in a non-linear way in the transmitter. With multipath propagation, some of the carriers are amplified by constructive signals, while others suffer destructive interference (frequency selective fading). Therefore, the OFDM system provides frequency interleaving by a re-arrangement of the digital bit-stream among the carriers, so that successive source samples are not affected by selective fade. In stationary receivers, this diversity in the frequency domain is the prime means to guarantee unimpaired reception; the time diversity due to time-interleaving provides further assistance to a mobile receiver. Consequently, multipath propagation is a form of diversity of which DAB takes advantage, in stark contrast to conventional FM or narrow- band digital systems, where it can completely destroy a service.

6. System Constraints

(1) System processing delay

The DAB system chain includes several blocks which introduce a significant processing delay. For example, the time interleaver introduces a delay of 384 ms, and the audio coder/decoder introduces a delay of several tens of milliseconds. The total delay in the system may vary from one implementation to the next. The system delay should be taken into account when the receiver switches between DAB and FM “simulcast” programmes, so that a seamless transition is obtained. It will become necessary for simulcast FM transmissions to be delayed by nominally the same amount, say one second, regardless of the receiver design. This nominal delay should be taken into account when signaling the current time information.

(2) Frequency accuracy in SFNs

In order not to reduce the performance of the DAB system, the difference in frequency between geographically-adjacent transmitters must be kept to an absolute minimum – of the order of a few hertz in 108. Consequently, the local oscillators of all transmitters must be locked to a rubidium oscillator, or to a common reference which is distributed to all the transmitters.

(3) Time accuracy in SFNs

The time difference between geographically adjacent transmitters will have an implication on the system’s capability to cope with “active echoes”. Therefore, all the transmitters operating in an SFN should be time-synchronized with an accuracy of better than 25 ms (i.e. approximately 10 % of the guard interval in Transmission Mode I).

(4) Bit-by-bit compliance in SFNs

In principle, the bit-streams emitted from all transmitters operating in an SFN should be identical. If this condition is not fulfilled, there will be a "mush area" (i.e. interference zone) between the transmitters where the DAB receiver may be confused. Tests are being undertaken to assess the size of the mush area in the case where a local transmitter "opts out" from an SFN, thus emitting a different bit stream to the other transmitters in the SFN.

(5) Receiver speed limit

As the speed of a vehicle increases, the performance of an on-board DAB receiver progressively degrades, due to the Doppler effect. The "receiver speed limit" may be considered as the vehicular speed at which the RF signal-to-noise ratio degrades by 4 dB, due to the Doppler effect. While this does not affect the audio quality, it may reduce the DAB coverage area slightly – but only in a fast-moving vehicle. In the case of an SFN operating at VHF, the receiver speed limit is about 200 km/h. When the receiver operates at 1.5 GHz and Transmission Mode IV is used, the speed limit is about 120 km/h.

7. DAB in India

Terrestrial DAB transmissions in India will be in VHF Band II and the satellite emissions will be in L-Band. Attempts to bring together all the major parties involved in DAB are being pursued by All India Radio and membership of the EuroDab Forum is being sought. DAB services in India will be implemented in three phases[1]. In the first phase, due to commence in 1998, a limited terrestrial DAB service – based on current regional radio programmes – will be initiated in four metropolitan cities: Delhi, Bombay, Calcutta and Madras. The regional programmes will be collected at New Delhi, via satellite contribution links, and subsequently distributed from New Delhi via an S-band transponder of the INSAT satellite. The received DAB signals will be converted to VHF Band II frequencies and then simulcast using the existing FM transmitting antennas and towers. In the second phase, independent local services – carrying a mix of local, regional, national and sponsored programmes – will be added gradually to a number of FM stations by the year 2003. Finally, DAB services via satellite could commence after 2003. So far, a number of preliminary propagation studies have been carried out in L-Band. Experiments using the Eureka 147 system will start shortly, covering both terrestrial and satellite delivery.

8. Conclusion

Going through the content of the digital audio broadcasting we have gained a lot about the fundamentals of the real communication systems and the advantage of digital communication over the conventional analog communication.

REFERENCES

[1] EBU Recommendation R79 (1994): "Recommended system for digital sound broadcasting to mobile, portable and fixed receivers in the appropriate frequency bands in the range 30 MHz to 3 GHz".

[2] http://www.worlddab.org

[3] http://www.dlr.de/DAB/

Comparative Analysis of Ultra Low Power & Ultra Low Voltage CMOS Miller OTAs

Drashti Chavda

Email:Drashti.chavda@gmail.com

Electronics & Communication Engineering Department, Silver Oak College of Engineering & Technology, Ahmedabad

Abstract:

Recently so many portable devices like mobile, laptop, palmtop, digital camera are invented which are battery operated. Due to downscaling of technology & long lasting batteries, CMOS circuits should be provided with low supply voltage and should also consume low power.OTA can be designed at very low supply voltage less than 1V and its power dissipation is also low. Recently so many improved CMOS Miller OTA architectures are reported. Here comparison of simple Miller OTA & improved CMOS Miller OTA analog circuits in 45nm, 90nm & 180nm Technology is done using Ngspice simulator.

Keywords: Operational trans conductance amplifier (OTA), Improved Miller OTA, Unity gain frequency, Open loop gain.

1. Introduction

The operational transconductance amplifier (OTA) is a voltage controlled current source (VCCS) device. The transconductance of the amplifier is usually controlled by an input current, denoted I_{abc} ("amplifier bias current"). The amplifier's transconductance is directly proportional to this current. OTAs are used in implementing electronically controlled applications such as variable frequency oscillators, filters and variable gain amplifier stages which are more difficult to implement with standard op-amps, multiplexer, timer, sample and hold circuits.

2. Miller OTA

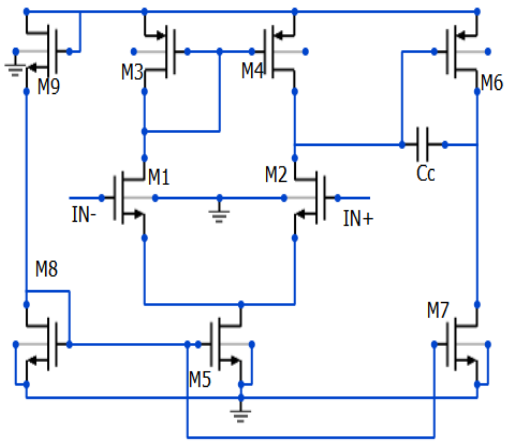

Fig.1 Miller's OTA [1]

In fig.1, circuit consists of differential pair (M1, M2) with transistor loads (M3, M4).It also consists of current mirror sub-circuit (M9, M8, M5, M7) and output stage (M6, M7). Its gain is 74 db in 180nm technology. Table 1 shows values when supply voltage is 2V or 1V for 180nm technology, but when supply voltage is 0.6V in180nm

technology then only W/L ratio of M5, M7 & M9 will be changed from 1.2u/1u to 3u/1u and all other W/L ratios will be same.

TABLE 1

TRANSISTOR AND OTHER ELEMENTS OF MILLER OTA IN 180NM TECHNOLOGY (2V & 1V SUPPLY VOLTAGE) & 90NM TECHNOLOGY (1V & 0.6V SUPPLY VOLTAGE)

$(W/L)_{M1}$ 5.43u/1u	$(W/L)_{M5}$ 1.2u/1u
$(W/L)_{M2}$ 5.43u/1u	$(W/L)_{M6}$ 60.6u/1u
$(W/L)_{M3}$ 20u/1u	$(W/L)_{M7}$ 1.2u/1u
$(W/L)_{M4}$ 20u/1u	$(W/L)_{M8}$ 80u/1u
$(W/L)_{M9}$ 1.2u/1u	Cc 0.01nf
C_L 0.01pf	

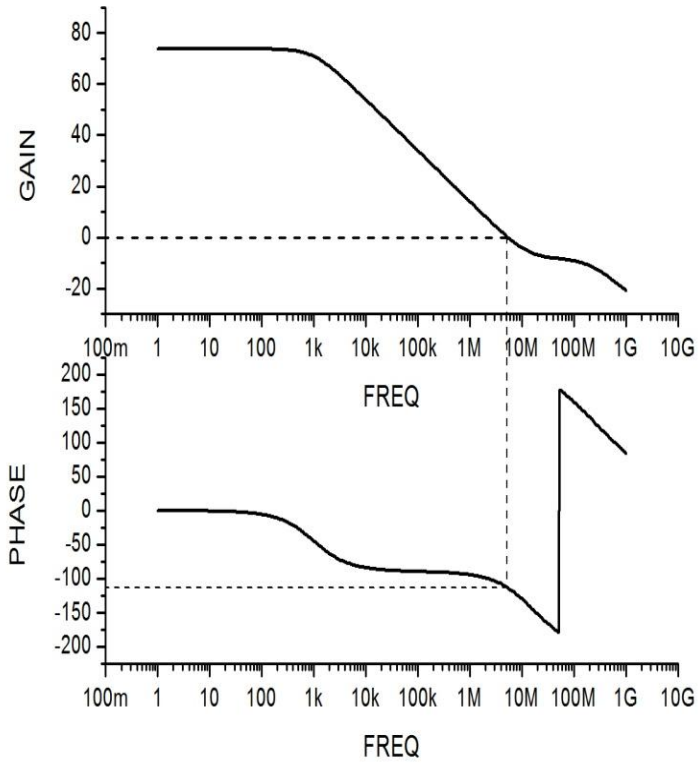

Fig. 2 Simulated Open loop gain and Phase of Miller OTA

TABLE 2

MILLER OTA PERFORMANCE BENCHMARK INDICATORS

Technology	**180nm**	**180nm**	**180nm**	**90nm**	**90nm**	**90nm**
Power supply	2V	1V	0.6V	2V	1V	0.6V
Open loop Gain	74.1db	73.1db	70db	50db	56.5db	56.5db
Unity Gain Freq	5.1MHz	813KHz	577KHz	511MHz	316MHz	304MHz
Phase Margin	71°	67°	65°	65°	60°	67°
Power dissipation	533uW	15uW	98nW	22mW	0.72mW	26uW
Slew rate	5.3V/us	1.68V/us	50V/ms	635V/us	152V/us	10V/us

3. Improved Miller OTA

Bulk driven Floating gate Threshold voltage tuning. The best approach for low-voltage CMOS circuits is the bulk-driven differential pair, since it allows a large signal swing without cutting off the transistor. Leakage current is also low in bulk-driven differential pair type of architecture.

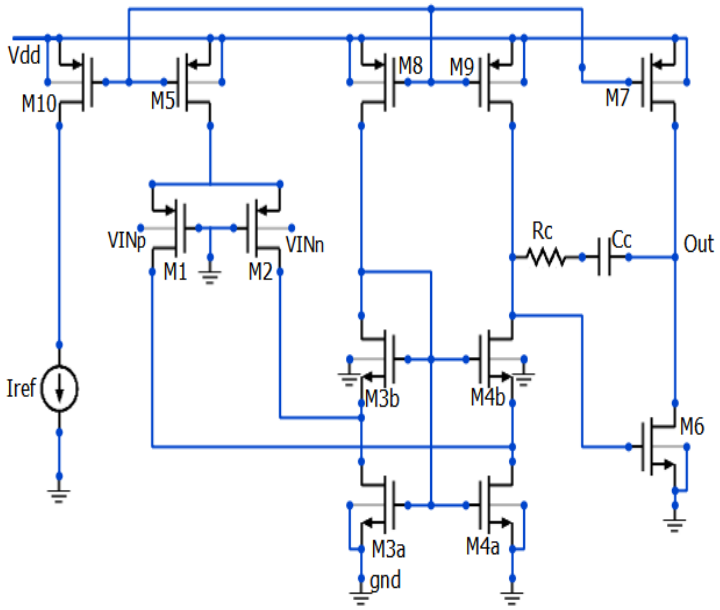

Fig.3 Improved bulk driven Miller OTA circuit [3]

In this architecture transistor pairs 3a–3b and 4a–4b form composite transistors. They allow the differential pair active load and the common gate amplifier to be biased by the same potential, without the use of additional biasing sources [3].

TABLE 3

TRANSISTORS AND OTHER ELEMENTS OF IMPROVED MILLER OTA IN 180NM & 90NM TECHNOLOGY

$(W/L)_{M1}$ 126.5u/1u	$(W/L)_{M5}$ 94.5u/9u
$(W/L)_{M2}$ 126.5 u/1u	$(W/L)_{M6}$ 55.56u/1u
$(W/L)_{M3a}$ 20u/1u	$(W/L)_{M7}$ 180u/9u
$(W/L)_{M4a}$ 20u/1u	$(W/L)_{M8}$ 17.5 u/9u
$(W/L)_{M3b}$ 90 u/1u	$(W/L)_{M9}$ 17.5u/9u
$(W/L)_{M4b}$ 90u/1u	R_C 5k
$(W/L)_{M10}$ 50u/9u (180nm) & 69.5u/9u(90nm)	
C_c 7p(180nm) & 5p(90nm)	
Iref 3u(180nm) & 25u(90nm)	
C_L 15p(180nm) & 20p(90nm)	

TABLE 4

TRANSISTOR AND OTHER ELEMENTS OF IMPROVED MILLER OTA IN 45NM TECHNOLOGY

$(W/L)_{M1}$ 143.44u/1u	$(W/L)_{M5}$ 177.45u/9u
$(W/L)_{M2}$ 143.44 u/1u	$(W/L)_{M6}$ 4.65 u/1u
$(W/L)_{M3a}$ 77.18u/1u	$(W/L)_{M7}$ 10.91 u/9u
$(W/L)_{M4a}$ 77.18u/1u	$(W/L)_{M8}$ 92.33u/9u
$(W/L)_{M3b}$ 174.34 u/1u	$(W/L)_{M9}$ 92.33 u/9u
$(W/L)_{M4b}$ 174.34u/1u	$(W/L)_{M10}$ 140.92u/9u
C_c 4f	R_C 34k
Iref 27u	C_L 1f

TABLE 5

IMPROVED MILLER OTA PERFORMANCE BANCHMARK INDICATORS

Technology	**[3]**	**180nm**	**90nm**	**45nm**
Power supply	0.6V	0.6V	0.6V	0.6V
Open loop Gain	69.4dB	71.0dB	77.9dB	73.4dB
Unity Gain Freq	11.35kHz	683kHz	26MHz	142MHz
Phase Margin	65.1°	72.7°	71.2°	65.4°
Power dissipation	550nW	11uW	77uW	50uW
Slew rate	14.6V/ms	200V/ms	500V/ms	280V/ms

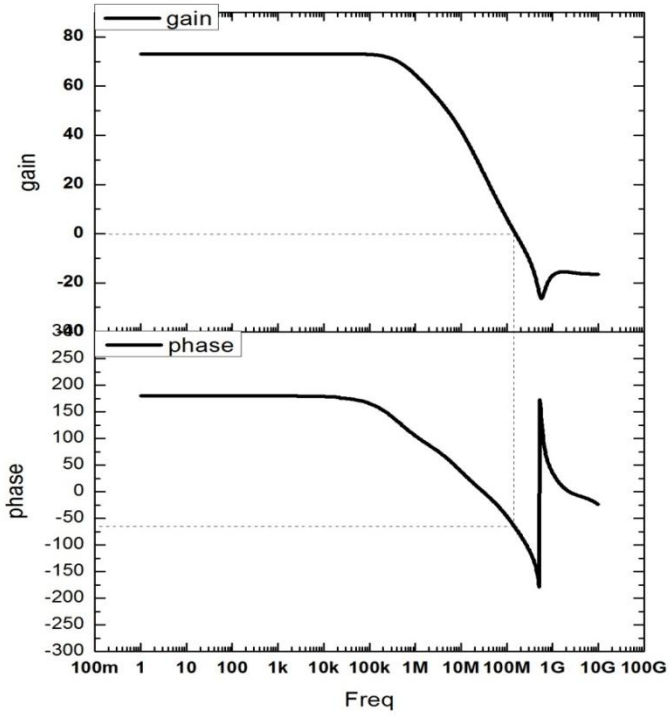

Fig.4 Gain-phase plot of improved Miller OTA at 45nm

4. Most recent improved Miller OTA

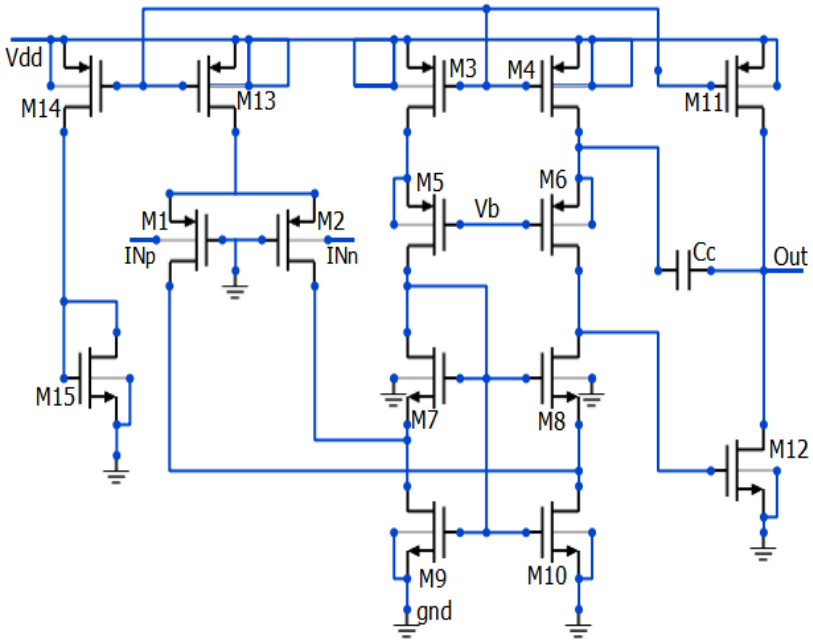

Fig.5 Most recent improved Miller OTA [4]

The proposed topology based on a bulk-driven input differential pair employed a gain-stage in the Miller capacitor feedback path to improve the "pole-splitting" effect [4].

TABLE 6

MILLER OTA PERFORMANCE BENCHMARK INDICATORS

Technology	**[4]**	**180nm**	**90nm**
Power supply	0.5V	0.5V	0.5V
Open loop gain	88.5dB	75dB	71dB
Unity Gain Freq	83.88kHz	607kHz	296kHz
Phase Margin	66.3°	72.2°	74.5°
Power dissipation	1.02uW	0.77uW	2.9uW
Slew rate	52V/ms	100V/ms	20V/ms

5. Conclusion

From the literature study, it has been observed that improved Miller operational transconductance amplifier achieves more gain, unity-gain frequency and slew rate at the cost of higher power dissipation. The technology used in reported work on OTA is either 180nm or 250nm. Therefore, this study focuses design and simulation of various architectures of OTA in technology files such as 45nm, 90nm and 180nm and to compare results with reported work. The circuits are simulated using Ng-Spice simulator. By simulation of improved Miller OTA which is reported in [4], it has been observed that we are getting lesser gain but improvement observed in unity gain frequency and slew rate. It leads to conclude that improved Miller OTA circuit reported in [3] is successfully optimized in 90nm technology at 0.6V supply voltage for all the specifications.

These circuits in this work are designed manually with specific design steps. Due to process voltage and temperature (PVT) variation, we could not achieve better performance measures. So, it inspires to design OTA circuits using automatic design approach for better performance in future.

REFERENCES

[1] Design of CMOS OTA core for Practical Education

[2] "Utilizing the Bulk-driven Technique in Analog Circuit Design" by Fabian Khateb, Dalibor Biolek,Nabhan Khatib 978-1-4244-6613-9/10,2010 IEEE.

[3] Luis H C. Ferreria ,T.C pimenta and R L moreno "An Ultra Low Voltage Ultra Low Power CMOS Miller OTA With Rail To Rail Input/Output Swing" IEEE trans.vol 549-7747,Oct 2007

[4] Milad Razzaghpuor,Abbas Golmakani. "An Ultra Low Voltage Ultra Low Power OTA With Improved Gain-Bandwidth Product" 1-4244-2370-5,2008 IEEE.

[5] Text book of operational transconductance amplifier and Analog integrated circuits by Tahira parveen.

[6] Sensors and Low-Power Signal Processing by Syed K. Islam and Mohammad R. Haider.


SILVER OAK COLLEGE OF ENGINEERING & TECHNOLOGY
Robotics Lab